THE UPPER DEVONIAN RHINESTREET BLACK SHALE OF WESTERN NEW YORK STATE – EVOLUTION OF A HYDROCARBON SYSTEM

GARY G. LASH

Department of Geosciences
State University College
Fredonia, NY 14063 USA

and

DAVID R. BLOOD

Chesapeake Appalachia L.L.C.
Charleston, WV

INTRODUCTION

Organic-rich, low permeability, sometimes fractured, shale deposits, once ignored by drillers seeking more readily understood plays and faster returns on their investments, are boosting the fortunes of midsized producers across the United States and becoming an increasingly important resource base. This burgeoning interest is driven largely by increased natural gas prices, improved completion technologies and a lack of conventional reservoir targets. However, there is no universal model applicable to each and every unconventional or continuous-type reservoir. Indeed, most vary in terms of basic stratigraphic facies distribution, mineralogy (i.e., quartz content and clay type and content), fracture parameters (length, orthogonal spacing, connectivity, anisotropy), porosity and permeability, and rock mechanical properties. There clearly is a need to further our understanding of these economically important deposits. This fieldtrip focuses on the evolution of the heavily fractured Upper Devonian Rhinestreet black shale, which has served not only as a hydrocarbon source rock, but also as its own seal and reservoir, the essence of the unconventional reservoir. Specifically, we address the Rhinestreet shale in terms of the hydrocarbon system, which comprises three basic elements (Demaison and Huizinga, 1994). The first component, *charge*, is the hydrocarbon volume available for entrapment and is dependent upon source rock richness and volume. *Migration*, the second parameter, can be thought of in terms of the lateral movement of hydrocarbons via permeable carrier beds versus vertical migration via faults and, more to the point of the Rhinestreet shale, fractures. The final component of the petroleum system is *entrapment*, which involves consideration of those rock properties that would favor the arrest of migrating hydrocarbons.

We will consider the Rhinestreet shale from deposition through early diagenesis, including mechanical compaction, followed by the early and relatively shallow generation of abnormally high pore fluid pressures caused by a marked increase in sedimentation rate at the end of the Devonian. Soon after this, at the onset of the Alleghanian orogeny, the Appalachian Basin of western New York state and western Pennsylvania was uplifted resulting in the initial phase of fracturing in the Rhinestreet shale. This was followed by rapid burial of the organic-rich rocks to the oil window and the generation of natural hydraulic fractures (joints) in response to catagenesis. Indeed, the jointing history of these rocks provides a record of the complex overpressure history of the Rhinestreet shale and other black shale units of the western New York state region of the basin.

Results reported herein represent the record of six years of work on the Upper Devonian shale-dominated succession exposed along the Lake Erie shoreline and general vicinity, the Lake Erie District (LED). This work is now being extended into the subsurface of western New York state, northwest

Pennsylvania, and northeast Ohio by use of wireline logs. During his involvement in the study of the Rhinestreet shale, DRB was supported by two SUNY Fredonia Summer Undergraduate Research Fellowships. Most recently, his work, which constitutes the better part of his MS thesis at the University of Buffalo, was supported by an AAPG grant-in-aid. We acknowledge Peter Bush and his staff at the University of Buffalo, South Campus Instrumentation Center, School of Dental Medicine, for their unflagging help with the electron microscopy, Ross Giese and Anja Dosen, University of Buffalo, for the XRD analyses, and Taury Smith, Rich Nyahay, and James Sandor of the Reservoir Characterization Group at The New York State Museum, Albany, New York. Finally, we thank Terry Engelder for many fruitful discussions on compaction, jointing, the geology of the Catskill Delta Complex, and more in the field, over the phone, and via E-mail.

GENERAL STRATIGRAPHY OF THE RHINESTREET SHALE

The Upper Devonian (Frasnian) Rhinestreet shale, West Falls Group, is best exposed along Eighteenmile Creek in northern Erie County, western New York state, where it comprises ~54 m of heavily jointed, finely laminated organic-rich grayish-black to medium-dark-gray (herein referred to as black) shale (~ 85% of the unit in this area), thin (2-3 m-thick) intervals of greenish-gray, dark-greenish-gray, and medium gray shale, thin black shale beds, discontinuous concretionary carbonate layers, the so-called "scraggy layers" of Luther (1903), several horizons of ellipsoidal carbonate concretions, and rare thin siltstone beds (Fig. 1). The Rhinestreet is underlain by the Cashaqua shale, the contact being abrupt and easily recognized in the field. The upper 2.75 m of the Cashaqua shale is composed of brownish-black to olive-gray finely laminated shale. Below this, the Cashaqua comprises dark-greenish-gray shale and discontinuous diagenetic carbonate horizons (Fig. 1). The top of the Rhinestreet is transitional into the overlying Angola gray shale and marked by an interval of interbedded black and gray shale (Fig. 1). We follow Luther (1903) and Pepper et al. (1956) in placing the upper contact of the Rhinestreet shale at the base of the upper scraggy layer (Fig. 1), a horizon readily recognized in the field and even on wireline logs as discussed below.

The Rhinestreet shale was named for exposures of black shale near Rhinestreet Road at Naples, Ontario County, New York (Clarke, 1903). However, the Rhinestreet shale at its type locality is markedly different from that of Erie County where black shale comprises more than 80% of the unit. Indeed, black shale is found only in the lower part of the Rhinestreet shale in Ontario County (Pepper et al., 1956). Recently, Lash (2006a) demonstrated a rapid eastward reduction in the thickness of the black shale interval (based on gamma-ray and bulk density wireline logs) of the Rhinestreet shale in the subsurface in eastern Allegany County, New York (Fig. 2). It is tempting to attribute this abrupt facies change to penecontemporaneous movement on the Clarendon-Linden Fault System, the trace of which trends ~ north-south in eastern Cattaraugus County (CLF; Chadwick, 1920; Jacobi, 2002) (Fig. 2). If this fault were active during Rhinestreet sedimentation, and relative offset was down-to-the-east, then the rapid eastward reduction in organic rich-sediment at the expense of organic-lean shale and siltstone (e.g., Pepper et al., 1956) may reflect the existence of a hinge that ponded more clastic-rich deposits to the east (hinge position 2, Fig. 3). Such a scenario accords with the interpretation of Jacobi and Fountain (1993) who suggested that during accumulation of the Genesee Group, the axis or hinge of the foreland basin lay to the east of the CLF (hinge position 1, Fig. 3) whereas by Dunkirk shale time, the basin axis had migrated to the west of the CLF (hinge position 3, Fig. 3). This intriguing question awaits further study of the Rhinestreet shale in the subsurface.

The Rhinestreet shale is one of several black shale units that comprise part of the Upper Devonian succession of the western New York state region of the Appalachian Basin (Fig. 3). Each organic-rich unit occupies the basal interval of an unconformity-bound sequence and is conformably overlain by organic-lean gray shale and siltstone (Fig. 3). Accumulation of black shale records the episodic cratonward advance of the Acadian fold and thrust load accompanied by rapid subsidence of the basin and deposition of clastic-starved, carbonaceous sediment (Ettensohn, 1985, 1987, 1992). Overlying organic-lean shale and siltstone reflects tectonic relaxation, establishment of terrestrial drainage systems and delta progradation (Ettensohn, 1985, 1992). Nevertheless, the correlation of some black shales with global marine transgressions suggests that eustatic oscillations and/or fluctuations, too, may have played a role in the accumulation of Upper Devonian black shale in the Appalachian Basin (Johnson et al., 1985; Algeo et al.,

1995; Brett and Baird, 1996; Werne et al., 2002). Indeed, the two gray shale intervals within the Rhinestreet shale (Fig. 1) that reflect sedimentation in somewhat more oxygenated, and perhaps shallower, water than the black shale, are probably elements of fourth-order progradational/retrogradational marine cycles of glacio-eustatic origin like those recognized in late Frasnian deposits throughout much of the Appalachian Basin (Filer, 2002).

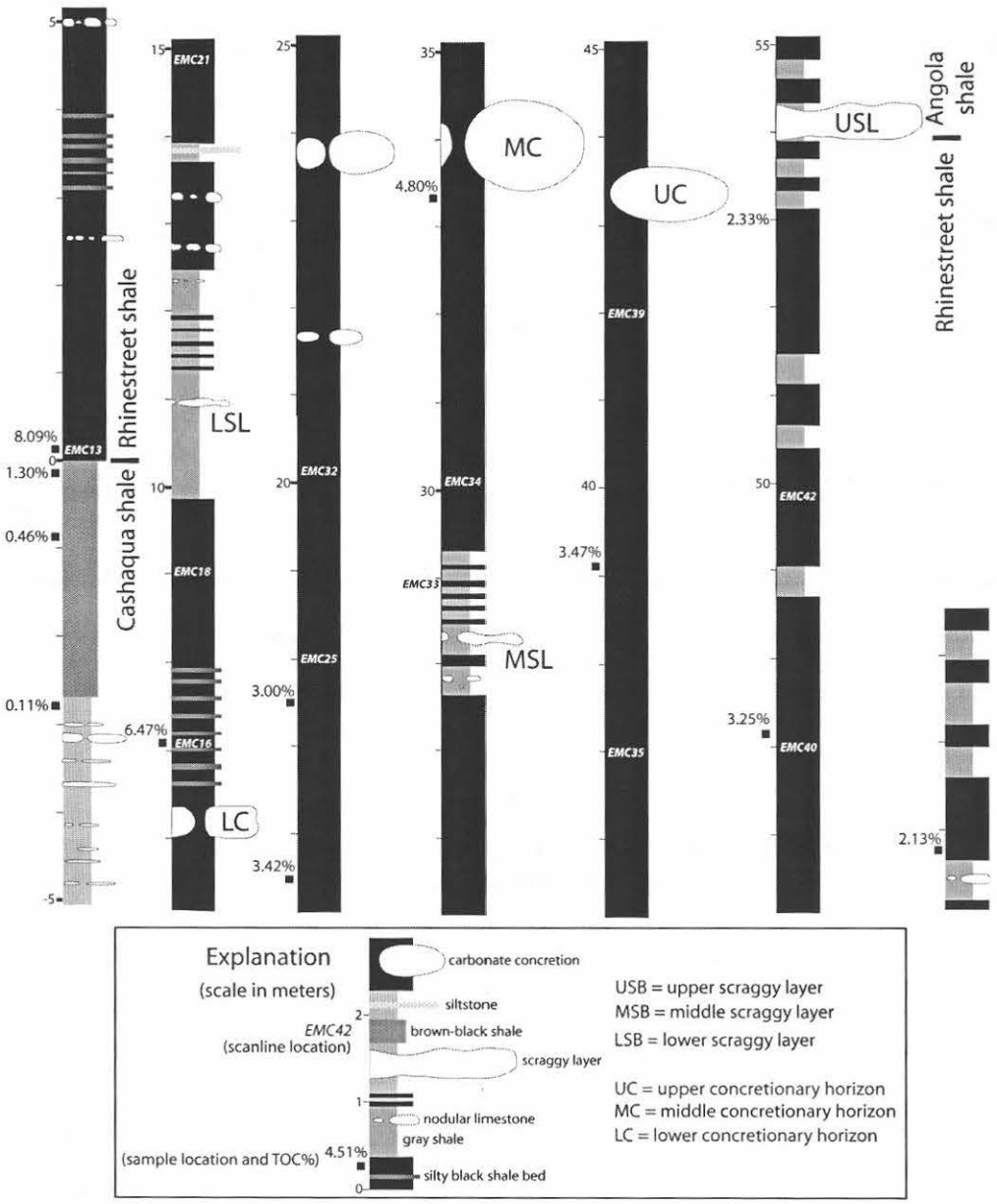

Fig. 1: Stratigraphic log of the Rhinestreet shale, Eighteenmile Creek.

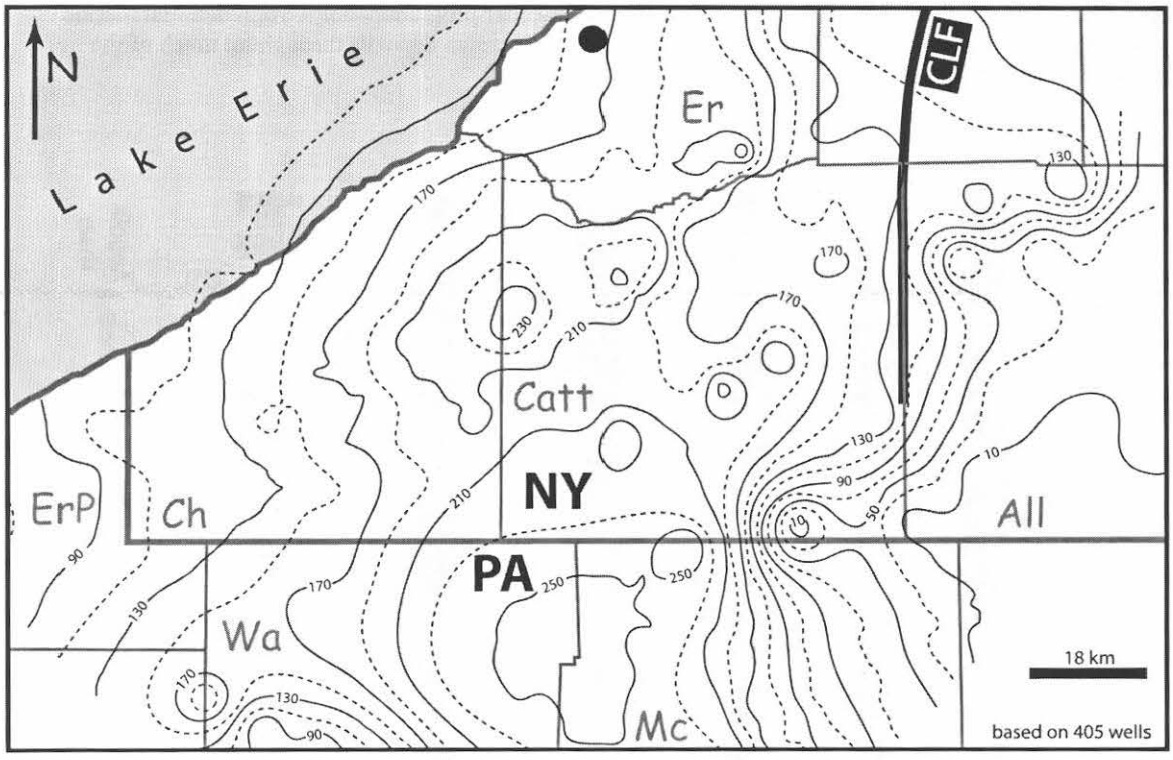

Fig. 2: Isopach map of the Rhinestreet shale in western New York state and northwest Pennsylvania showing the trace of the Clarendon-Linden Fault System (CLF). The thickness of the Rhinestreet shale is based on estimated TOC (Lash, 2006a). Contours in feet; filled circle marks the location of the Eighteenmile Creek measured section. New York state counties: Ch = Chautauqua; Catt = Cattaraugus; All = Allegany; Er = Erie. Pennsylvania counties: ErP = Erie; Wa = Warren; Mc = McKean.

RESERVOIR AND SOURCE ROCK CHARACTERISTICS AND BURIAL/THERMAL HISTORY

There is little doubt that the Rhinestreet shale of the Chautauqua-Cattaraugus-Erie counties region of western New York state and to the south into Pennsylvania has the makings of a quality source and reservoir rock. X-ray diffraction (XRD) analysis of three samples each of the Rhinestreet and Casahqua shales reveals noteworthy mineralogic differences. The Rhinestreet samples contain more quartz (Fig. 4), including non-detrital (i.e., lack of sharp edges) grains recognized in thin section and scanning electron microscopic (SEM) analysis. Clay minerals comprise a greater proportion of the Cashaqua samples than they do the Rhinestreet samples (Fig. 4). Illite is by far the dominant clay mineral in samples of both units, followed by chlorite and kaolinite. However, based on other thermal indicators, including vitrinite reflectance and Rock-Eval parameters, we suggest that the bulk of the illite is more a reflection of a low-grade metamorphic source terrane than a high level of thermal stress sustained by the Rhinestreet and Cashaqua shale samples (e.g., Lash, 2006b). Chlorite is consistently more abundant than kaolinite in Cashaqua shale samples; the reverse is the case for the Rhinestreet samples. Feldspar (microcline and plagioclase) averages 5.8% (±0.6%) in the Rhinestreet samples and 2.9% (±0.3%) in analyzed Cashaqua shale samples. Calcite, dolomite, and siderite, in decreasing order of abundance, are present in variable amounts in the Rhinestreet (0.9 – 2.2%) and Cashaqua (1.9 – 5.2%) shales. Indeed, gray shale of the LED, including the Cashaqua and Angola shales, typically contain more calcite in the form of cement

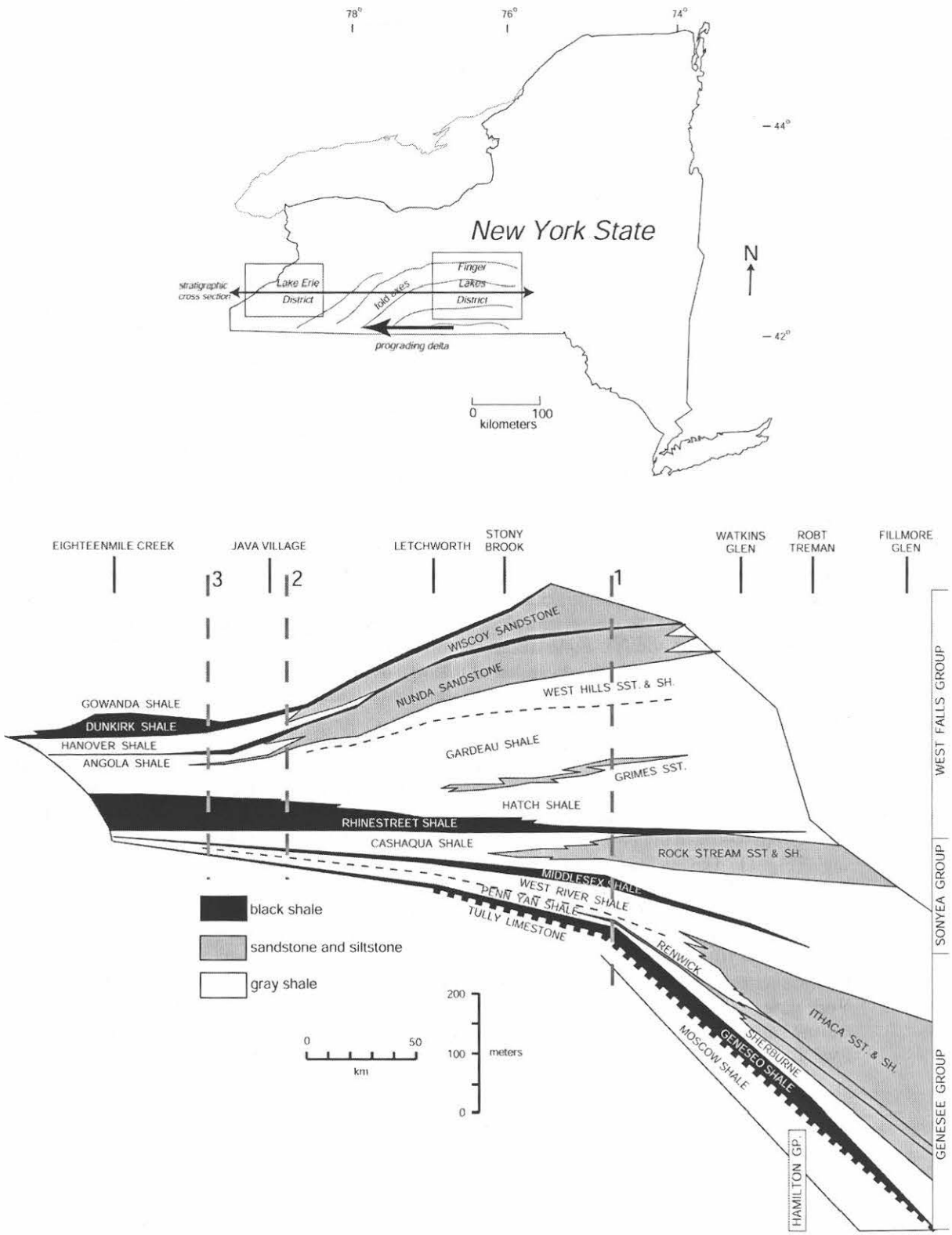

Fig. 3: Location map of the Lake Erie and Finger Lakes districts and a generalized east-west stratigraphic cross-section through the Catskill Delta Complex (modified after Woodrow et al., 1988) showing inferred positions of basin hinges.

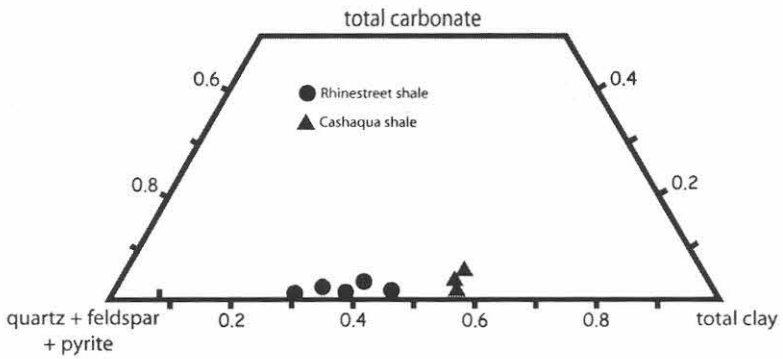

Fig. 4: Compositional plots for Rhinestreet and Cashaqua shale samples examined in this study.

(occasionally > 25%) than organic-rich shale, perhaps a reflection of the higher pre-lithification porosity of the former (Lash, 2006b).

Reservoir characteristics of the Rhinestreet and Cashaqua shales were investigated by mercury injection capillary pressure (MICP) measurements made on those samples analyzed by XRD. Samples were prepared so that pressure measurements were made perpendicular to bedding. Capillary entry measurements (10% saturation levels) for both sets of samples are quite high; however, the Rhinestreet entry pressures (~10,007 psia) are more than five times those of the Cashaqua shale samples (~1,800 psia) (Fig. 5). The calculated porosity of the Rhinestreet shale is 3.9% (±0.9%), less than one-half that of the Cashaqua shale (8.5% ±1.2%). MICP measurements indicate that the Rhinestreet shale is two orders of magnitude less permeable than the Cashaqua shale (10^{-20} m^2 vs. 10^{-18} m^2, respectively), which seems at odds with the generally coarser grained nature of the former. This likely reflects the very small average pore throat diameter of the Rhinestreet shale (8 nm) as opposed to that of the Cashaqua shale samples (19.2 nm). There are three possible explanations for this: (1) the strongly oriented planar microfabric of the black shale (see below), (2) the generation of bitumen during catagenesis of the Rhinestreet shale that clogged pore throats; and (3) the squeezing of abundant ductile organic matter in the Rhinestreet shale into void spaces (e.g., Lash, 2006b).

Total organic carbon (TOC) content of the Rhinestreet shale at its base along the Eighteenmile Creek section is 8.09%, diminishing irregularly upward to 2.3 % at its contact with the Angola shale (Fig. 1). TOC in the Cashaqua shale typically is less than 0.5%; however, TOC in the 2.75 m-thick brownish-black laminated shale interval at the top of the Cashaqua shale immediately beneath the Rhinestreet shale varies from 0.46% at the bottom of this interval to 1.3% at its top, 13 cm below the base of the Rhinestreet shale (Fig. 1). TOC in the Cashaqua gray-green shale 17 cm below its contact with the brownish-black interval is 0.11%, a value more typical of the Cashaqua shale (Fig. 1). Organic matter in the Rhinestreet shale consists principally of unstructured lipids (proprietary data); however, algal remains have been recognized in thin section and SEM analysis. The organic matter of the Rhinestreet is a combination of Type II/Type III oil and gas prone material (Fig. 6). The measured vitrinite reflectance, $\%R_o$, of Rhinestreet shale samples collected from both field exposures and gas well cuttings from western New York state range from 0.52% to 0.77% (Fig. 7). The bulk of the samples fall within the oil window for marine kerogen ($\%R_o$ > 0.6%; Tissot and Welte, 1984; Espitalie, 1986), as suggested by the plot of Rock-Eval T_{max} vs. hydrogen index (HI) as well as calculated production index values (Fig. 8).

The EASY$\%R_o$ kinetic model of vitrinite reflectance (Sweeney and Burnham, 1990) was used to model the burial/thermal history of the Rhinestreet black shale. This algorithm requires knowledge of (1) the age(s) of the unit(s) of interest (the base of the Rhinestreet shale), (2) at least a partial thickness of the local stratigraphic sequence, and (3) the measured vitrinite reflectance of the unit(s) of interest (average vitrinite reflectance of the base of the Rhinestreet shale = 0.74%). We estimate that the Cashaqua shale in the western New York state area was overlain by as much as 1,155 m of Devonian strata (Lindberg, 1985) and that the age of the base of the Rhinestreet shale can be dated by the Belpre ash bed at ~ 381 Ma (Kaufmann, 2006). Finally, our model assumes a geothermal gradient of 30° C km^{-1} and a 20° C seabed temperature (e.g., Gerlach and Cercone, 1993). We will make reference to the burial/thermal model of the Rhinestreet shale (Fig. 9) throughout the text. However, in light of the fact that vitrinite reflectance suppression has been recognized in Devonian black shales (e.g., Rimmer and Cantrell, 1988; Rimmer et al., 1993; Nuccio and Hatch, 1996; Rowan et al., 2004), including those from northwest Pennsylvania and

western New York state (see Stop 2 discussion), we caution that the estimated 3.1 km maximum burial depth of the Rhinestreet shale (Fig. 9) should be viewed as a minimum maximum burial depth.

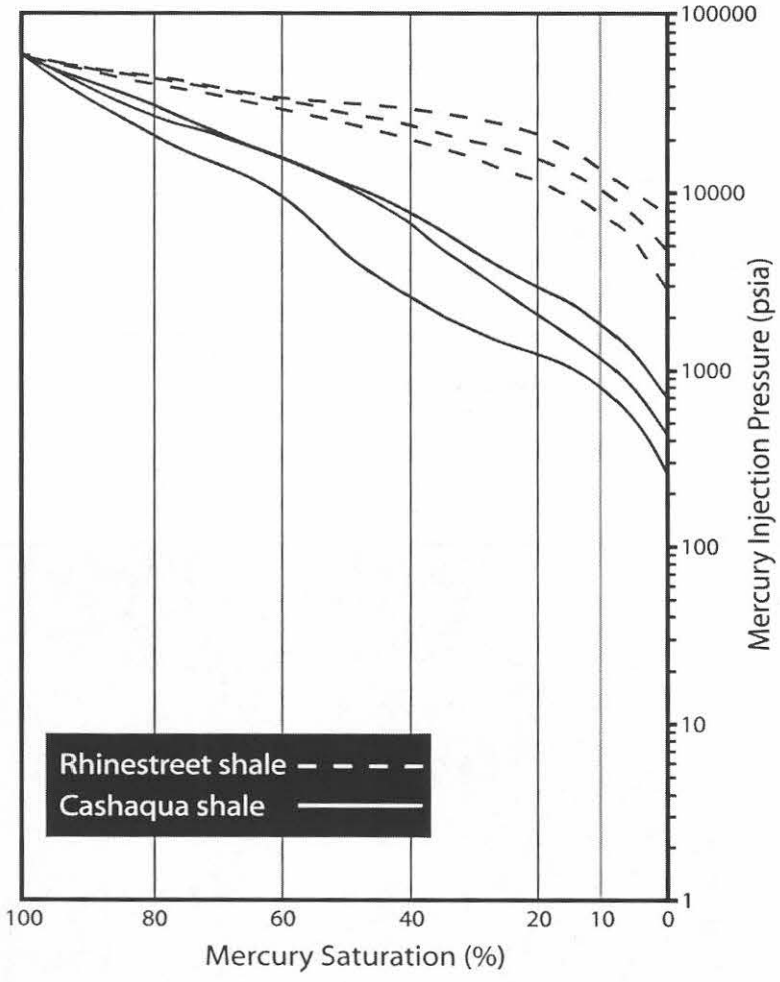

Fig. 5: Mercury injection capillary pressure curves for Rhinestreet and Cashaqua shale samples. Note the line denoting the 10% mercury saturation pressure (a proxy for saturation; see Lash, 2006b).

EARLY COMPACTION AND DIAGENESIS OF THE RHINESTREET SHALE

Mechanical Compaction

The important part that gravitational pressure plays in the progressive consolidation of mud and clay has been recognized for well over fifty years (Hedberg 1926, 1936) and perhaps longer (Sorby 1908). More recent studies (e.g., Heling 1970; Bennett et al. 1977, 1981; Faas and Crocket 1983; O'Brien and Slatt 1990; O'Brien 1995) have presented compelling evidence for the early diagenetic development of a strongly oriented particle orientation in response to burial-related compaction of high-porosity, water-rich flocculated clay. However, other studies have demonstrated that the strongly planar microfabric observed in some shales can form during progressive illitization of smectite by dissolution and re-precipitation under an anistropic stress field (Ho et al., 1999; Charpentier et al., 2003; Aplin et al., 2003).

Carbonate concretions hosted by the Rhinestreet shale provide the opportunity to study pre- and post-compaction clay fabrics of the encapsulating carbonaceous shale. Recently, we (Lash and Blood, 2004a) presented results of an SEM analysis of microfabric variations observed in Rhinestreet black shale samples collected from around early diagenetic carbonate concretions. Crucial to this was establishing that the internally laminated compaction-resistant concretions formed rapidly and, most importantly, close to the sediment-water interface. Field observations, including the wrapping of shale around concretions (Fig.

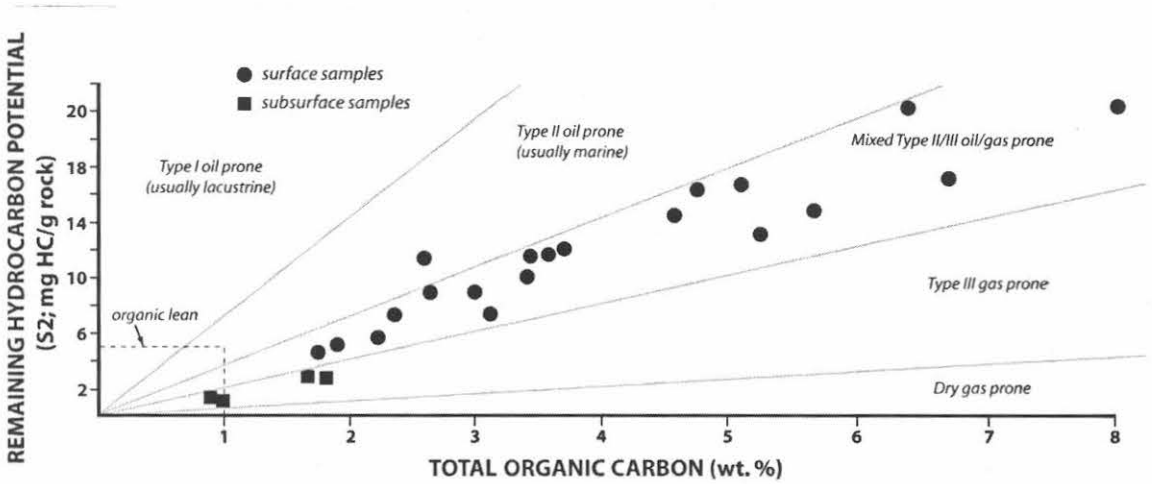

Fig. 6: Plot of TOC vs. Rock-Eval hydrogen index (HI) for Rhinestreet shale samples.

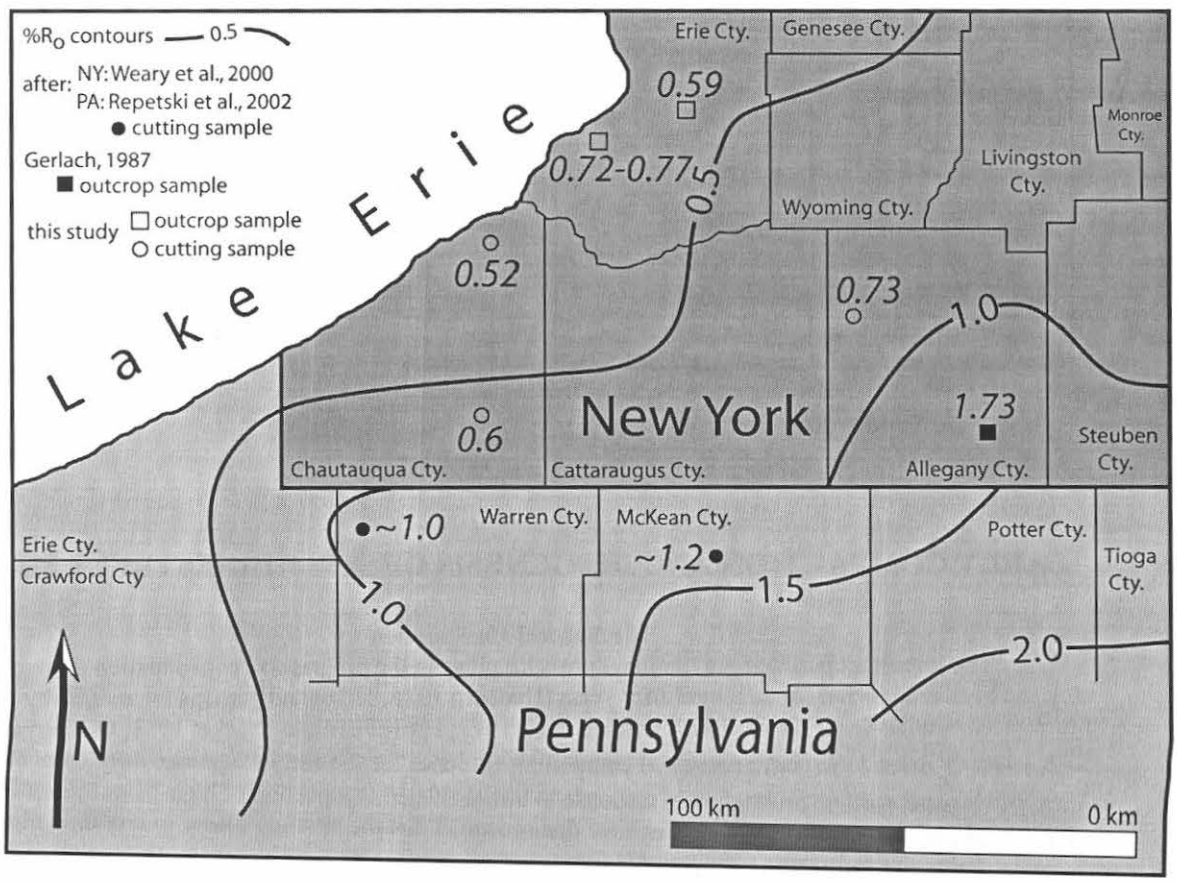

Fig. 7: Map of western New York state and northwest Pennsylvania showing thermal maturity data collected in this study and previous studies of Upper Devonian black shale.

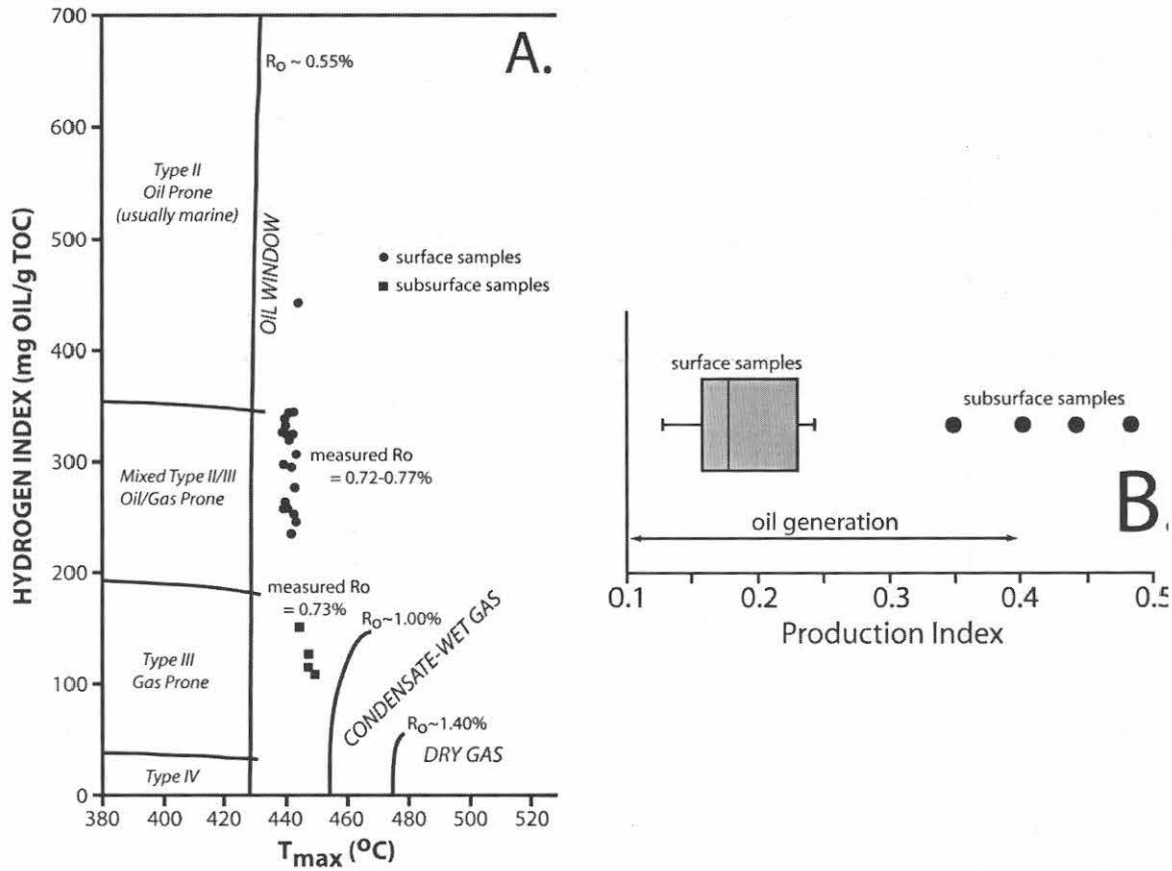

Fig. 8: (A) Van Krevelen plot of HI versus Rock-Eval T_{max} for the Rhinestreet shale samples; (B) box and whisker plot showing the range of production index (Rock-Eval S1/S1+S2) values for the Rhinestreet shale samples.

10A), the lack of center-to-edge deviation in laminae thickness (Fig. 10B), and the tilting of some concretions (Fig. 10C), demonstrate that the concretions formed rapidly at shallow burial depths, perhaps a meter or so below the seafloor (Lash and Blood, 2004a,b). A shallow depth of concretion growth is further suggested by estimates of host sediment porosity based on the assumption, addressed in more detail below, that carbonate cement precipitated passively within the water-filled pore space of the organic-rich clay (e.g., Lippmann 1955; Raiswell 1971; Gautier 1982). Accordingly, the volume percent of carbonate cement in the concretion matrix is a proxy for the porosity of the host sediment at the time of concretion growth (Raiswell 1971). Volume percent of 21 Rhinestreet concretion matrix samples collected from four concretions varies from 74 to 93% (mean = 83%), a range that encompasses the high end of porosity of modern marine clay deposits near the sediment-water interface (e.g., Müller 1967; Velde 1996). In summary, carbonate concretions of the Rhinestreet shale formed at very shallow depth, perhaps within a meter of the sea floor, by rapid, near-uniform, precipitation of diagenetic carbonate in void spaces of the host carbonaceous sediment (see Lash and Blood, 2004a,b for details). The shallow burial depth and rapid rate of growth of Rhinestreet concretions will allow us to use the thickness of layers within concretions (Fig. 10B) as a proxy for the original seafloor thickness of the carbonaceous mud layers immediately prior to, and coeval with, carbonate precipitation (e.g., Raiswell, 1971; Oertel and Curtis, 1972).

Our approach to defining the precompaction microfabric of the Rhinestreet black shale reflects the low compressibility of concretions relative to surrounding unconsolidated clay. The ellipsoidal concretions affected the local compaction-related elastic stress field such that sediment immediately adjacent to lateral edges of concretions - the concretion strain shadow - was shielded from overburden stress. The shielding effect of carbonate concretions in the Rhinestreet shale is obvious at the macroscopic scale. Argillaceous rock within strain shadows is not fissile (Fig. 11, see "ss") and is properly classified as mudstone (Pettijohn 1975). However, these *same* mudstones become fissile less than 30 cm distant the strain shadows, necessitating their reclassification as shale (Fig. 11, see "sh"; Pettijohn 1975). These observations alone

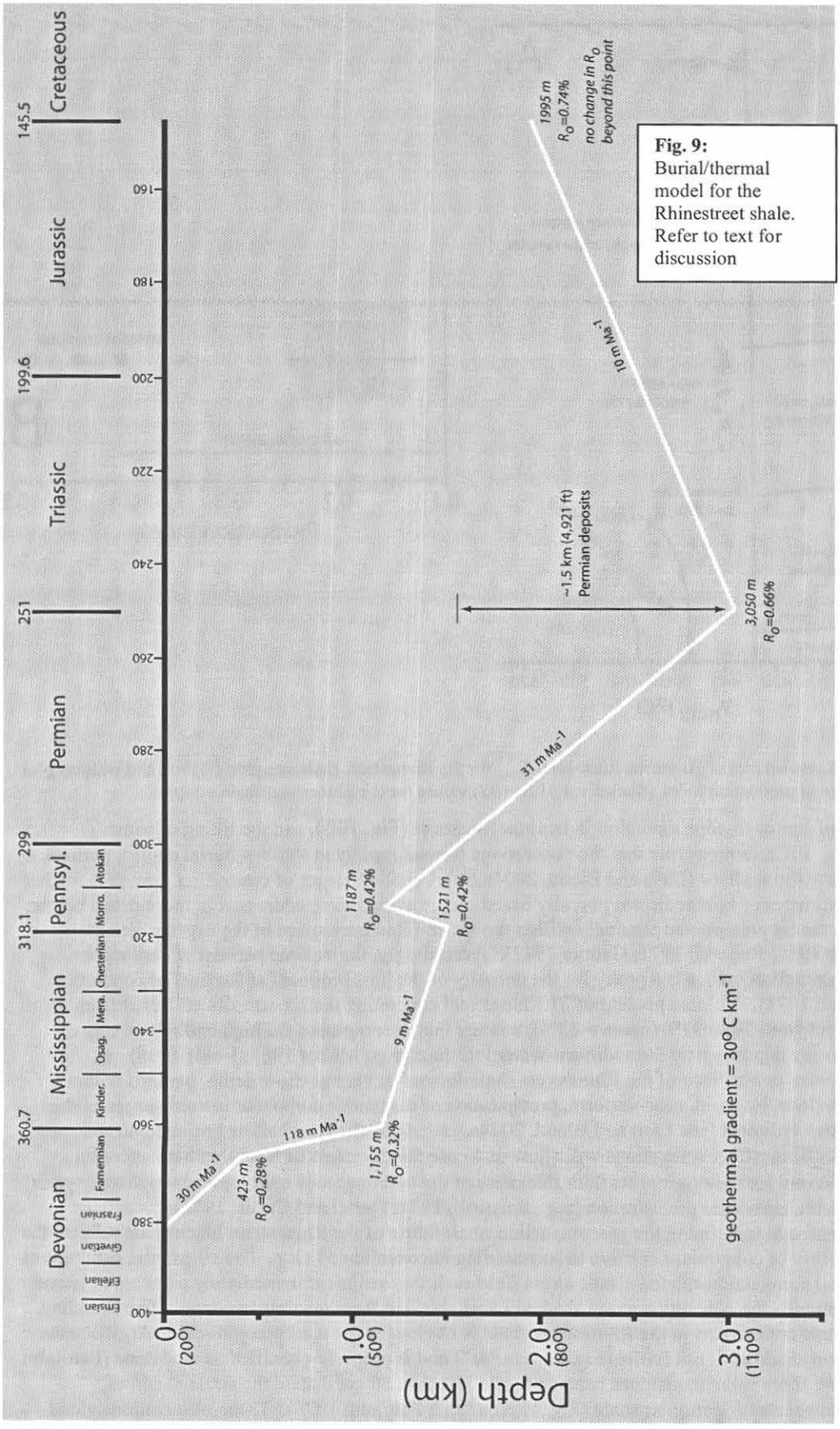

Fig. 9: Burial/thermal model for the Rhinestreet shale. Refer to text for discussion

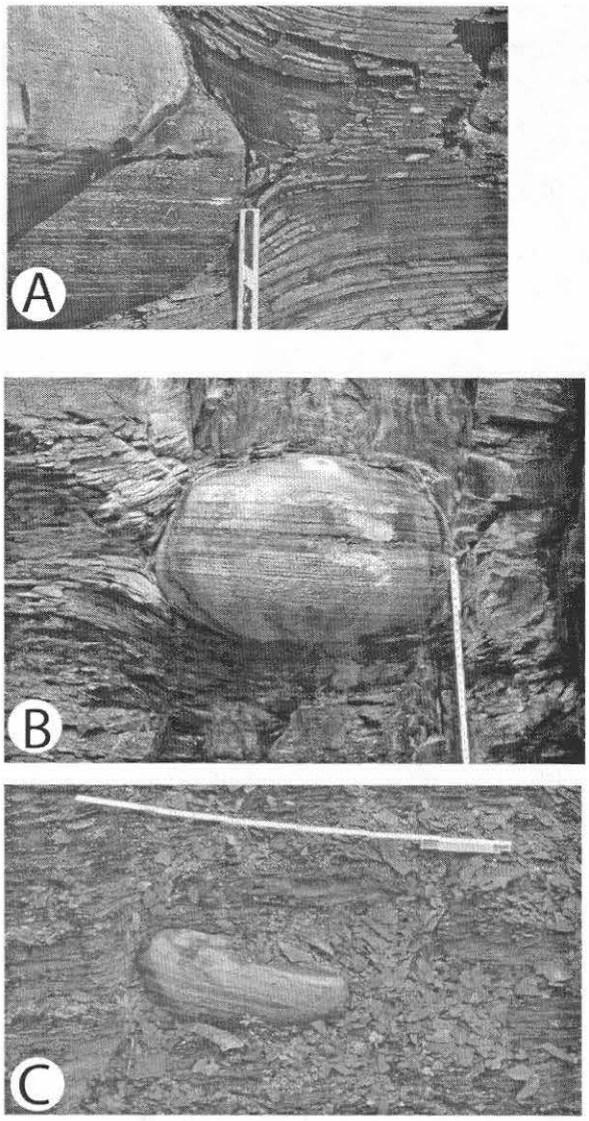

Fig. 10: Carbonate concretions of the Rhinestreet shale:: (A) close-up of differential compaction (note internal laminae); (B) internally laminated concretion; (C) tilted concretion (rule = 1 m).

suggest that the fissility was induced by mechanical compaction and that mudstone within the strain shadows preserves a physical record of the depositional (i.e., pre-mechanical compaction) fabric.

SEM analysis of mudstone samples collected from concretion strain shadows reveals an open fabric of randomly oriented platy particles, which higher magnification proves to be face-to-face clay flake stacks or domains (Fig. 12A). Domains typically are arranged in a low-density network or cardhouse fabric of edge-to-edge and edge-to-face contacts marked by large voids relative to the thickness of clay flakes and domains (Fig. 12B). Secondary electron images of fissile shale samples collected 20 to 30 cm from strain shadows, however, reveal a generally low-porosity microfabric marked by a moderately to strongly preferred orientation of clay flake domains (Fig. 12C). The almost negligible degree of compaction sustained by strain shadow mudstone confirms that gravitational compaction of the Rhinestreet shale was minimal until *after* carbonate concretions had become incompressible thereby affirming the shallow diagenetic origin of the concretions (Lash and Blood, 2004a). Moreover, SEM observations of concretion samples evince an open cardhouse arrangement of detrital clay grains typical of newly deposited flocculated clayey sediment preserved by precipitation of carbonate cement (Fig. 12D; Lash and Blood, 2004b).

The foregoing discussion suggests that the Rhinestreet black shale accumulated in dysoxic to anoxic bottom water as flocculated carbonaceous sediment that underwent rapid gravitational mechanical compaction resulting in the observed strongly anisotropic planar microfabric. Nevertheless, the possible role of chemical dissolution and re-precipitation in producing the planar microfabric documented from the Upper Devonian black shale deposits of the LED cannot be dismissed out of hand. Clues to this question can be gained by microfabric analysis of samples collected from gray shale intervals within the Rhinestreet shale (Fig. 1). Thin section and SEM analysis of these deposits confirms what appear to be the effects of pervasive bioturbation judging from field observations, including the lack of well-defined bedding planes. Notably, the microfabric of the gray shale typically is characterized by an irregular distribution of silt grains throughout a mottled clay matrix (Fig. 13A), the result of bioturbation that homogenized the sediment by mixing silt grains with the clay (e.g., O'Brien and Slatt 1990; Bennett et al. 1991). SEM observations reveal an open microfabric of variably oriented platy grains, many of which appear to be individual clay grains (Fig. 13B). Angular silt grains dispersed throughout the "swirled" clay matrix by bioturbation propped open larger voids during compaction precluding complete reorientation of the disrupted fabric (Fig. 13C). It is obvious that these deposits lack the strongly anisotropic microfabric of the immediately under- and over-lying organic-rich deposits.

We believe that the Rhinestreet gray shale deposits would have acquired a strongly planar microfabric had they had been buried deep enough for illitization kinetics to initiate. Charpentier et al. (2003) point out that this transition in the deepwater Gulf of Mexico sedimentary column occurs at ~5,600

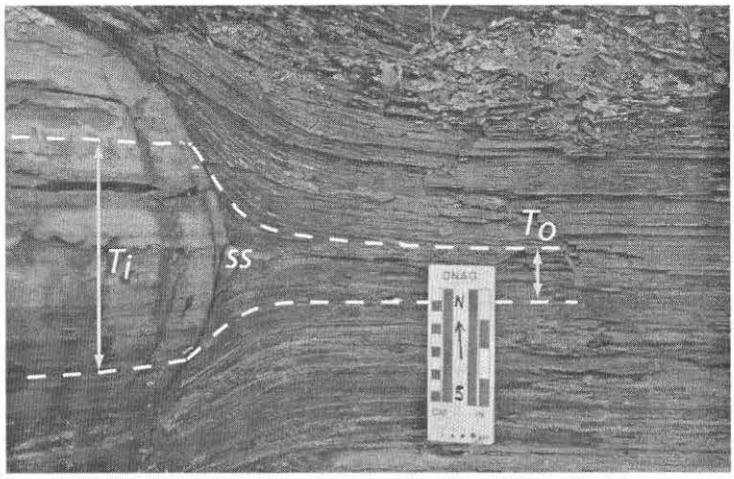

Fig. 11: Rhinestreet shale carbonate concretion and host shale showing elements that were measured for compaction strain analysis. T_i is the thickness of the measured bedding interval within the concretion (the depositional thickness); T_o is the thickness of the measured interval traced into the encapsulating black shale (the compacted interval); ***ss*** is the strain shadow of the concretion (it is here that the incompressible concretion perturbed the local compaction-related elastic stress field so that the sediment was shielded from overburden stress; Lash and Blood, 2004a). The calculated compaction strain of the Rhinestreet shale at this location is -0.56 (56%). The relative thicknesses of T_i and T_o are distorted because the concretion projects ~ 20 cm from the exposure toward the viewer.

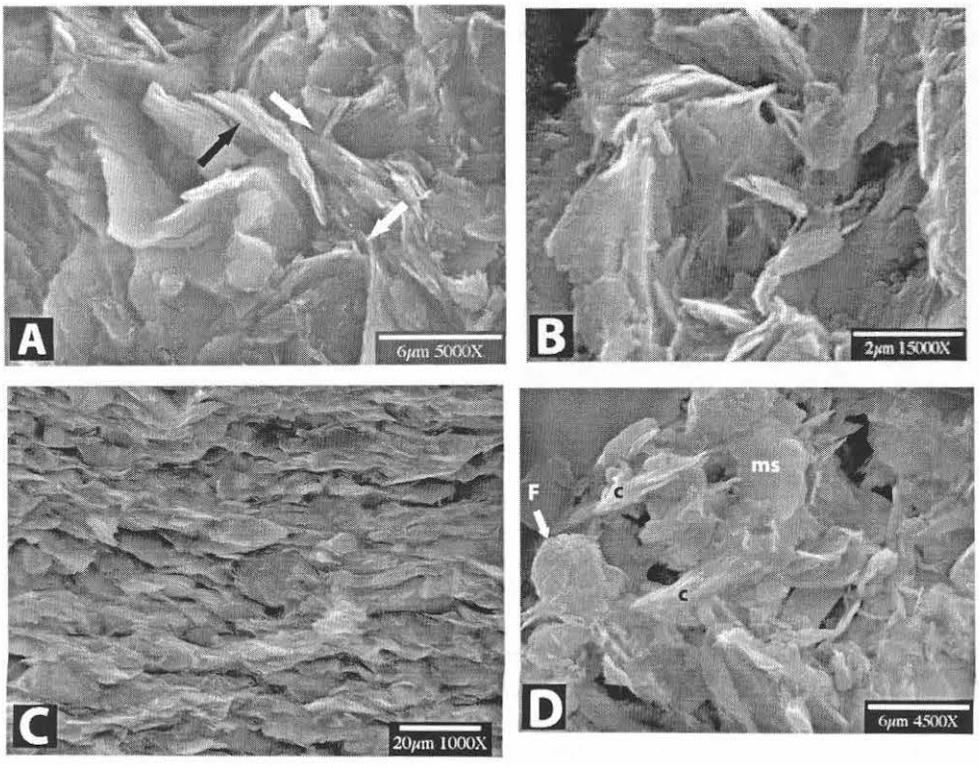

Fig. 12: Secondary electron images of Rhinestreet shale and concretion samples: (A) detail of clay domains and mudstone microfabric. Note face-to-face clay domains (black arrows) and edge-to-edge and edge-to-face domain contacts (white arrows); (B) detail of edge-to-edge domain contacts that define the cardhouse clay fabric. The porous nature of this fabric compares favorably with that of modern flocculated clay; (C) strongly planar (shale) fabric; (D) view of open framework of Rhinestreet carbonate concretions showing a framboid (**F**), randomly oriented clay grain domains (**c**), and microsparite (**ms**).

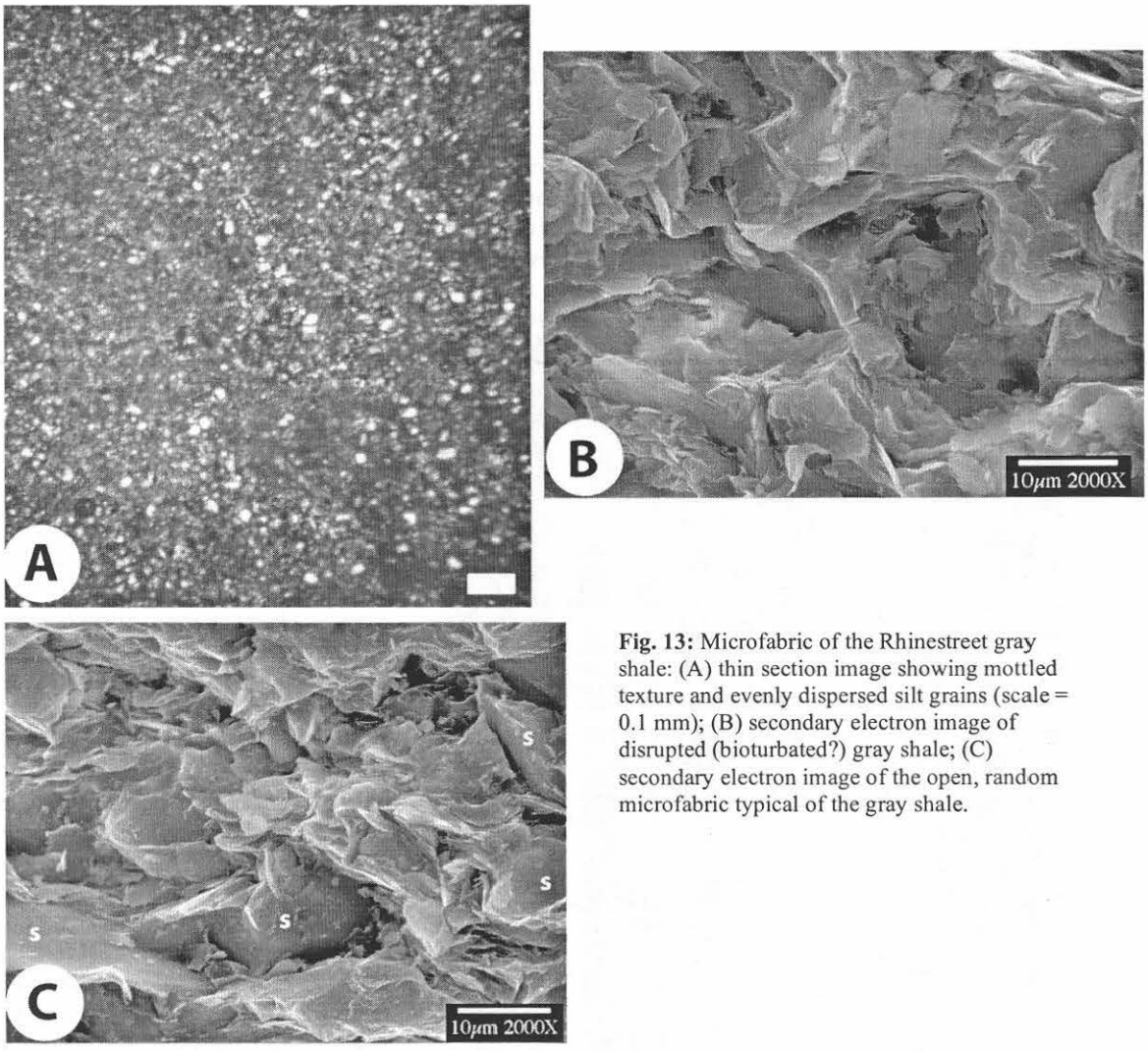

Fig. 13: Microfabric of the Rhinestreet gray shale: (A) thin section image showing mottled texture and evenly dispersed silt grains (scale = 0.1 mm); (B) secondary electron image of disrupted (bioturbated?) gray shale; (C) secondary electron image of the open, random microfabric typical of the gray shale.

m, well in excess of the modeled maximum burial of the Rhinestreet shale. However, Pearson and Small (1988), in their analysis of clay mineral diagenesis in North Sea deposits, demonstrated that illitization occurs at depths of 2.4 to 3.5 km, within a vitrinite reflectance range of 0.54 and 0.72% and a temperature range of 87 to 100° C, placing the Rhinestreet shale within this zone. As described above, illite is by far the most common clay mineral in analyzed Rhinestreet shale samples, and most Devonian shale samples of the Appalachian Basin for that matter (Hosterman, 1993). However, rather than reflecting a high degree of thermal maturation, the plentiful illite probably tells of a source terrane rich in illite. Strickler and Ferrell (1989), for example, argued that the great abundance of illite in Louisiana Gulf Coast clays reflects derivation from the Appalachian orogen. Moreover, the location of the Rhinestreet shale in the LED, a region of very low illite crystallinity (Hosterman, 1993), is consistent with some of the low $\%R_o$ values measured in samples of Upper Devonian black shale collected from along the Lake Erie shoreline (see Fig. 7). It is difficult at best to envision the development of the strongly aligned microfabric of Rhinestreet black shale samples as a consequence of the smectite-illite transition while not seeing any evidence for this phenomenon in Rhinestreet gray shale samples. We suggest, instead, that the gray shale retained its relatively open fabric because the Rhinestreet was not buried deep enough for smectite-illite reaction kinetics to initiate. Thus, the planar microfabric of the Rhinestreet black shale was acquired rapidly and very early in the compaction history of the organic-rich clay, which, based on comparison with modern carbonaceous fine-grained sediment, was probably water-rich (e.g., Meade, 1966; Keller, 1982) and very compressible.

Carbonate Concretion Growth

Mechanical compaction is only one type of diagenetic modification of the Rhinestreet sediment; the other is the precipitation of carbonate cement in the form of concretions and the scraggy layers (Fig. 1). The majority of carbonate concretions of the Rhinestreet shale are found in three laterally persistent horizons (Fig. 1; Lash and Blood, 2004b). Most concretions are oblate ellipsoids with maximum diameters and thicknesses ranging up to 2.7 m and 1.1 m, respectively (Fig. 14A). Septarian fractures, where they can be observed, extend outward from concretion centers, narrowing to termination near the edges. Brown Fe-poor calcite lines fracture walls and is post-dated by yellow siderite. Pyrite, marked by low but uniform abundance throughout much of the interior of concretions, is concentrated along concretion carapaces as well as halos along septarian fractures. Broken and weathered concretions reveal depositional laminae inherited from the host Rhinestreet black shale that show no obvious systematic changes in thickness across concretions (Fig. 14B).

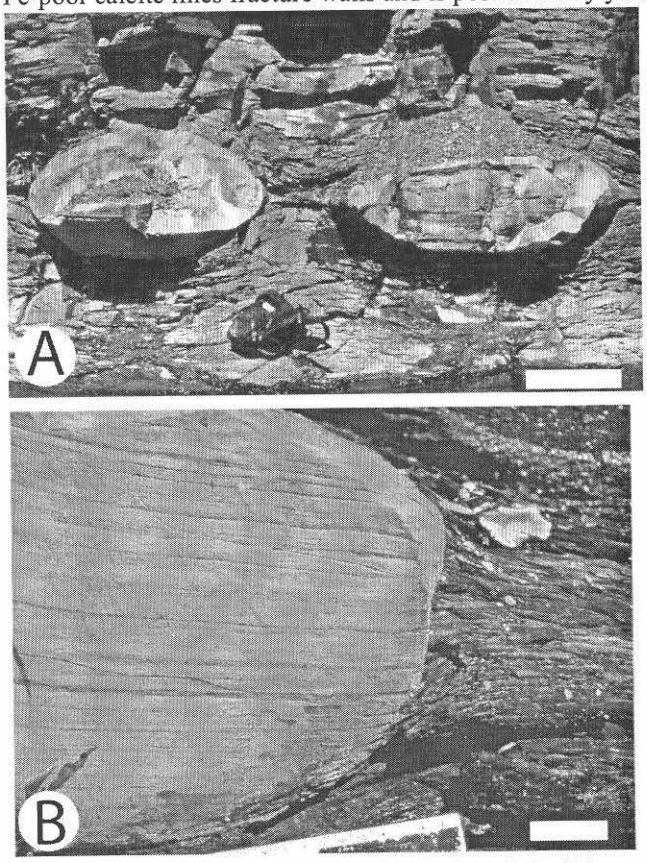

Fig. 14: Carbonate concretions of the Rhinestreet shale: (A) two of the larger ellipsoidal concretions of the middle concretion horizon (scale bar = 0.5 m); (B) carbonate concretion displaying laminae (bar = 3 cm).

The conventional explanation for the formation of carbonate concretions assumes that growth occurred concentrically by addition of successive layers of cement during burial (Oertel and Curtis, 1972; Mozley, 1996). Such a sequential growth history has been recognized by decreasing diagenetic carbonate percentage from the centers to edges of concretions reflecting progressively decreasing pore-space volume of the host sediment during concretion growth (e.g., Raiswell, 1971; Oertel and Curtis, 1972). Five studied Rhinestreet concretions show diminishing carbonate in center-to-edge traverses, the maximum reduction being 8% to a value of 74% at the edge of concretion EMC29 (Fig. 15), suggesting only a minor reduction in porosity of the host sediment during concretionary growth. One concretion (concretionUC5) is characterized by more than 90% carbonate in samples collected from the interior of the concretion whereas center and edge samples contain ~ 85% carbonate (Fig. 15). The minimal radial carbonate gradients exhibited by Rhinestreet concretions indicate that the concretions grew largely by rapid near-uniform precipitation of carbonate cement throughout the concretion body thereby confirming a similar interpretation based on the lack of center-to-edge deviation in laminae thickness (Lash and Blood, 2004b). Moreover, microscopic observations described earlier in this section indicate that concretions grew as compaction resistant frameworks of calcite micrite and microspar in porous organic-rich clay perhaps a meter or so below the seafloor (Fig. 12D; Lash and Blood, 2004b)). The open framework of the newly formed concretions provided strength yet reduced the mean density of most concretions precluding their sinking into the weak, low-density clay (e.g., Wetzel, 1992; Raiswell and Fisher, 2000).

Stable element isotopic data adds to our understanding of the diagenetic history of the Rhinestreet shale and its concretions. The range of $\delta^{13}C$ values is rather wide (-13.9 to +1.7 ‰ PDB) while that of $\delta^{18}O$ is limited (-6.8 to –3.8 ‰ PDB) (Fig. 16). Isotopic values of concretions sampled in the middle and lower

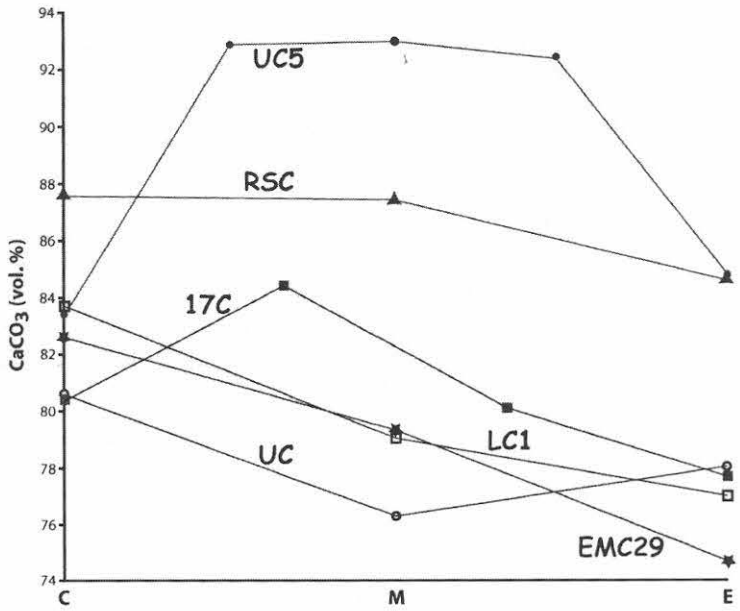

Fig. 15: Plot of diagenetic volume percent carbonate versus sample location within the concretion (C = center; M = middle; E = edge).

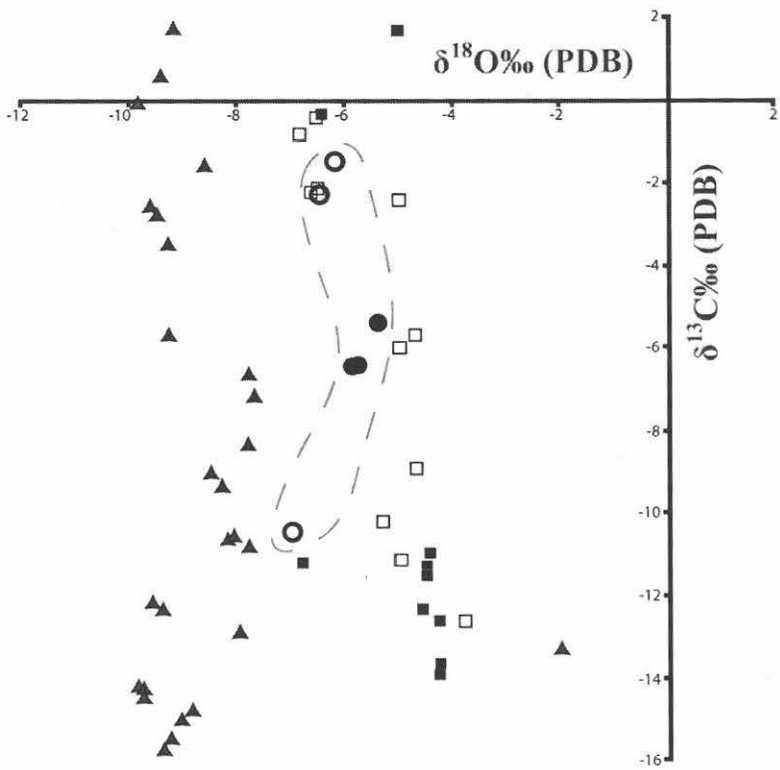

Fig. 16: $\delta^{18}O$ and $\delta^{13}C$ scatter diagram for Rhinestreet carbonate concretions (filled squares = lower concretion horizon; open squares = middle concretion horizon) and scraggy layers (filled circles = middle scraggy layer; open circles = upper scraggy layer). The plot includes the data of Dix and Mullins (1987) represented by triangles for comparison.

concretionary horizons are similar though less depleted ^{13}C values appear to be somewhat more common to concretions of the middle horizon (Fig. 16). Four of the six studied concretions show radial enrichment in ^{13}C (Fig. 17A). Nevertheless, concretion 17C displays minimal radial variation in $\delta^{13}C$, and center and edge $\delta^{13}C$ values of concretion UC5 are more enriched in $\delta^{13}C$ than samples collected from the mid-interior region of the concretion (Fig. 17A). Oxygen isotope compositions of the studied Rhinestreet concretions show minor radial variations (Fig. 17B). Four concretions display slight center-to-edge depletion in ^{18}O, and one concretion (concretion 17C) shows no change in $\delta^{18}O$. Center and edge samples collected from concretion UC5 are characterized by equally depleted $\delta^{18}O$ compositions whereas samples recovered from the interior of this concretion are less depleted (Fig. 17B). Concretions UC and EMC29 display center-to-edge enrichment in ^{13}C that is complemented by depletion in ^{18}O. However, concretions LC1 and RSC show almost identical radial increases in heavy carbon but dissimilar center-to-edge variations in $\delta^{18}O$. The significance of these seemingly random radial variations in stable element isotopes will be addressed below.

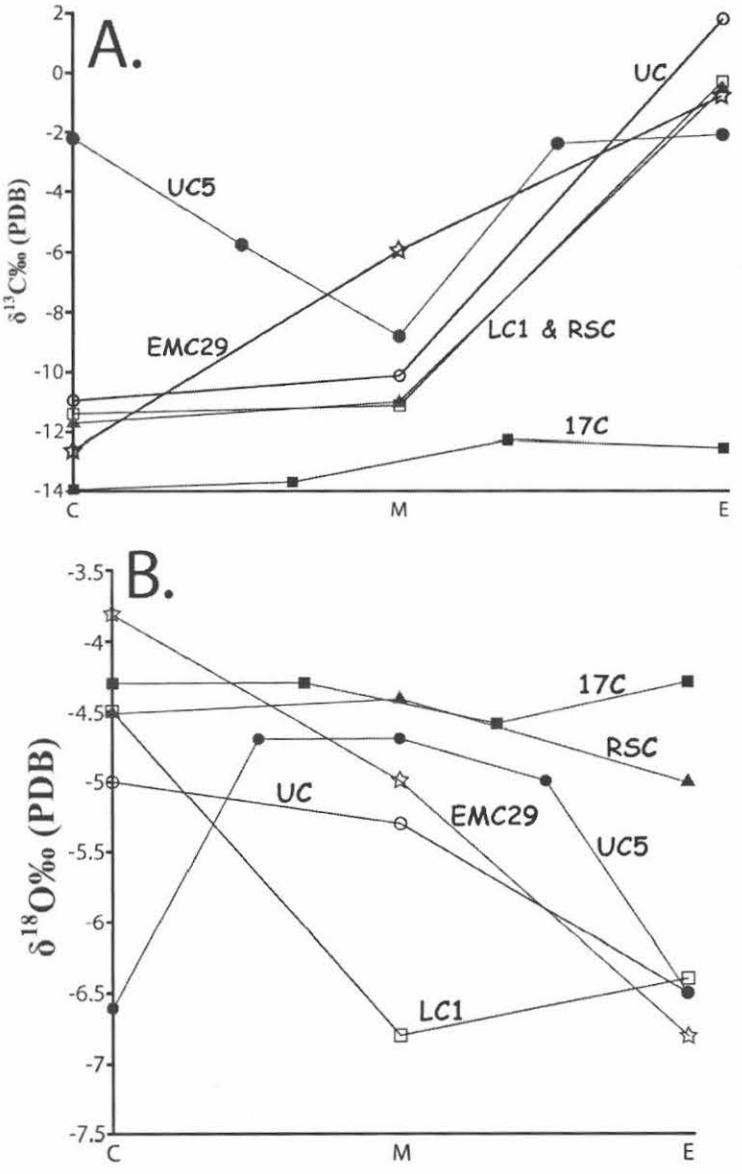

Fig. 17: Plots of $\delta^{13}C$ (A) and $\delta^{18}O$ (B) versus sample location within the concretion (C = center; M = middle; E = edge).

The formation of Rhinestreet concretions along specific horizons, an occurrence common to other black shale units (e.g., Raiswell, 1971; Hudson, 1978; Raiswell and White, 1978; El Albani et al., 2001), requires explanation. The siting of carbonate concretions has been related to the microbial reduction of locally concentrated organic matter, including skeletal remains and tissue (e.g., Weeks, 1957; Zangerl et al., 1969; Berner, 1980). However, we observed no textural evidence to suggest such a siting mechanism for the Rhinestreet concretions, nor do the concretions show a predilection for the organic-rich base of the unit (see Fig. 1). Moreover, organic matter within concretions is strikingly less than that in encapsulating shales (Lash and Blood, 2004b), though compaction-related volume loss of the shale no doubt elevated host rock TOC. Nevertheless, depleted carbon isotopic compositions (Figs. 16 and 17A) indicate that concretionary carbonate originated in part from the anaerobic bacterial reduction of organic matter. The large size of the Rhinestreet concretions suggests that the limited amount of *in situ* organic carbon was augmented by carbon derived from other sources during diagenetic precipitation of carbonate cement. A likely source of the additional carbon was the oxidation of biogenic methane at the base of the sulfate reduction zone by anaerobic methane oxidation (AMO) (Fig. 18; Raiswell, 1987, 1988). According to this mechanism, biogenic methane produced by microbial decomposition of organic matter in the zone of methanogenesis diffuses upward to the base of the sulfate reduction zone where carbonate precipitation occurs, usually within less than a meter of the seabed (Fig. 18). The isotopically light methane leaves behind a pool of ^{13}C-enriched carbon dioxide (Irwin et al., 1977) some of which migrates upward through the sediment. The siting of concretions within a concretionary horizon reflects the locations of permeable vertical pathways capable of conducting methane to the base of the sulfate reduction zone (Raiswell, 1987). Moreover, differences among $\delta^{13}C$ gradients of the studied Rhinestreet concretions (Fig. 17A) probably reflect local variations in the flux of methane and dissolved carbonate diffusing upward from the zone of methanogenesis (e.g., Raiswell, 1988).

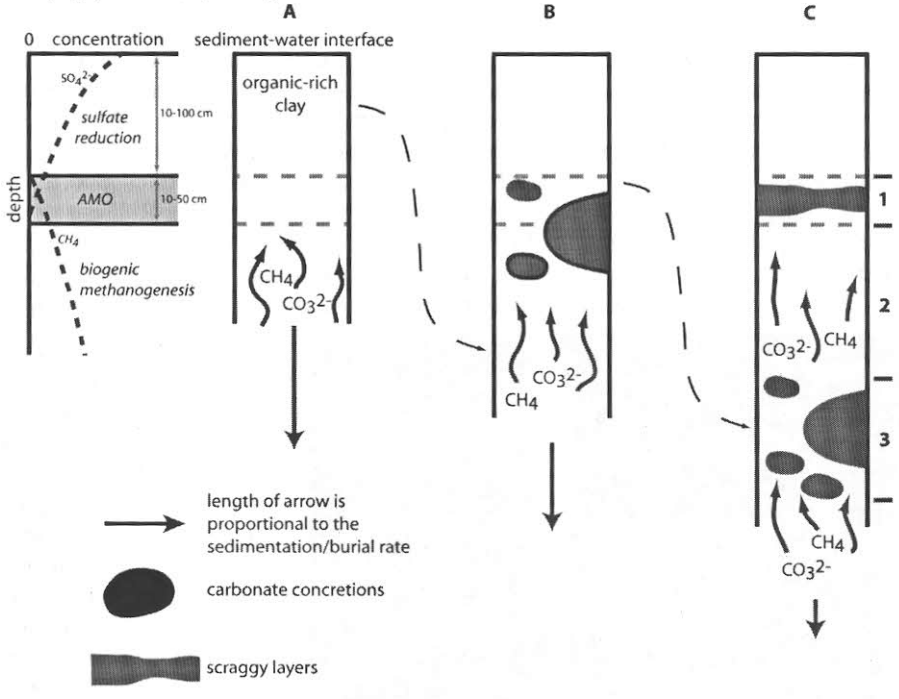

Fig. 18: Schematic representation of the inferred role of subsidence/burial rate in the growth of carbonate concretions by anaerobic methane oxidation (modified from Raiswell, 1987, 1988). The column on the left shows the diagenetic zones in anaerobic sediment; AMO = zone of anaerobic methane oxidation. Depth and thickness of the zone of AMO is based on Raiswell (1987) and references therein. Column A: subsidence/burial rates are high enough to carry sediment through the zone of AMO so fast that little more than the diffuse precipitation of diagenetic calcium carbonate occurs. Column B: a reduced burial rate enables concretions to grow in a relatively wide zone as sediment passes slowly through the zone of AMO (e.g., the lower concretionary horizon in the Rhinestreet shale and level 3 in column C). Column C: a near or complete cessation of sedimentation (very slow passage of sediment through the zone of AMO) results in the formation of a scraggy layer. Level 2 in column C reflects an increase in subsidence/burial rate following formation of the concretionary horizon represented by level 3.

Crucial to the precipitation of diagenetic carbonate as a consequence of AMO is a marked reduction in, or complete stoppage of, sedimentation/burial, which would stabilize the AMO zone thereby enabling protracted carbonate precipitation (Fig. 18; Raiswell, 1987, 1988). Two observations provide indirect evidence of a reduction in sedimentation/burial rate during concretion growth: 1) minimal change in estimated porosity (based on carbonate volume percentage) outward from the centers of studied concretions and 2) negligible variation in laminae thickness within concretions (see Figs. 10B and 14B). Both points suggest that the concretions grew in the near-absence of sedimentation/burial and associated compaction while the concretions formed (e.g., Raiswell, 1971).

Oxygen isotopic compositions of calcite are known to be a function of the temperature of precipitation and the $\delta^{18}O$ of the water from which the calcite precipitated (Hudson, 1977). If one variable is reasonably well known, the other can be estimated (Hudson, 1978). We used the equation of Anderson and Arthur (1983) to calculate paleotemperatures of concretionary calcite precipitation:

$$T^{o} = 16.0 - 4.14\,(\delta C - \delta W) + 0.13\,(\delta C - \delta W)^2 \qquad (1)$$

in which $\delta C = \delta^{18}O$ PDB of diagenetic calcite and $\delta W = \delta^{18}O$ of seawater on the SMOW scale. Estimates of seawater $\delta^{18}O$ for the Late Devonian include –1 ‰ SMOW of van Geldern et al. (2001) and –2 ‰ SMOW of Hudson and Anderson (1989). A Devonian seawater isotopic composition of –2 ‰ SMOW yields a temperature range of carbonate precipitation of 24° – 39° C, slightly to moderately in excess of the inferred 20° C bottom water temperature of the subtropical Catskill Delta basin (e.g., Gerlach and Cercone, 1993) and, therefore, incompatible with a shallow depth (~ 1 m below the seafloor) of concretion growth argued for by textural and field observations. Indeed, the range of oxygen isotopic values of Rhinestreet concretionary carbonate suggests that diagenetic precipitation occurred 130 to 630 m below the seafloor, assuming a geothermal gradient of 30° C/km.

An influx of ^{18}O-depleted meteoric water through the forming Rhinestreet concretions could account for their isotopic compositions, yet the location of the Rhinestreet depocenter, far distant from the Devonian shore would seem to preclude such a scenario. Direct precipitation of the Rhinestreet concretions from seawater at the temperatures suggested by the depleted oxygen isotopic values would require abnormally warm bottom waters during the Late Devonian, a hypothesis not supported by any geological data. We suggest, instead, that the oxygen isotope compositions of the Rhinestreet concretions resulted from the incomplete recyrstallization of primary calcite micrite to microspar (e.g., Folk, 1965) and re-equilibration of isotopic values at depth, perhaps by warm fluids migrating through the section. Although four of the Rhinestreet concretions studied by us show minor center-to-edge depletion in ^{18}O (Fig. 17B), estimated temperatures of precipitation of the centers of these concretions are too high to suggest precipitation from normal seawater. Further, concretion 17C shows no radial oxygen isotope gradient, and the center of concretion UC5 is marked by an especially depleted (-6.6 ‰ PDB) value (Fig. 17B). It appears, then, that warm fluids had some degree of access to concretion interiors. Dix and Mullins (1987) described a similar occurrence of recrystallized carbonate concretions in the more deeply buried Middle Devonian sequence of central New York state that they attributed to the migration of warm connate fluids, as much as 30°C warmer than those fluids inferred to have affected the Upper Devonian Rhinestreet concretions of western New York state (see Fig. 16).

Fig. 19: Upper scraggy layer, Eighteenmile Creek.

Finally, we consider the mode of formation of the scraggy layers (Fig. 19). The occasional presence of ellipsoidal carbonate concretions embedded within scraggy layers indicates that they, too, are

diagenetic and likely formed in a manner similar to the concretions; i.e., AMO. Indeed, stable isotope values of samples recovered form the middle and upper scraggy layers (see Fig. 1) fall within the range of values of the carbonate concretions (Fig. 16). The geometry of the scraggy layers, noticeably different from the ellipsoidal concretions, is interpreted to reflect a near stoppage of sedimentation/burial. Building upon our discussion of AMO, the thickness of a diagenetic carbonate horizon is interpreted to be proportional to the change in sedimentation/burial rate; i.e., a complete hiatus yields the minimum vertical range of carbonate precipitation because burial is halted and the zone of AMO is stabilized (Raiswell, 1987, 1988). The thickness and geometry of the scraggy layers likely reflects a greater duration of the break in sedimentation/burial during their growth than during the development of the concretionary horizons and, therefore, a protracted period of time that isotopically light methane and ^{13}C-enriched dissolved carbonate were delivered to the stationary AMO zone (compare columns B and C, Fig. 18; Raiswell, 1987, 1988). That is, the near cessation of sedimentation and, most importantly, burial, resulted in the confinement of carbonate precipitation to a narrow, fixed zone defined by the upper limit of methane and CO_3^{2-} diffusion and the maximum depth to which seawater sulfate can diffuse (Raiswell, 1988). The scraggy layers, by virtue of their thickness and their semi-continuous geometry, then, probably formed as a consequence of the stoppage of sedimentation and burial so that the zone of AMO was held in place long enough for diagenetic carbonate to accumulate laterally rather than vertically.

We have recognized the upper scraggy layer in wireline logs from hydrocarbon wells as distant as Chautauqua County (Fig. 20). Assuming that basinwide dynamics were responsible for the prolonged cessation of sedimentation and burial, the scraggy layers might be used both in outcrop and subsurface work to create a time-stratigraphic framework in the Rhinestreet shale. This is a fertile direction for future work.

EARLY (ACADIAN) OVERPRESSURE EPISODE – DISEQUILIBRIUM COMPACTION

The Rhinestreet shale likely followed a normal compaction history that can be described in terms of the exponential decay function for shale first proposed by Athy (1930),

$$\phi = \phi_i e^{-cz} \qquad (2)$$

where z is depth in meters, ϕ_i is the initial porosity at $z = 0$, and e is the compaction coefficient, for some time, perhaps to its maximum burial depth. Burial-induced normal mechanical compaction of argillaceous sediment is accomplished by a loss of porosity as sediment particles respond to increasing effective stress by reorienting into more mechanically stable arrangements (i.e., perpendicular to overburden stress) and pore fluid is expulsed (Hedberg, 1936; Terzaghi and Peck, 1948; Hamilton, 1976; Magara, 1978; Jones and Addis, 1985; O'Brien and Slatt, 1990; Goulty, 2004). The majority of porosity-depth algorithms created from empirical data (e.g., Sclater and Christie, 1980; Huang and Gradstein, 1990; Hansen, 1996; among others) define by a rapid reduction in porosity at shallow depth, followed by a reduced rate of porosity occlusion in progressively older, more deeply buried sediment.

Under certain conditions, however, notably when fluid expulsion during burial is retarded due to low permeability and/or rapid sedimentation, mechanical compaction fails to keep pace with increasing vertical effective stress such that pore pressure is greater than hydrostatic (Swarbrick et al., 2002). This phenomenon, termed *disequilibrium compaction*, has been documented from modern basins including the Carnarvon Basin, western Australia (van Ruth et al., 2004), the Gulf Coast Basin, offshore Louisiana (Dickinson, 1953; Harrison and Summa, 1991; Hart et al., 1995; Audet, 1996), the Caspian Sea (Bredehoeft et al., 1988), offshore eastern Trinidad (Heppard et al., 1998), the North Sea (Mann and Mackenzie, 1990; Audet and McConnell, 1992; Swarbrick and Osborne, 1998), and southeast Asia (Harrold et al., 1999). Overpressure caused by disequilibrium compaction begins at that depth where sediment permeability becomes so low that mechanical compaction and, therefore, porosity reduction is retarded (e.g., Swarbrick et al., 2002). The onset of overpressure occurs at the *fluid retention depth*, which is recognized on porosity-depth profiles as that depth at which porosity shows no reduction with increasing burial depth and on pressure-depth profiles as that depth where pore pressure exceeds hydrostatic (Fig. 21; Audet, 1996; Harrold et al., 1999; Swarbrick et al., 2002).

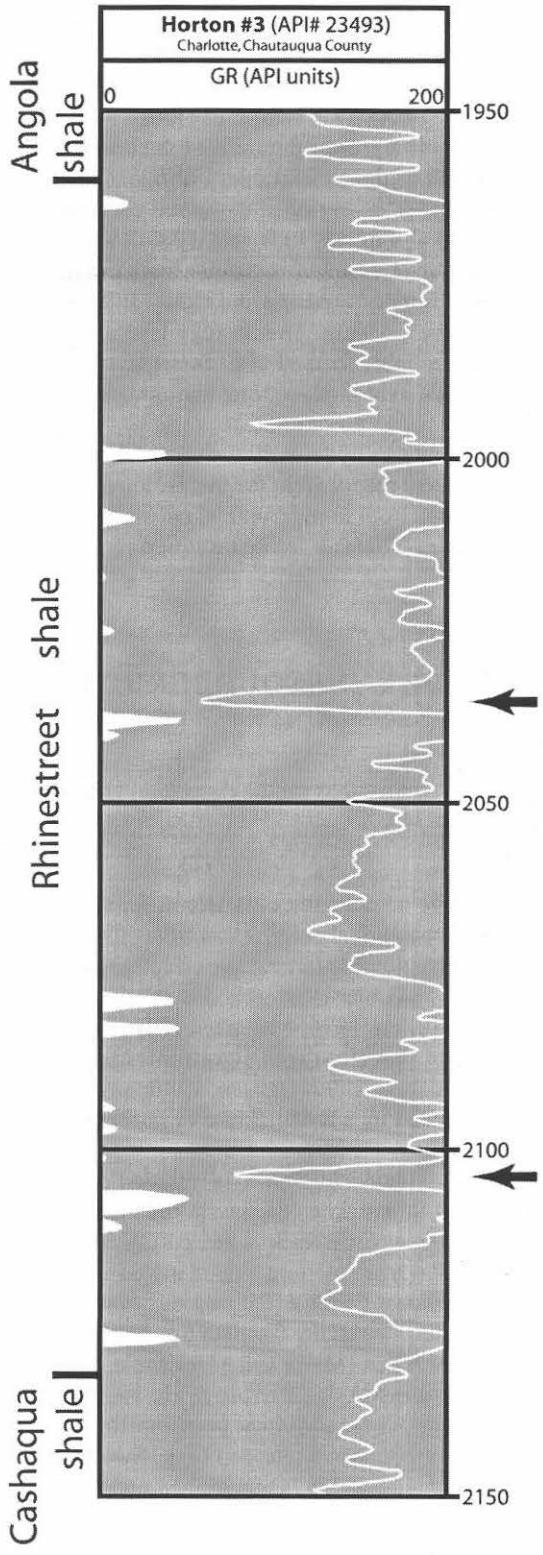

Fig. 20: Gamma-ray log of the Horton #3 well, Chautauqua County, New York. Black arrows point to inferred scraggy layers of the Rhinestreet shale.

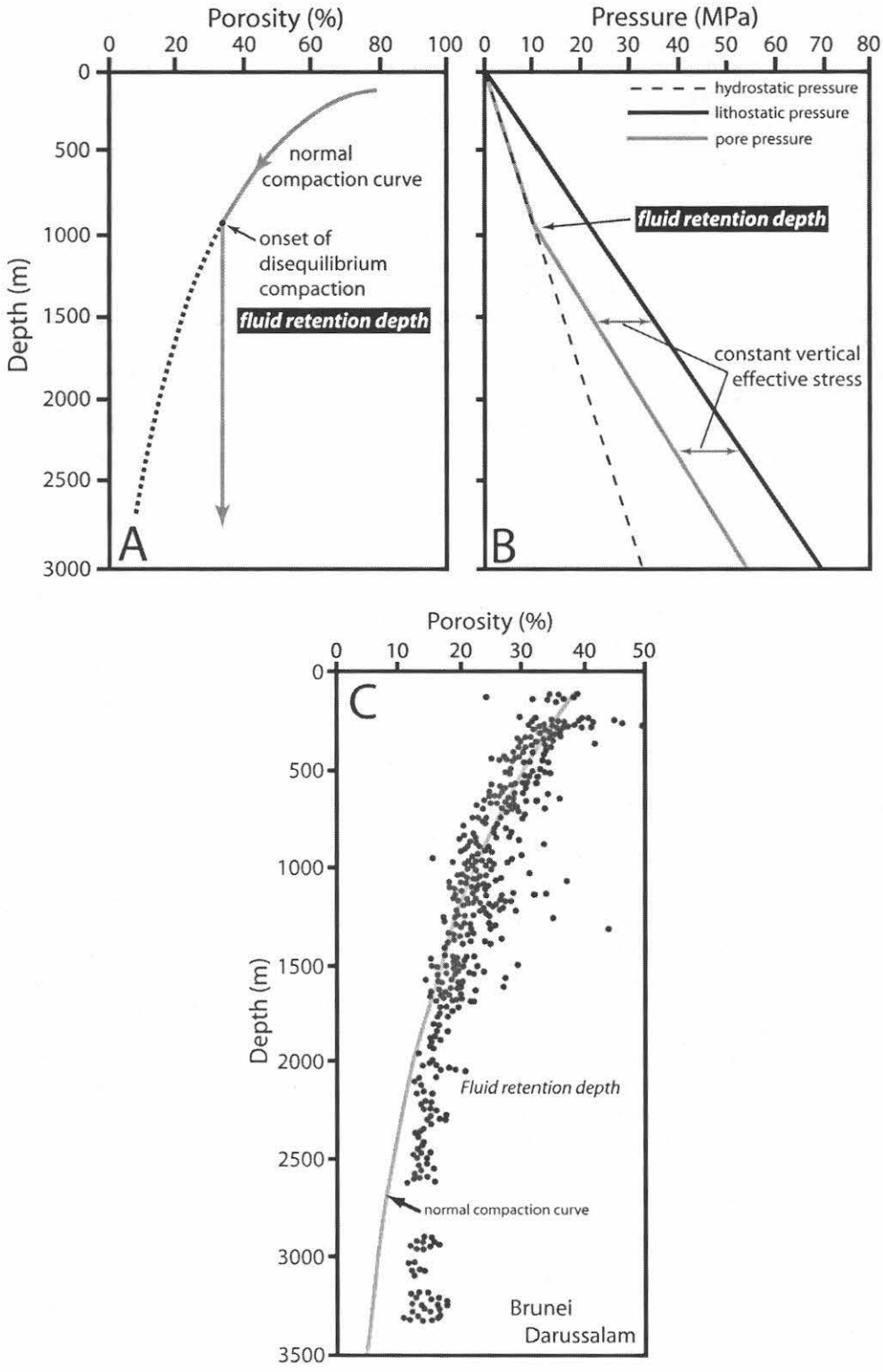

Fig. 21: Relationship between (A) porosity and depth and (B) pressure and depth for a shale that becomes overpressured by disequilibrium compaction at the fluid retention depth (modified after Harrold et al., 2000). (C) Porosity-depth profile for Brunei Darussalam (modified after Tingay et al., 2000).

Abundant natural hydraulic fractures (NHFs) or joints in the Upper Devonian shale-dominated succession of the western New York state region of the Appalachian Basin indicate that these deposits were episodically overpressured during their burial history (Engelder and Oertel, 1985; Lacazette and Engelder, 1992; Lash et al., 2004; Lash and Engelder, 2005). As described below and elsewhere, overpressuring of the shale and resultant natural hydraulic fracturing resulted from the transformation of kerogen to hydrocarbons in organic-rich source rocks and occurred close to or at maximum burial depth during the Alleghanian orogeny (Lash et al., 2004; Engelder and Whitaker, 2006). Because disequilibrium compaction alone is insufficient to generate pore pressures, P_p, capable of driving NHFs (Hart et al., 1995; Kooi, 1997), such an overpressuring event in the burial history of a basinal succession may go unrecognized. However, analysis of compaction strain data described below suggests that the Rhinestreet shale became overpressured well before attaining its maximum burial depth.

The most obvious measure of gravitational compaction strain sustained by a volume of sediment following accumulation on the seafloor is the change in layer thickness from the concretion into correlative layers of the encapsulating shale (see Fig. 11). We measured the thickness of bedding or a bedding interval inside concretions (T_i) and the thickness of that same interval in the shale (T_o), a presumed proxy for the original seafloor thickness of the host sediment as argued above (Fig. 11). Gravitational compaction strain of the shale outside the strain shadow of the concretion, ε_3, is calculated by the following expression,

$$\varepsilon_3 = \frac{T_i - T_o}{T_i}. \qquad (3)$$

The mean ε_3 of the Rhinestreet black shale based on the analysis of 118 concretions and encapsulating shale throughout the unit, expressed as a negative value, is –0.518 or 51.8% (± 4.9%). This value is noteworthy because normally compacted marine shales typically compact more than 65% upon burial to depths comparable to the maximum burial depth of the Rhinestreet shale (Burland, 1990).

The compaction strain of the Rhinestreet shale can be used as a measure of the porosity achieved at the termination of gravitational mechanical compaction if we assume that all volume loss was caused by vertical shortening, a reasonable assumption based on the lack of layer-parallel shortening caused by Alleghanian tectonics in these rocks (Hudak, 1992). Compaction strain is converted to paleoporosity, ϕ_p, by the following equation derived by Jacob (1949),

$$\phi_p = \frac{\phi_o + 100\varepsilon_3}{\varepsilon_3 + 1} \qquad (4)$$

in which ϕ_p is expressed as volume percent. However, in order to calculate the ϕ_p of the Rhinestreet shale, we first must obtain a reasonable value for the porosity of the sediment at the onset of normal compaction, ϕ_o. Textural evidence described above and in more detail by Lash and Blood (2004b) relates the formation of Rhinestreet concretions to the passive precipitation of diagenetic carbonate in void spaces of the clayey organic-rich host sediment. As noted earlier, the porosity of the Rhinestreet sediment at the time of concretion growth ranged from 74 to 93%. However, some authors have suggested that the porosity of newly deposited clayey sediment decreases from as much as 90% to perhaps 60-65% within ten m or so of the seafloor (Weller, 1959; Von Engelhardt, 1977; Magara, 1978; Luo et al., 1993). Moreover, Kawamura and Ogawa (2004) demonstrated an especially rapid reduction in void ratio of pelagic clay equal to a 5% drop in porosity down to a depth of 10 cm below the seafloor. Luo et al. (1993) maintain that such marked losses of porosity within several meters to a few tens of meters of the seafloor should be considered a continuation of the depositional process rather than the initial phase of normal load-induced mechanical compaction. Thus, we interpret the range in $CaCO_3$ volume in analyzed Rhinestreet concretions to reflect the rapid occlusion of porosity as the carbonaceous clay entered and passed through the sulfate reduction zone where concretionary growth occurred (Lash and Blood, 2004b). However, minor geochemical (i.e., $CaCO_3$) zonation observed in individual Rhinestreet concretions (see Fig. 15) suggests that concretionary growth occurred rapidly relative to the rate of porosity reduction.

In light of the preceding discussion, we arbitrarily set $\phi_o = 70\%$ for our calculation of the Rhinestreet shale ϕ_p. This value is a bit higher than the 60-65% porosity level that Luo et al. (1993) consider to mark the onset of normal compaction principally because of the typically high water content of organic-rich clays (e.g., Meade, 1966; Keller, 1982). Our calculated Rhinestreet shale ϕ_p using equation (4) is 37.8% (±7.1%), a value markedly higher than that expected for shale normally compacted to the 3.1 km maximum burial depth of the Rhinestreet shale (see Fig. 9). Because porosity reduction by normal

compaction is essentially nonelastic (Harrold et al., 1999), uplift of the Rhinestreet shale cannot account for the high ϕ_p. Indeed, the present porosity of the Rhinestreet shale based on MICP measurements is 3.9% (±0.9%), roughly one-tenth the calculated ϕ_p based on compaction strain analysis. We suggest that the Rhinestreet shale ϕ_p reflects the arrest of gravitational compaction short of its maximum burial depth. The reduction of porosity from the ϕ_p to the present porosity likely reflects a combination of processes, including pressure solution (Towarak, 2006), precipitation of cement, neoformation of clay minerals (chlorite, kaolinite), the production of bitumen when the Rhinestreet shale entered the oil window (Lash, 2006c), and the crushing and/or squeezing of soft grains, including kerogen, into pore throats and voids (e.g., Lash, 2006b).

The relatively low ϕ_p of the Rhinestreet shale suggests that normal compaction of the low-permeability organic-rich clay was arrested at some depth shy of its maximum burial depth by P_p in excess of hydrostatic. This depth, the paleo-fluid retention depth (PFRD), can be estimated in two ways; (1) comparison of the Rhinestreet ϕ_p with published porosity-depth profiles for shale and (2) calculation of the depth at which a porosity of 37.8% is reached during normal compaction of shale by use of empirical porosity-depth algorithms. Published porosity-depth relationships vary among basins as a consequence of such factors as the age of the sediment, effective mean stress, mineral composition, sedimentation rate, lateral stress, and pore fluid chemistry (e.g., Rieke and Chilingarian, 1974; Magara, 1980; Hermanrud, 1993; and many others). Indeed, there is no universal porosity-depth profile (Liu and Roaldset, 1994). Recognizing this, we seek only to bracket the PFRD of the Rhinestreet shale. Plotting the calculated mean Rhinestreet ϕ_p and its upper and lower standard deviation limits on Rieke and Chilingarian's (1974) summary plot of normal compaction curves for shale suggests that the PFRD could have ranged from a depth of ~690 m to ~1,380 m, less than half-way to the modeled maximum burial depth (Fig. 22).

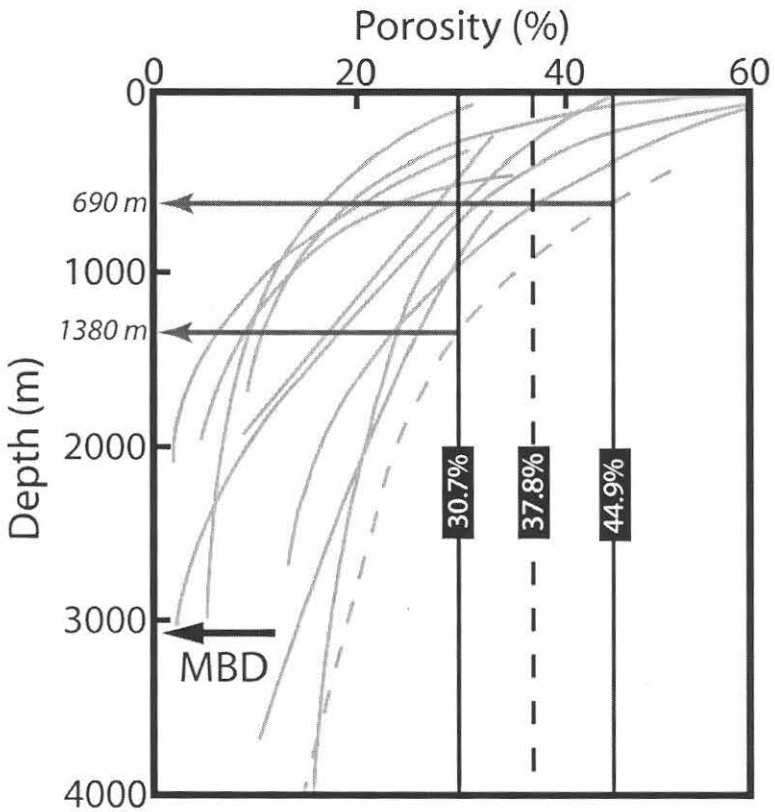

Fig. 22: Porosity versus depth of burial relationships for shale and clayey sediments (modified after Rieke and Chilingarian, 1974) showing the estimated maximum Rhinestreet paleo-fluid retention depth (PFRD) range based on the mean and the upper and lower standard deviation ranges for the calculated paleoporosity of the Rhinestreet shale. The dashed normal compaction trend, which was used to define the maximum depth of the PFRD, is from Ham (1966). MBD = modeled maximum burial depth of the Rhinestreet shale.

Our second approach to estimating the PFRD of the Rhinestreet shale involves the use of some of the more widely cited empirically derived porosity-depth algorithms for normally compacted shale (Gallagher, 1989). The majority of these functions describe a reduction in porosity that varies exponentially with depth, following, to various degrees, the relationship proposed by Athy (1930). The Rhinestreet shale PFRD was estimated using the shale exponential functions of Hansen (1996; Norwegian Shelf), Huang and Gradstein (1990; deep sea claystone), Tingay et al. (2000; Baram Basin, Brunei Darussalam), Hermanrud et al. (1998; offshore mid-Norway), Sclater and Christie (1980; North Sea), Gallagher and Lambeck (1989; Eromanga Basin, Australia), and Hegarty et al. (1988; southern margin of Australia). Estimated depths at which a porosity of 37.8% is reached during equilibrium compaction range from a low of 456 m based on the porosity-depth function of Hegarty et al. (1988) to 1,543 m, half the maximum burial depth of the Rhinestreet shale, using the algorithm of Tingay et al. (2000) (Fig. 23). Most calculated depths derived from exponential functions fall within the depth range defined by comparison of the Rhinestreet ϕ_p with normal compaction curves (Fig. 23). Three linear shale porosity-depth relations were used to calculate the Rhinestreet PFRD; Hansen (1996; Norwegian Shelf), Velde (1996; clay-rich sediments and Recent and Tertiary sediments from Japan and Italy; burial depths > 500 m), and Falvey and Deighton (1982). These functions yield PFRDs of 1,344 m, 622 m, and 500 m, respectively (Fig. 23). The minimum PFRD, 295 m, was obtained from the power-law equation of Baldwin and Butler (1985) for normally compacted shale. Finally, the parabolic porosity-depth function of Liu and Roaldset (1994) placed the PFRD of the Rhinestreet shale at 2,100 m, one km above its modeled maximum burial depth (Fig. 23).

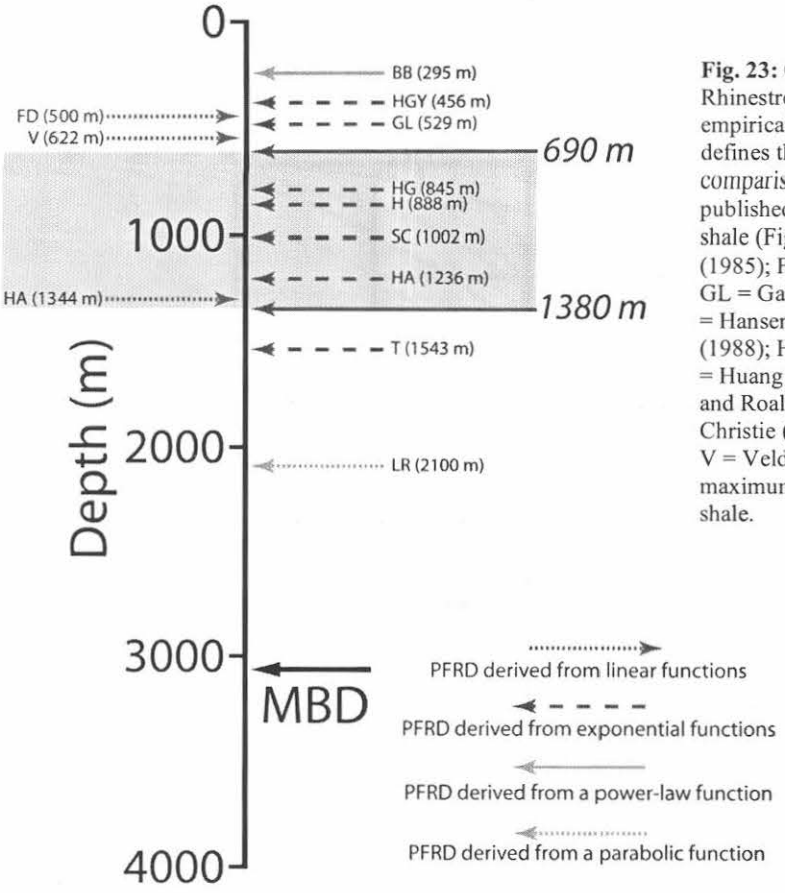

Fig. 23: Calculated PFRD values for the Rhinestreet shale (ϕ_p = 37.8%) using empirical algorithms. Shaded interval defines the PFRD range based on comparison of the Rhinestreet ϕ_p with published normal compaction curves for shale (Fig. 22). BB = Baldwin and Butler (1985); FD = Falvey and Deighton (1982); GL = Gallagher and Lambeck (1989); HA = Hansen (1996); HGY = Hegarty et al. (1988); H = Hermanrud et al. (1998); HG = Huang and Gradstein (1990); LR = Liu and Roaldset (1994); SC = Sclater and Christie (1980); T = Tingay et al. (2000); V = Velde (1996); MBD = modeled maximum burial depth of the Rhinestreet shale.

Normal gravitational mechanical compaction of sediment with a ϕ_o of 70% to > 2 km burial depth typically reduces porosity to ≤ 20% (Rieke and Chilingarian, 1974; Magara, 1978; Giles et al., 1998). Estimation of the Rhinestreet PFRD by use of published porosity-depth curves for normally compacted shale and empirically derived porosity-depth functions suggests that this organic-rich unit departed its

normal compaction trend at a depth of 850 to 1,380 m, short of its maximum burial depth (Fig. 23). The relatively shallow depth range of the Rhinestreet PFRD indicates that the overpressure mechanism was not linked to the transformation of kerogen to hydrocarbons, which did occur in the Rhinestreet shale of the LED, but at much greater depth (Lash, 2006c). The most likely candidate for the early generation of overpressure in the Rhinestreet shale is disequilibrium compaction. Disequilibrium compaction, while capable of pushing P_p above hydrostatic at a given depth, the fluid retention depth, cannot drive it high enough to create an effective tensile stress of zero as the increase in P_p is linked inextricably to the rate of loading or the lithostatic gradient (see Fig. 21; Hart et al., 1995; Kooi, 1997; Swarbrick et al., 2002). Indeed, this phase of overpressuring in the shale-dominated succession of the LED did not result in the propagation of NHFs.

There is widespread agreement that the principal controls of disequilibrium compaction include sedimentation (loading) rate and sediment permeability, and, secondarily, sediment compressibility (Luo and Vasseur, 1992; Kooi, 1997; Swarbrick et al., 2002; among others). Swarbrick et al. (2002) argue convincingly that the fluid retention depth in low permeability/highly compressive rocks, like the organic-rich Rhinestreet shale, would be shallower than that expected for more permeable, less compressible sand- and/or silt-rich deposits. Further, given the same sediment type, the fluid retention depth will be relatively shallow in those rocks that have been affected by high sedimentation rates. For example, Grauls (1998) points out that a slow sedimentation rate (~50 m Ma^{-1}) in offshore Angola resulted in fluid retention at a depth of 1,200 m; on the Nile Delta, on the other hand, where sedimentation rates > 800 m Ma^{-1}, disequilibrium compaction begins at a depth of only 800 m (Mann and Mackenzie, 1990).

In order to better evaluate the timing of disequilibrium compaction in the Upper Devonian shale succession of the LED, we need to fully understand the Upper Devonian-Mississippian stratigraphy of this region of the basin (Fig. 24). Exhumation caused by passage of a peripheral bulge at the onset of the Alleghanian orogeny across western New York state (Faill, 1997, and discussed below) resulted in the loss of much of the Mississippian section in the LED (Fig. 24; Lindberg, 1985). However, the presence of the lower Kinderhookian Knapp conglomerate conformably overlying Devonian strata along the New York state-Pennsylvania border immediately south of the LED suggests that the Cashaqua shale is overlain by 1,155 m of Upper Devonian deposits (Fig. 24). Approximately 148 m of Frasnian strata, including the Rhinestreet shale, were deposited on top of the Cashaqua shale at a rate of 30 m Ma^{-1}. The remaining 1,007 m of Upper Devonian sediment accumulated during the Famennian stage at an average rate of 65 m Ma^{-1}, a more than two-fold increase in sedimentation rate from the Frasnian stage. Moreover, the sedimentology of the lower part of the Famennian succession in the LED, the Dunkirk black shale and overlying Gowanda gray shale (see Fig. 3), suggests that the relatively low Frasnian sedimentation rate continued into the Famennian (Baird and Lash, 1990). However, overlying progressively siltier deposits that record a regressive shift from delta front to shallow-marine shelf environments (Baird and Lash, 1990; Dodge, 1992) evince an increase in sedimentation rate in post-Gowanda shale time. Accumulation of the 275-m-thick Dunkirk shale-Gowanda shale succession (Lindberg, 1985) at the above-cited 30 m Ma^{-1} Frasnian sedimentation rate would have encompassed 9.2 Ma of the 15.4 Ma Famennian stage (Kaufmann, 2006). The remaining 732 m of Famennian deposits, then, would have accumulated at the markedly higher rate of 118 m Ma^{-1}.

The transition from the Devonian to the Mississippian in the Appalachian Basin of northwest Pennsylvania is defined by a marked drop in sedimentation rate to 25 m Ma^{-1} based on 172 m of Kinderhookian deposits preserved in this area (Fig. 24; Lindberg, 1985). However, if the Knapp conglomerate accumulated at the very end of the Devonian, as suggested by Dodge (1992), the postulated drop in sedimentation rate would have occurred shortly before the Mississippian. Regardless, the sedimentation rate appears to have diminished throughout the Mississippian (e.g., Beaumont et al., 1987) as evidenced by a calculated sedimentation rate of 9 m Ma^{-1} for the 366 m (Lindberg, 1985) of Kinderhookian to Chesterian deposits preserved in north-central Pennsylvania, immediately south of the Finger Lakes District of western New York state (Fig. 24). The marked reduction in sedimentation rate at the Devonian-Mississippian boundary in Finger Lakes and Lake Erie districts appears to confirm Bond and Kominz's (1991) contention that the Early Carboniferous of the central Appalachians lacked significant tectonic activity.

We believe that the early and relatively shallow onset of disequilibrium compaction in the low-permeability shale-dominated Upper Devonian succession of the LED was induced by the marked increase in sedimentation rate in the latter half the Famennian related to an acceleration, perhaps glacio-eustatic in origin (Veevers and Powell, 1987), in the rate of progradation of the Catskill Delta Complex. Moreover,

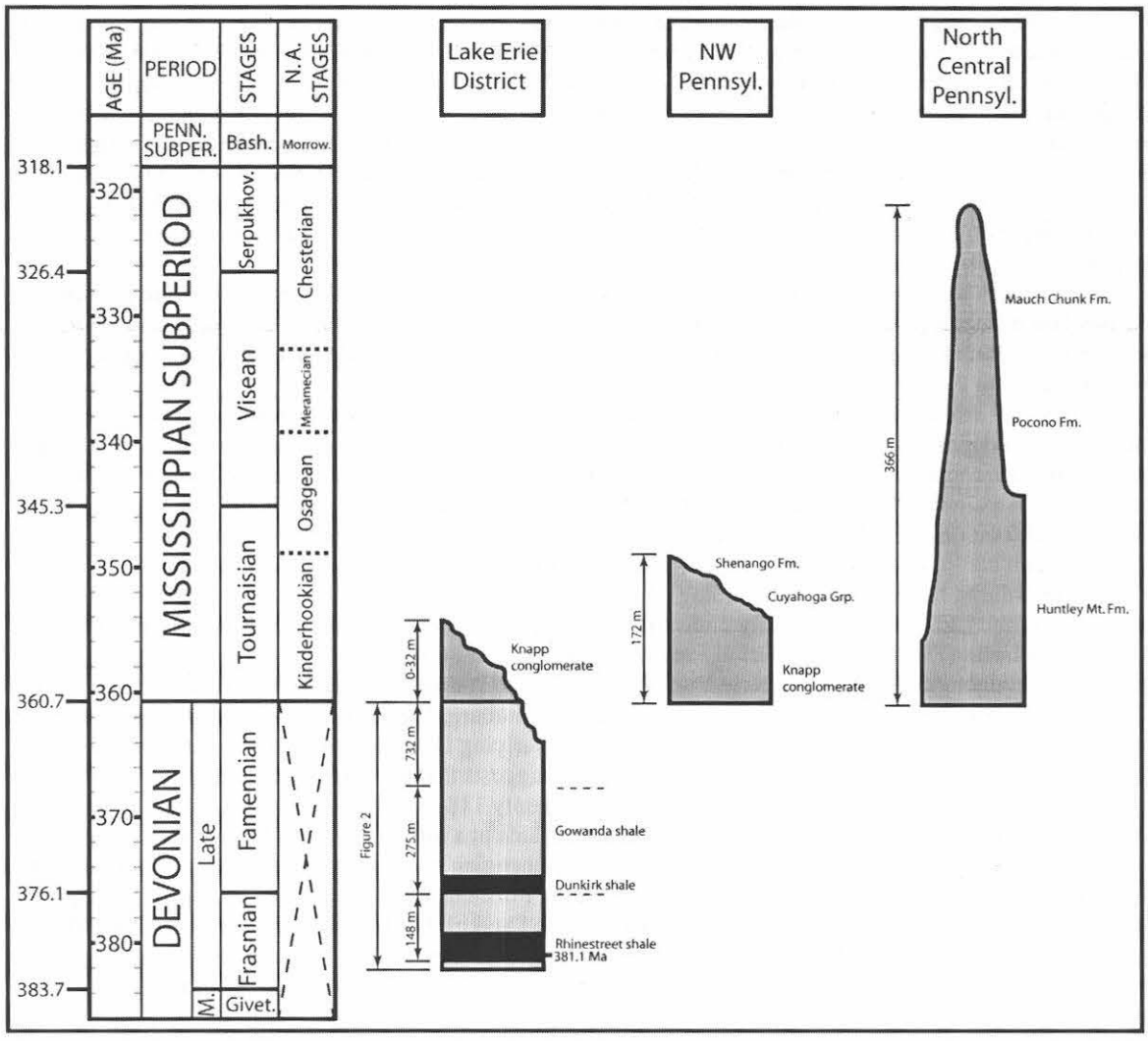

Fig. 24: Upper Devonian-Mississippian stratigraphic relations of western New York state (Lake Erie District) and northwest and north-central Pennsylvania. Stratigraphic columns, including thicknesses, are modified from Lindberg (1985). Devonian time scale (including the Devonian-Mississippian boundary) is from Kaufmann (2006); Mississippian time scale is from Gradstein et al. (2004).

the presence of a 1,100 to 1,200 m of Devonian strata on the Cashaqua shale-Rhinestreet shale contact suggests that the onset of disequilibrium compaction in the Upper Devonian succession occurred at a depth of ~1.1 km, well within the depth range defined by comparison of the Rhinestreet shale ϕ_p with normal compaction curves and porosity-depth algorithms for shale (see Fig. 23). The earlist overpressure episode recorded by rocks of the LED, then, is an Acadian event that finds recent analogues in the Louisiana Gulf Coast (Dickinson 1953) and the Mahakam Delta, Indonesia (Burrus, 1998). Indeed, our estimated PFRD of the Rhinestreet shale and the maximum Famennian sedimentation rate of 118 m Ma^{-1} are consistent with data from modern basins overpressured by disequilibrium compaction (Fig. 25; Swarbrick et al., 2002).

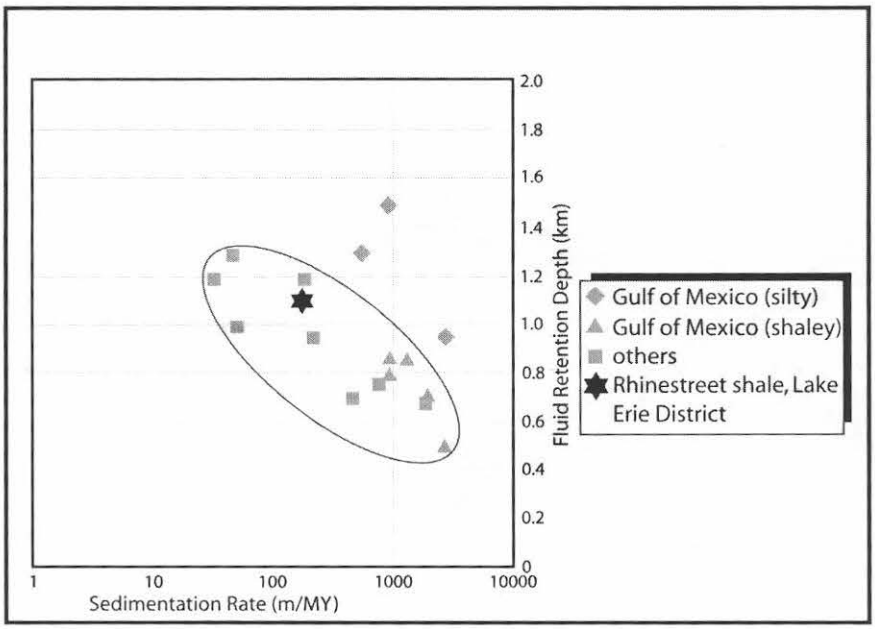

Fig. 25: Plot of sedimentation rate versus fluid retention depth showing data from the Gulf of Mexico and other basins and the Rhinestreet shale (modified after Swarbrick et al., 2002). Refer to text for discussion of the sedimentation rate that induced disequilibrium compaction of the Rhinestreet shale and estimation of the Rhinestreet PFRD.

ONSET OF THE ALLEGHANIAN OROGENY - FRACTURE EVIDENCE FOR PASSAGE OF A PERIPHERAL BULGE

The Rhinestreet shale was overpressured as a consequence of the Acadian orogeny, yet the nature of the overpressuring mechanism – disequilibrium compaction – could not have driven P_p high enough to induce NHFs. Thus, jointing of the Upper Devonian shale-dominated sequence did not occur until after the Acadian orogeny. The following discussion emphasizes joint-driving mechanisms; thus, this is an appropriate time to introduce the dominant joint sets represented in the Rhinestreet black shale and other shale units of the LED. It is worth noting that even relatively recent publications relate the pervasive fractures carried in Upper Devonian black shales of western New York state and western Pennsylvania to glacial unloading and differential isostatic rebound (e.g., Schmoker and Oscarson, 1995). Although we have catalogued joints that formed under these conditions (Lash et al., 2004), the systematic joints readily observed in shale exposed along the lakeshore formed much earlier and under very different loading configurations. Indeed, the pioneering work of Terry Engelder and his students at Penn State, grounded in linear elastic fracture mechanics, has demonstrated the variety of natural loading configurations and related joint-driving mechanisms under which rocks can fracture (Engelder, 1985, 1987; Engelder and Lacazette, 1990; Engelder and Gross, 1993; Engelder and Fischer, 1996; Lacazette and Engelder, 1992). Moreover, each loading configuration may be represented during a single tectonic cycle (Engelder, 1985).

The Rhinestreet shale carries as many as five systematic joint sets (e.g., Lash et al., 2004). The most pervasive sets, regionally and stratigraphically, are NW (298°-313°)- and ENE (060°-075°)-oriented sets (Fig. 26). Systematic NS (352°-007°)-trending joints, while displaying a strong stratigraphic control as described below, are also recognized over much of the LED (Fig. 27). Abutting relations among joints of the three sets indicate that the NS joints are the oldest structures and systematic ENE-trending joints are the youngest (Lash et al., 2004). Both the ENE- and NW-trending joints show a strong affinity for black shale, especially the basal, more organic-rich intervals of these units (Lash et al., 2004). Joints of these two sets seldom extend downward from the bases of black shale units into underlying gray shale; instead, they appear to have propagated farther upward into the black shale and then into overlying gray shale (Fig. 28; Lash et al., 2004).

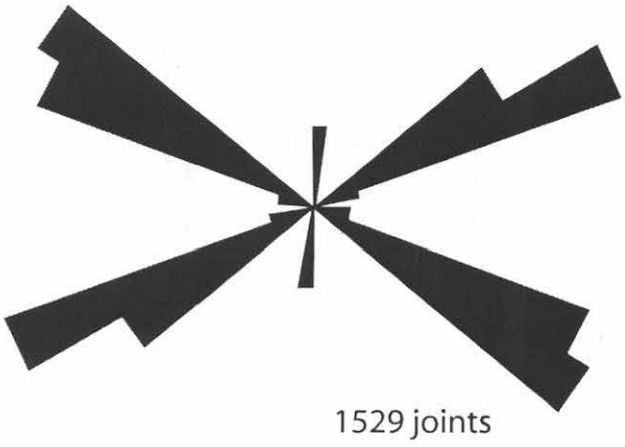

Fig. 26: Rose plot of joints in the Rhinestreet shale, northern Erie County, New York.

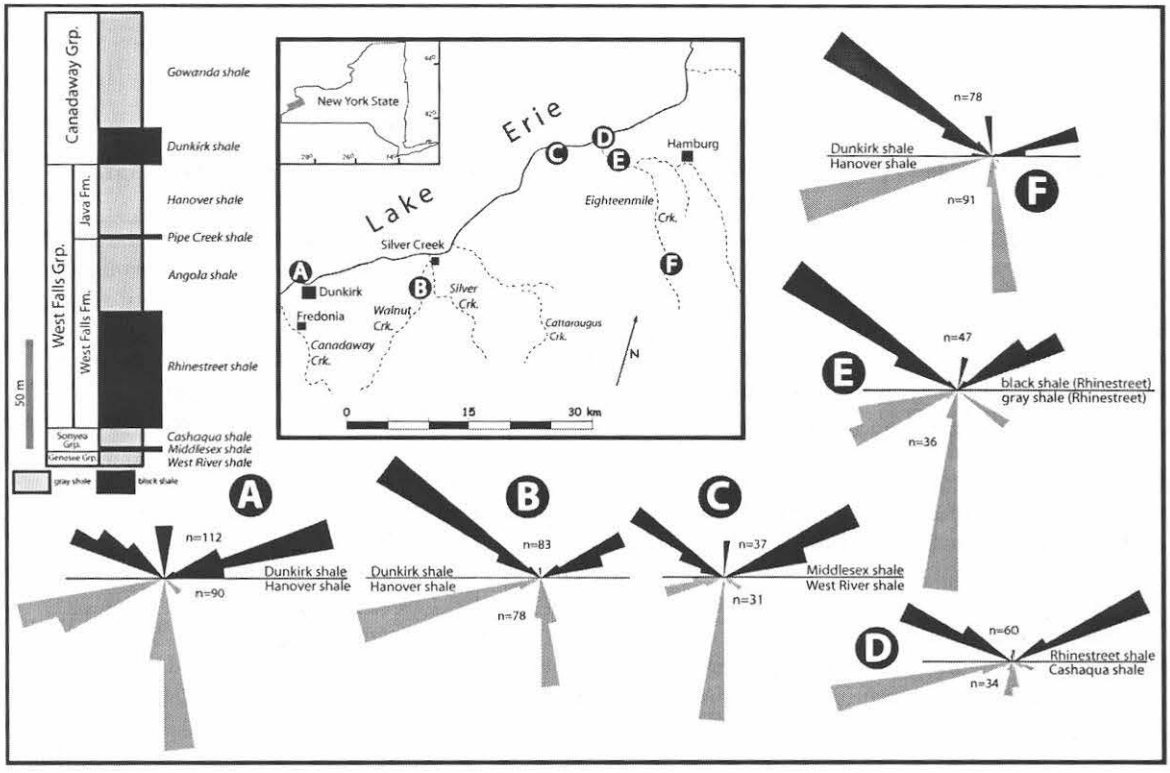

Fig. 27: Generalized stratigraphic column showing the Upper Devonian shale succession of the Lake Erie District and selected rose plots of systematic NS, NW, and ENE joints at gray shale-black shale contacts throughout the Lake Erie District. The lettered rose plots are keyed to the location map.

Fig. 28: Tall, close-spaced NW joints at the contact (dotted line) of the Dunkirk shale and underlying Hanover gray shale along Eighteenmile Creek.

Systematic NS joints formed preferentially at the tops of gray shale units and basal intervals of overlying black shale deposits (Fig. 27; Lash, 2006b). These joints have been observed at the bottom contacts of all Upper Devonian black shale units of the LED and at almost all exposures of these contacts (Fig. 27). However, they are most densely developed (i.e., lowest median orthogonal spacing) at the Hanover shale-Dunkirk shale contact, the Cashaqua shale-Rhinestreet shale contact, and at contacts of gray shale intervals and overlying black shale within the Rhinestreet shale (Fig. 27). Few NS joints observed in gray shale (~20%) extend more than 20 cm into overlying black shale (Fig. 29A); roughly 50-60% of all NS joints examined by us either were arrested below or at the base of the overlying black shale unit (Fig. 29B). Finally, NS joints are rarely found exclusively in black shale; indeed, >90% of NS joints observed in black shale units can be readily traced into underlying gray shale from which they appear to have propagated.

The joint-driving mechanism(s) for the three dominant systematic joint sets carried in Upper Devonian shale of the LED is not immediately obvious. Few joint surfaces of these fine-grained rocks contain any sort of ornamentation that might be informative regarding the origin of the joints. However, rare plumose structures consistent with incremental propagation decorate ENE and NW joint surfaces. Such morphology is typical of fluid loading during natural hydraulic fracturing (Lacazette and Engelder, 1992). Moreover, the close orthogonal spacing of joints of each set relative to their height offers further evidence for their propagation under conditions of fluid loading (Ladeira and Price, 1981; Fischer et al., 1995; Engelder and Fischer, 1996). Indeed, it is tempting to attribute the seemingly similar nature of the NS joints to the same loading configuration as the NW and ENE joints. However, further insight into differences in joint-driving mechanisms among the three dominant joint sets carried in the LED may be found in the nature of joint-carbonate concretion interactions (e.g., McConaughy and Engelder, 1999). Studied diagenetic carbonate concretions in the Upper Devonian shale succession of the LED exist in two general forms that appear to be controlled by host shale type: (1) large ellipsoidal (aspect ratio ~ 2) internally laminated concretions most common to black shale units as described above (Lash and Blood, 2004a,b) and (2) smaller lenticular (aspect ratio > 4) internally massive concretionary bodies most frequently found in bioturbated gray shale.

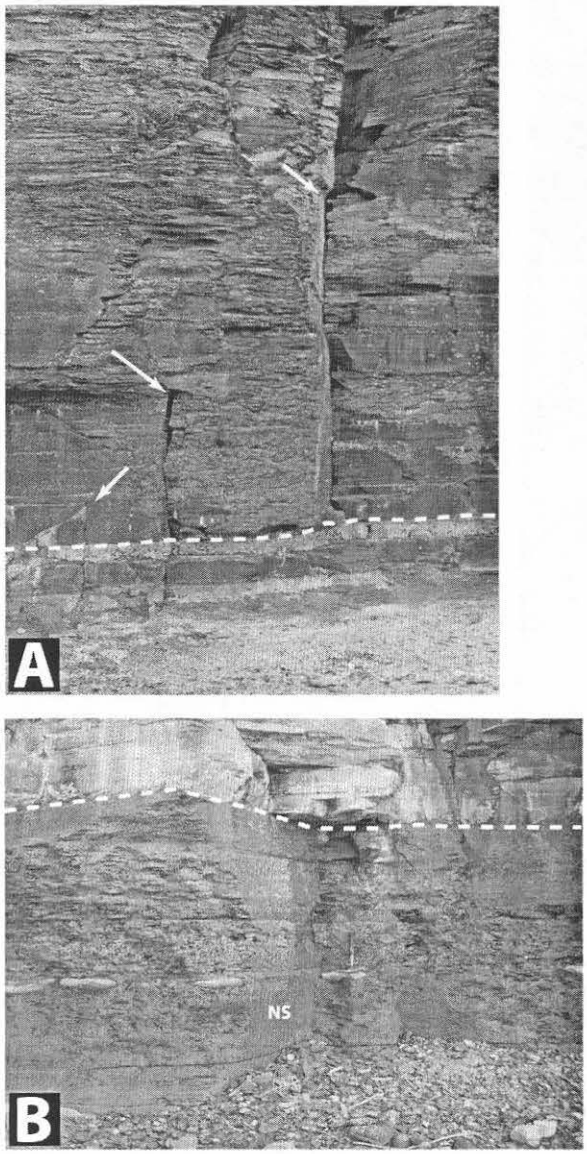

Fig. 29: NS joints terminating at gray shale-black shale contacts: (A) close-spaced NS joints at the Hanover shale-Dunkirk shale contact (dashed line). Arrows point to tips of NS joints that have propagated from the Hanover shale into the Dunkirk shale; (B) NS joint (**NS**) arrested at the contact of a gray shale (below white dashed line) interval and overlying black shale within the Rhinestreet shale. Note concretionary carbonate horizon in the gray shale at the hammer.

Systematic NW and ENE joints show no deflection in propagation path as they approach concretions; instead, the joints propagated in-plane above and below the concretions (Fig. 30A). However, the occasional joints confined to a mechanical layer narrower than the width of the concretion define propagation paths that deflected into an orientation approximately normal to the interface. The majority of systematic NW and ENE joints (>90%) failed to penetrate concretions (Fig. 30B); one in ten ENE joints were observed to have propagated no more than a centimeter into concretions before arresting.

Systematic NS joints, while grossly similar to NW and ENE joints, differ from their younger counterparts in the nature of their interactions with embedded concretions. Anywhere from 30% to 70% of NS-trending joints, depending upon one's field location, completely cleave lenticular concretions (Fig. 31A). Few NS joints interface with larger ellipsoidal concretions common to black shale. However, the infrequent NS joints that propagated upward from gray shale into concretion-bearing interval within black shale typically penetrate deeply (> 4 cm) into the concretions (Fig. 31B). Occasionally, NS joints in gray shale can be observed cutting concretions in one stratigraphic interval but are arrested at interfaces with concretions in immediately over- and/or under-lying horizons (Fig. 31C). The few NS joints whose width is less than that of the concretions with which they interact display propagation paths that curve toward interfaces (Fig. 31D).

NW- and ENE-trending joints of the LED are NHFs that propagated as a consequence of the transformation of kerogen in the organic-rich black shale to hydrocarbons at burial depths >2.3 km (Lash et al., 2004; Lash and Engelder, 2005), an interpretation confirmed by their interactions with embedded concretions. Specifically, P_p in black shale was driven well above hydrostatic by catagenesis and sustained by a tight, strongly anisotropic microfabric (e.g., Lash and Engelder, 2005). Increasing P_p ultimately reduced the compressive minimum horizontal stress to an effective tensile stress initiating the NW- and later ENE-trending fluid loaded joints. The relatively stiff (i.e., high modulus) concretions embedded in the overpressured black shale, however, remained under effective compressive stress thereby suppressing penetration by NHFs beyond the carapace of the concretion (McConaughy and Engelder, 1999).

The critical difference between systematic NW and ENE joints and the older NS joints is that the latter penetrate deeply and/or completely cut many, but by no means all, concretions. We suggest that these joints originated within the higher modulus concretionary carbonate by a thermoelastic contraction

driving mechanism. This scenario requires a uniform level of extensional elastic strain distributed over the entire Upper Devonian shale succession of the LED. Presuming elastic extension, the higher modulus diagenetic carbonate would fail in tension before the lower modulus shale, which remained under effective compression at a given depth of burial (e.g., McConaughy and Engelder, 1999). This interpretation is borne out by the local presence of NS joints confined to lenticular concretionary carbonate at the tops of the gray shale units (Fig. 32). However, the fact that not all concretions originated NS joints may reflect variable $CaCO_3$ abundance among concretions and its effect on elastic properties. The lack of NS joints originating in the ellipsoidal (lower aspect ratio) concretions in black shale suggests that tensile stress builds most effectively in the higher aspect ratio concretionary carbonate.

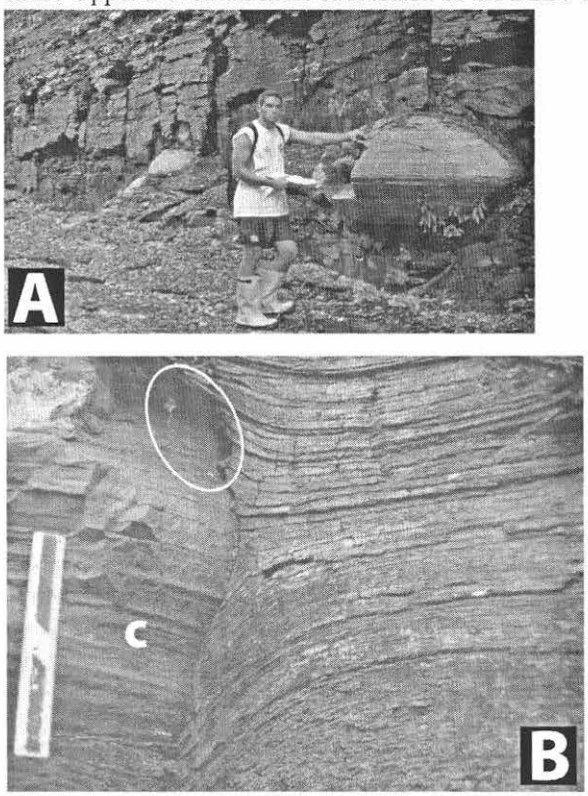

Fig. 30: (A) Tall ENE joint that propagated in-plane around two large concretions in the Rhinestreet shale. Person = 1.9 m; (B) Close-up of the interface of a concretion (**c**) and a NW joint that propagated in-plane around the concretion. Note the lack of penetration in the circled area where the black shale has been eroded. Scale = 14 cm.

Propagation of NS joints out of concretions and into the lower modulus host gray shale was likely aided by modestly overpressured pore fluid in the latter that migrated into the open joints. Elevated P_p within newly formed joints in the diagenetic carbonate would have enabled them to propagate through the shale under a fluid decompression mechanism. Indeed, the preferential growth of NS joints at the tops of the gray shale units probably reflects some degree of overpressure at these stratigraphic intervals. Deeper in the gray shale, however, lower (near hydrostatic) P_p would not have been high enough to create an effective tensile stress necessary for joint propagation. Thus, whereas NS joints were initiated in higher modulus diagenetic carbonate by thermoelastic contraction, they were driven through the lower modulus shale by fluid decompression. Evidence for this interpretation includes NS joints that cut concretions at one stratigraphic level (point of initiation) but failed to cleave or even penetrate concretions in immediately over- and under-lying stratigraphic intervals. Instead, the joints propagated in-plane around the rigid inclusions (Fig. 31C). Further, the curving of some NS joint trajectories toward normal to concretion interfaces (Fig. 31D) is more typical of fluid loaded joints than joints that originated by thermoelastic contraction (McConaughy and Engelder, 1999).

The switch in joint-driving mechanism recorded by the Rhinestreet shale from thermoelastic contraction supplemented by fluid decompression early in the deformation history of these deposits (*NS joints*) to a solely fluid decompression mechanism later in the tectonic cycle (*NW* and *ENE joints*) must be considered in terms of our present understanding of Alleghanian tectonics. The inception of the Alleghanian orogeny in the central Appalachian Basin is nominally dated by the initial accumulation of the Chesterian Mauch Chunk delta deposits shed from an eastern source area over the Greenbrier and Loyalhanna limestones (Hatcher et al., 1989; Faill, 1997). The end of the Mississippian, however, witnessed a change in sedimentary facies from the low-energy Mauch Chunk facies to westward spreading high-energy fluvial conglomeratic deposits of the Pottsville Formation (Meckel, 1967; Colton, 1970). This transition has been attributed to renewed uplift caused by crustal thickening during oblique convergence between the African portion of Gondwana and Laurentia, perhaps with microcontinents such as the Goochland terrane sheared between them (Faill, 1997). Oblique convergence early in the Alleghanian orogeny (Atokan and younger) is manifested by sequential dextral slip deformation along much of the central and southern Appalachian internides and development of ENE-trending (present direction) face cleat in coal in the central and southern Appalachians and ENE-trending joints in Frasnian black shales of

the Appalachian Plateau of New York state (Fig. 33; Gates and Glover, 1989; Hatcher, 2002; Engelder and Whitaker, 2006).

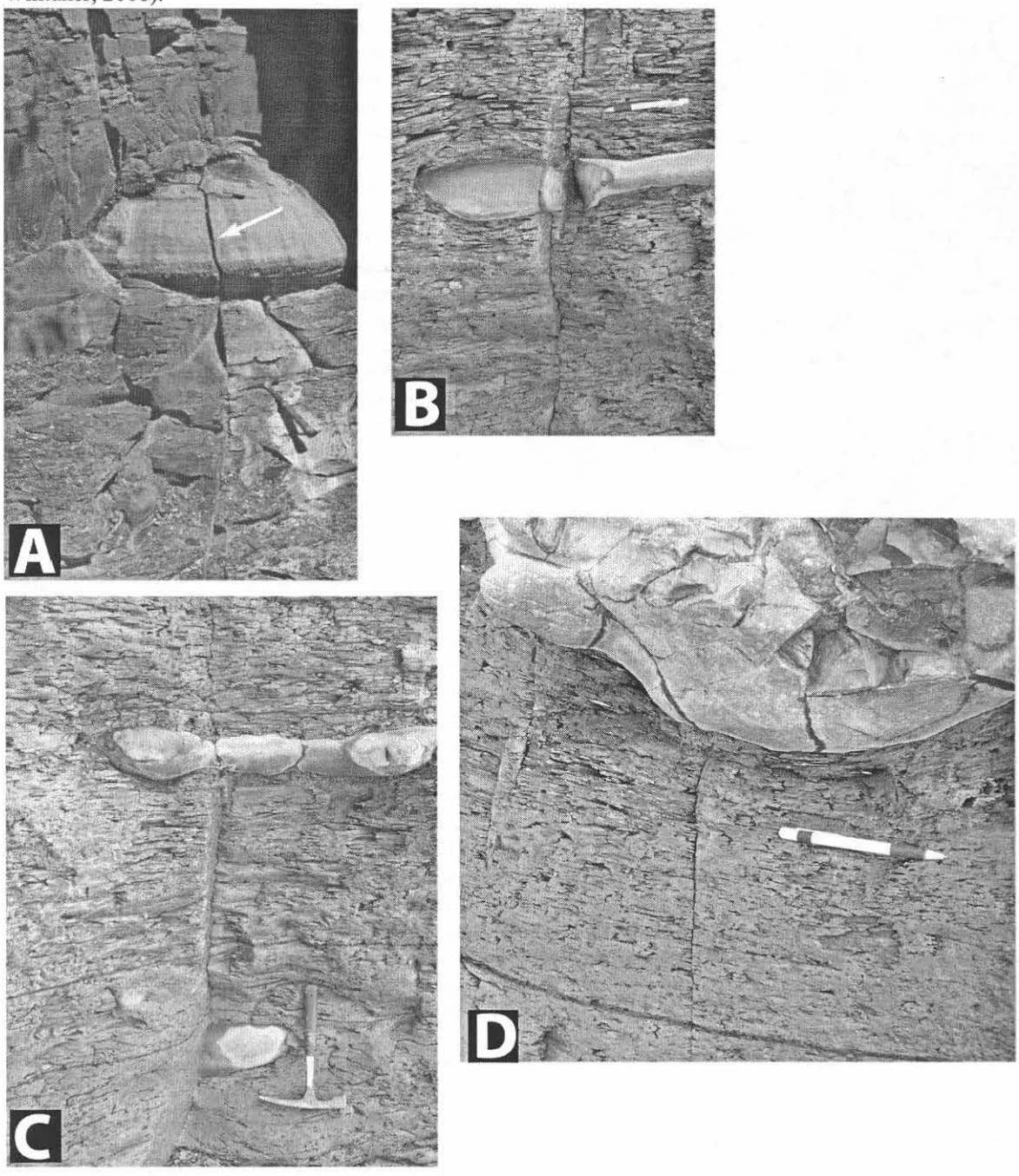

Fig. 31: (A) NS joint that cut a concretion in a gray shale interval of the Rhinestreet shale. Pen = 11 cm; (B) NS joint (indicated by arrow) that penetrated a large carbonate concretion in the Rhinestreet shale. An ENE joint (**ENE**) propagated in-plane (parallel to the picture) around the concretion. Note hammer for scale; (C) NS joint that cut the upper concretionary carbonate body but propagated in-plane around the lower concretion; (D) the propagation path of a narrow (relative to the width of the concretion) NS joint deflecting into a path perpendicular to the concretion interface. Pen = 11 cm.

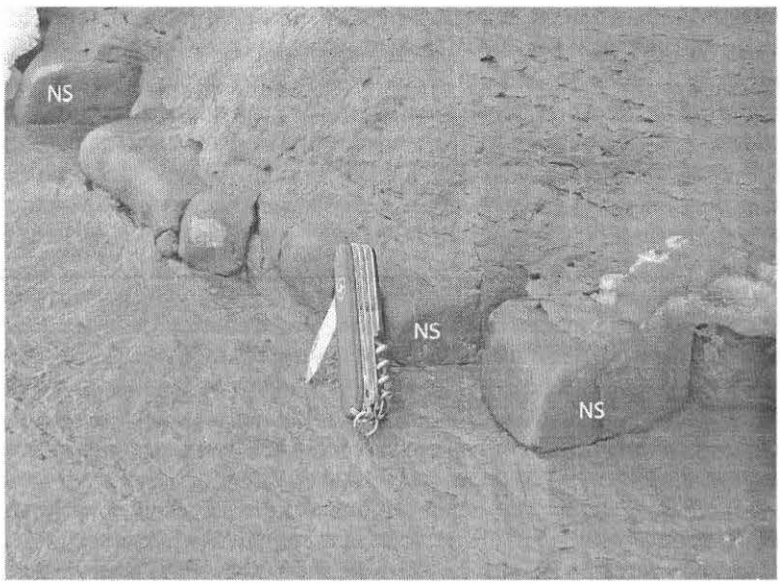

Fig. 32: NS joints (**NS**) that failed to propagate out of a thin carbonate layer at the top of the Hanover shale. Knife = 8 cm long.

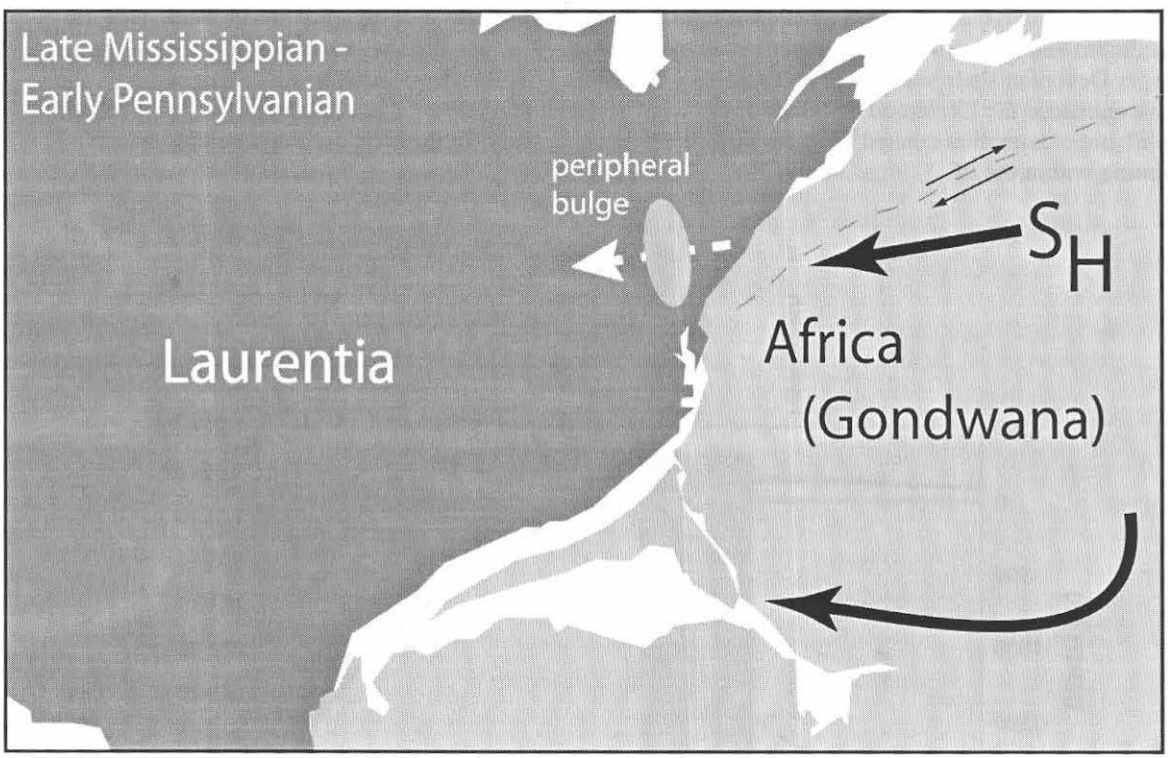

Fig. 33: Closure of the Theic ocean early in the Alleghanian orogeny by oblique convergence of Gondwana against Laurentia (modified after Hatcher, 2002). Refer to text for discussion.

The onset of Alleghanian tectonics is also manifested by a widespread Morrowan unconformity present in parts of the Appalachian system, including the southern tier of western New York state (e.g., Berg et al., 1983; Lindberg, 1985) (see Fig. 24). This unconformity is attributed to the cratonward migration of a peripheral bulge caused by early Alleghanian thrust loading in the southern Appalachians (Ettensohn and Chesnut, 1989). Similarly, loading during oblique convergence of Gondwana against Laurentia in New England and the Canadian Maritimes Appalachians drove a contemporary peripheral bulge across New York state and Pennsylvania (Fig. 33; Faill, 1997). The switch in joint-driving mechanism demonstrated by the jointing history of the Rhinestreet shale is consistent with passage of a peripheral bulge across the basin followed by burial of the shale succession to the oil window. The peripheral bulge was driven by crustal loading during the earliest stages of closure of Africa against the Laurentian plate in New England in Morrowan time (Fig. 33; Faill, 1997). The propagation of NS joints in gray shale of the LED prior to the formation of ENE-trending coal cleat elsewhere in the Applachian Basin (Engelder and Whitaker, 2006) and NW joints in the Rhinestreet shale indicates that the Upper Devonian shale succession of the LED had not yet been buried to the oil window by the time of the Morrowan unconformity, consistent with our burial/thermal model of the Rhinestreet shale (see Fig. 9). Indeed, the earliest coal cleat in the Appalachian Basin, which records oblique convergence in the New England Appalachians, post-dates the Morrowan (Engelder and Whitaker, 2006). Thus, the NS-trending joints in the LED are among the earliest structures that can be attributed to the Alleghanian orogeny.

Modeling of the peripheral bulge as having formed in response to the imposition of a line load at the edge of Laurentia and an overthrust fill of 2 km (Stewart and Watts, 1997) predicts that flexural curvature was highest in the approximate location of the Hudson Valley (Fig. 34). However, the great depth of burial and consequent high compressive stress in this more proximal area of the basin suppressed curvature-related tensile stress keeping the rocks under effective compression. Flexure-related uplift resulted in deep erosion in the LED and to the south in western Pennsylvania (Berg et al., 1983; Lindberg, 1985). Although the calculated tensile stress in this region of the Appalachian Basin was ~ one-half the maximum tensile stress magnitude generated by the bulge (Fig. 34), the shallow depth of burial of the Upper Devonian shale succession and resulting diminished overburden-related compressive stress would have enhanced the likelihood that these rocks were placed under effective tensile stress. Flexural-related uplift and exhumation created the near-surface tension necessary for thermoelastic contraction-driven jointing within the LED (Figs. 34 and 35).

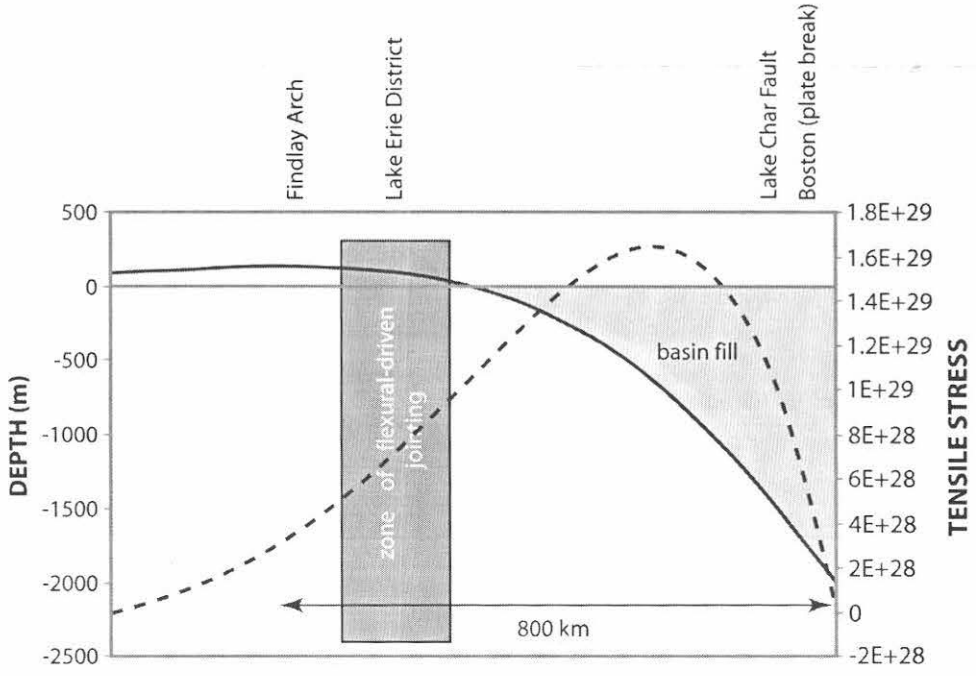

Fig. 34: Modeled peripheral bulge showing variations in the calculated tensile stress across the Appalachian Basin.

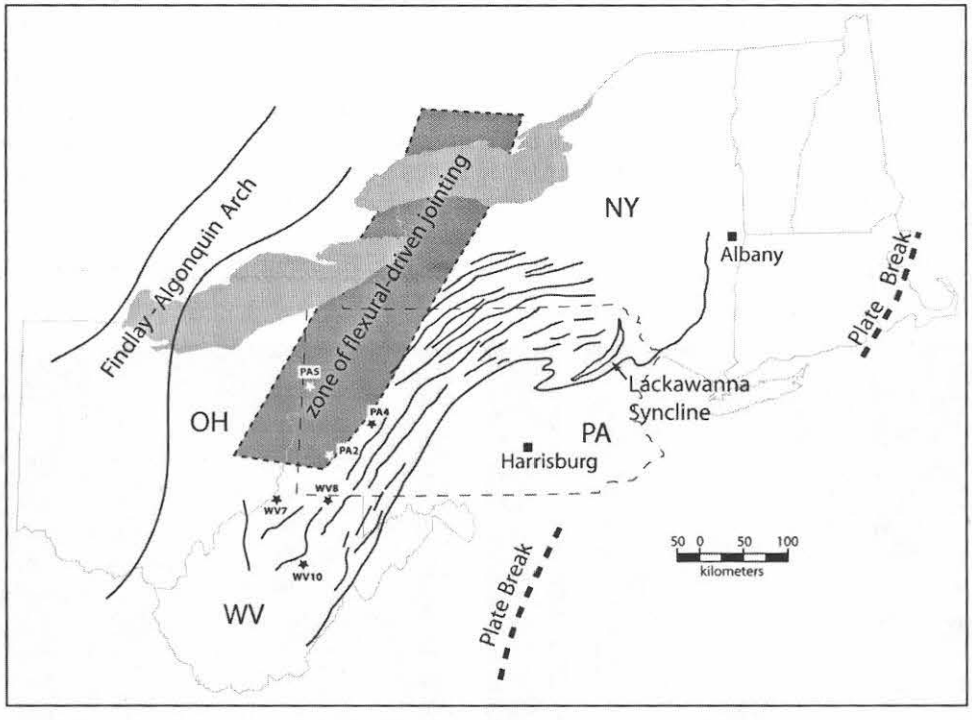

Fig. 35: Map showing the modeled area of NS jointing related to migration of the peripheral bulge. Black stars show locations of EGSP (Eastern Gas Shales Project) cores in which NS joints were observed in Middle Devonian rocks by Evans (1994).

NS joints initiated in higher modulus diagenetic carbonate by thermoelastic loading propagated through the host gray shale aided by modestly elevated P_p, which maintained an effective tensile stress in the lower modulus shale. Preferential propagation of NS joints by fluid decompression immediately beneath the black shale units suggests that the gray shale at these stratigraphic intervals was overpressured. Elevated P_p within the gray shale probably was caused by the increase in sedimentation rate at the end of the Devonian that attended rapid progradation of the Catskill Delta plain into the western New York region of the basin as described above. Overpressure generated by disequilibrium compaction may have been maintained by the formation of gas capillary seals induced by biogenic methanogenesis in the organic-rich Rhinestreet deposits (Blood and Lash, 2006; Lash, 2006b). Termination of the NS joints at the base of, or a short distance within, the black shale may reflect a somewhat lower modulus in the organic-rich deposits that suppressed the tensile stress carried by these rocks.

The proposed influence of the early Alleghanian peripheral bulge on the jointing history of the LED appears to have extended well to the south. The modeled region of the Appalachian Basin where uplift related to lithospheric flexure induced the systematic NS joints can be traced south into western and southwestern Pennsylvania where Evans (1994) described early NS-trending joints in Middle Devonian shale cores (Fig. 35). The locus of NS jointing in the Appalachian Basin was limited to the west by diminishing tensile stress; its eastern extent likely was controlled by the increasing depth of burial and consequent rise in compressive stress (Fig. 34).

MAIN STAGE JOINTING IN THE ALLEGHANIAN – EVOLUTION OF THE RHINESTREET FRACTURED RESERVOIR

The peripheral bulge had subsided by Atokan time when the Pottsville-equivalent Olean Conglomerate accumulated unconformably over eroded Upper Devonian and Kinderhookian strata (Edmunds et al., 1979; Berg et al., 1983; Lindberg, 1985; Dodge, 1992). Continued subsidence through the balance of the Pennsylvanian into Permian time carried the Upper Devonian shale succession of the LED into the oil window by ~ 275 Ma (Fig. 9; Lash, 2006c). The initial response to the Rhinestreet's entry into the oil window appears to have been the initiation of horizontal microcracks identical to those identified in the Upper Devonian Dunkirk shale (Lash and Engelder, 2005; Fig. 36). The intriguing aspect of these fractures is that they formed as open-mode cracks under a basinal stress field in which the greatest principal stress was vertical. Lash and Engelder (2005) explained this as a consequence of two factors: (1) a marked compaction-induced layer-perpendicular strength anisotropy and abundant flattened kerogen particles and (2) poroelastic deformation of these low permeability deposits pressurized by conversion of kerogen to bitumen and consequent establishment of a local *in situ* stress field favorable to the propagation of the microcracks in the horizontal plane.

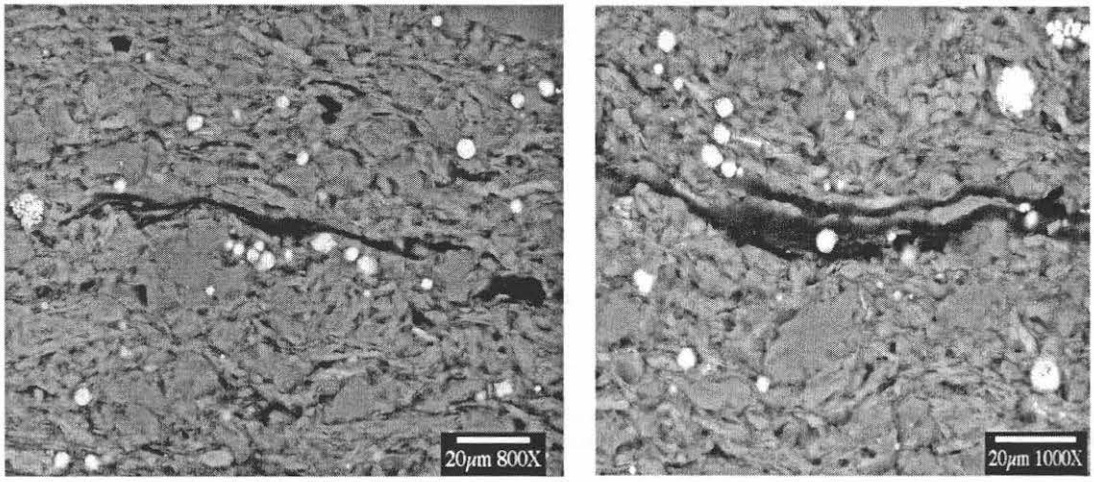

Fig. 36: Secondary electron images of bitumen-filled microcracks in Rhinestreet shale samples.

Continued burial of the Rhinestreet shale and further production of hydrocarbons resulted in the initiation of upward-propagating systematic fluid-loaded NW-trending joints or NHFs. The timing of the entry of these rocks into the oil window ties this phase of jointing to the emplacement of the Blue Ridge-Piedmont Megathrust sheet by rotational transpression of Gondwana along the southern Appalachians (Fig. 37; Hatcher, 2002). The transition from horizontal open-mode fractures to the propagation of vertical NHFs defies simple explanation. There is no evidence that the least principal stress direction flipped from vertical to horizontal. Indeed, in order to avoid violation of Occam's Razor, we assume that the regional stress field remained constant during the time that the horizontal microcracks and NW joints propagated. We propose that the switch from horizontal microcracks produced by catagenesis to vertical NHFs involved some degree of horizontal tensile stress that diminished the effective minimum horizontal stress induced by burial to zero enabling the vertical joints to form (e.g., Zhao and Jacobi, 1997). The origin of the hypothesized tensile stress may be found in the irregular nature of the Laurentian margin (i.e., the Pennsylvania salient; Hatcher, 2002) and its effect on plate edge stresses during rotational transpression of Gondwana along the central and southern Appalachians.

Systematic ENE joints formed toward the end of the Alleghanian tectonic cycle after the Rhinestreet shale had experienced greater hydrocarbon production (see Fig. 9). Further oblique convergence in the New England Appalachians, may have provided a level of lateral extension that, when combined with elevated P_p in the Rhinestreet shale, resulted in the propagation of the ENE joints. The stress field responsible for the ENE joints carried by the Rhinestreet shale had earlier produced ENE-trending systematic joints in Frasnian black shales in the Finger Lakes District as well as an early face cleat in coal deposits throughout the Appalachian system (Engelder and Whitaker, 2006). This stress system, unlike that which produced the NW joints, appears to have remained in place for the duration of the Alleghanian orogeny.

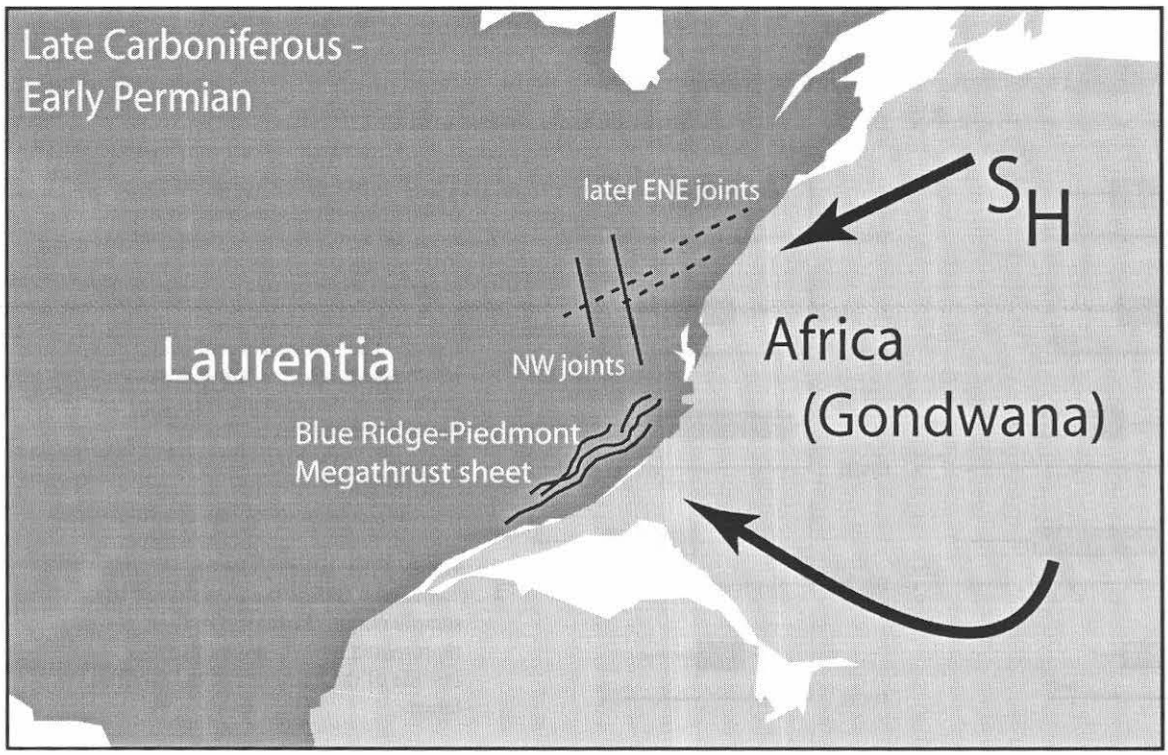

Fig. 37: Late Carboniferous-Early Permian head-on collision resulting in emplacement of the Blue Ridge-Piedmont Megathrust sheet (modified after Hatcher, 2002). Refer to text for discussion.

The Rhinestreet shale continued to undergo thermal maturation even as it was uplifted in post-Alleghanian time (see Fig. 9). ENE joints may have continued to propagate during this time, perhaps induced by post-Alleghanian flexural rebound of the Appalachian Basin (Blackmer et al., 1994). That is, at about the time the Rhinestreet shale had reached its peak thermal maturity (and hydrocarbon generation), unroofing of the Appalachian Plateau brought the overpressured black shale closer to the surface, resulting in thermoelastic contraction. Relaxation of the minimum horizontal compressive stress affecting the overpressured impermeable organic-rich deposits provided the mechanism for the preferential development of effective tensile stress within the black shale relative to gray shale units. Moreover, the ENE orientation of these joints may reflect the Early Cretaceous change in the remote stress system from one dominated by rift-related dynamics to one of compression caused by sea floor spreading of the North Atlantic Ocean (Miller and Duddy, 1989). Indeed, we are increasingly of the mind that there are, in fact, two sets of ENE joints – an older ENE set that was fluid-driven and a younger, less planar, set that may have been induced by thermoelastic contraction. As such, ENE joints in the LED may provide an example of similarly oriented joints having formed by different loading configurations. This intriguing story awaits much more work.

According to our jointing chronology for the Rhinestreet shale (as well as other Upper Devonian black shale units of the LED; Lash et al., 2004), fluid loaded ENE joints formed when the Rhinestreet had been in the oil window for a longer period of time than for formation of the NW joints. Evidence for this interpretation can be found in the relative density of joints of each set as manifested by their spacing characteristics. Joint spacing data for each joint set were obtained by simple scanline techniques (refer to Lash et al., 2004, for details of this method and statistical treatment of the data). Scanline analysis from the top of the Cashaqua shale through the Rhinestreet shale to its contact with the Angola shale reveals three trends regarding the degree of development of NW and ENE joints as measured by orthogonal spacing (Fig. 38). First, and perhaps most obvious, is the great range and high median spacing of ENE joints in the Cashaqua shale immediately below the Rhinestreet shale. NW joints are poorly represented at the top of the Cashaqua, an observation made of other gray shale units in the LED (see Fig. 27). Second, ENE joints

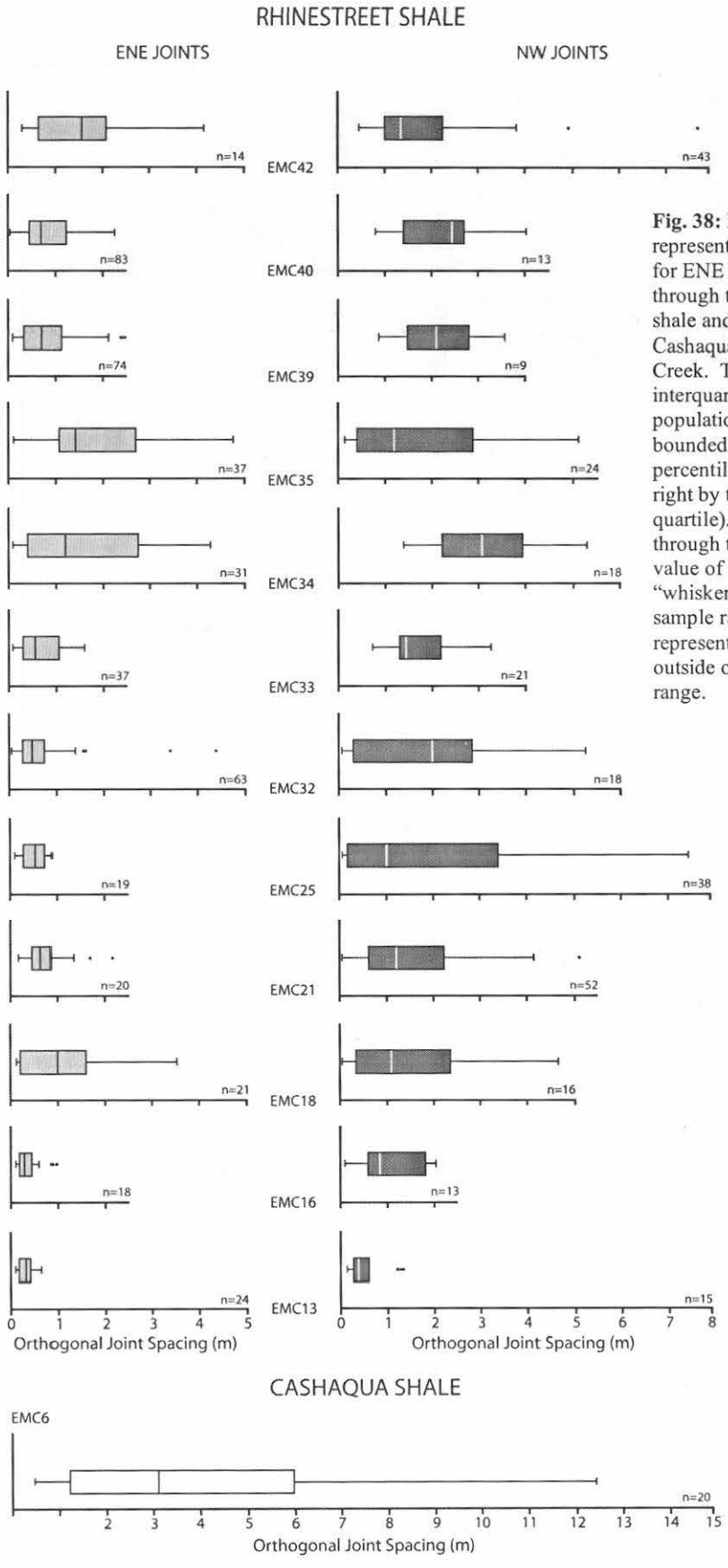

Fig. 38: Box-and-whisker diagrams representing joint spacing distribution for ENE and NW joints from the base through the top of the Rhinestreet shale and ENE joints at the top of the Cashaqua shale along Eighteenmile Creek. The box encloses the interquartile range of the data set population; the interquartile range is bounded on the left by the 25th percentile (lower quartile) and on the right by the 75th percentile (upper quartile). The vertical line drawn through the box defines the median value of the data population, and the "whiskers" define the extremes of the sample range. Statistical outliers are represented by data points that fall outside of the extremes of the sample range.

are more closely and uniformly spaced at a particular stratigraphic horizon than are NW joints at that same horizon. Finally, both NW and ENE joints demonstrate a subtle reduction in density upsection from the high TOC base of the Rhinestreet shale to its contact with the Angola shale (Fig. 38). The scanline data, then indicates that (1) both NW and ENE joints are most densely formed in the most organic-rich deposits, (2) within the Rhinestreet shale, ENE joints are more densely developed than are the older NW joints, and (3) the density of both NW and ENE joints correlate positively with TOC (Fig. 38). Trends similar to these have been described from elsewhere in the Middle and Upper Devonian succession of the Appalachian Plateau (Loewy, 1995; Lash et al., 2004).

Differences in spacing characteristics of the NW and younger ENE joints of the Rhinestreet shale can be thought of in terms of the progressive thermal maturation of a source rock. It is widely held that a set of natural fractures does not form instantaneously; rather, it evolves over a period of time becoming progressively denser (Fig. 39). Rives et al. (1992), for example, have demonstrated that the orthogonal spacing of a systematic joint set evolves from a negative exponential distribution early in its history to a log-normal distribution and finally to a normal distribution. Similarly, Narr (1991) and Becker and Gross (1996) maintain that as joint systems develop, orthogonal spacing becomes progressively smaller and more uniform. Ultimately, overlapping stress shadows between adjacent joints precludes the formation of new fractures in intervening unjointed volumes of rock (Fig. 39). The rock is said to be fracture saturated at this point. Time is a critical factor in this process - the longer the duration of fracturing under a given set of conditions, the closer a specific set approaches saturation. The Rhinestreet shale had just entered the oil window when it was affected by the remote stress field that gave rise to the NW joints. That is, production of hydrocarbons in the Rhinestreet shale had not proceeded long enough when the rocks reacted to the stress field responsible for emplacement of the Blue Ridge-Piedmont Megathrust sheet for the resultant joints to form with a density even close to saturation. Indeed, the wider range in joint spacing of the NW joints is more consistent with a negative exponential or log-normal distribution. Moreover, the general dearth of NW joints at the tops of gray shale units (see Fig. 27) may reflect a level of production in the underlying black shale incapable of driving these joints well up into the overlying gray shale. ENE-trending joints, having formed after the Rhinestreet had occupied the oil window for a prolonged period of time, are more densely and uniformly (close to saturation) developed than NW joints reflecting a greater level of production. Moreover, the great abundance of ENE joints at the tops of gray shale units (see Fig. 27) likely records the higher level of hydrocarbon production by the time the ENE joints were initiated in these rocks. An identical relationship of NW and younger ENE joints has been described from the Dunkirk shale (Lash et al., 2004).

CONCLUSIONS

The Rhinestreet shale is an unconventional or continuous-type hydrocarbon accumulation that satisfies most criteria of these systems, including a lack of obvious trap and seal. Indeed, the Rhinestreet shale, like other Devonian black shale units, is its own seal and reservoir; it is a self-sourced reservoir. However, in spite of general similarities among all continuous-type hydrocarbon accumulations, most differ in terms of more subtle parameters, including mineralogy (e.g., silt content, dominant clay mineral type), complexity of fractures and fracture history, reservoir thickness and internal stratigraphy, compaction and burial/thermal history, kerogen type, TOC and variations in TOC, both vertically and laterally. Thus, it is important to treat each continuous-type hydrocarbon accumulation as an individual situation and take from it what might be applied to the study of other similar accumulations.

The Rhinestreet shale has a rather complex burial/thermal history (see Fig. 9). Its early compaction history records the fitful burial of the sediment resulting in the formation of the laterally persistent concretionary horizons that could have influenced fluid migration. The marked increase in sedimentation rate in the latter half of the Famennian, likely induced by rapid progradation of the Catskill Delta complex, perhaps the result of glacio-eustacy, brought normal mechanical compaction of the Rhinestreet shale to an end, well shy of its maximum burial depth. However, this initial overpressure event caused by disequilibrium compaction, an Acadian event, failed to initiate fractures.

Morrowan time was marked by uplift of the Devonian-Mississippian succession in western New York state and western Pennsylvania, a result of the westward migration of a peripheral bulge produced by loading of the Laurentian plate edge at the onset of the Alleghanian orogeny. Burial/thermal modeling of

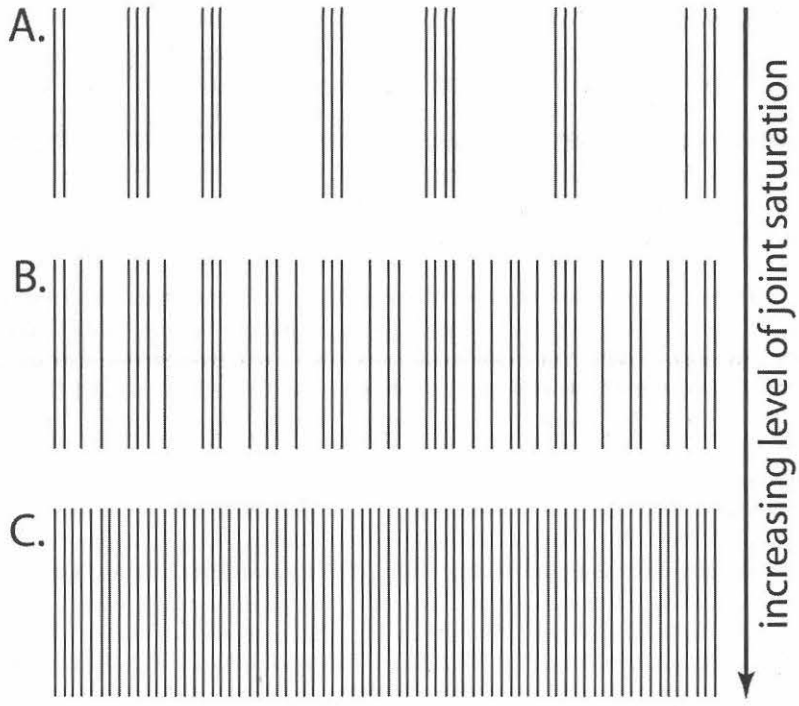

Fig. 39: Schematic diagram showing the evolution of fracture spacing (modified after Peacock and Mann, 2005). Refer to text for discussion.

measured vitrinite reflectance of the Rhinestreet shale suggests that the organic-rich rocks had not yet been buried to the oil window when they were uplifted (see Fig. 9). Thermoelastic contraction of the uplifted sequence in concert with reduced burial-related stress induced NS-trending joints in the higher modulus diagenetic carbonate. Moderately elevated P_p in the host gray shale as a consequence of the above-mentioned disequilibrium compaction enabled the newly formed joints to propagate through the shale as natural hydraulic fractures.

Renewed subsidence in Atokan time carried the Rhinestreet shale into the oil window by ~275 Ma. The initial result of catagenesis was the formation of horizontal bitumen-filled microcracks, which caused this tight unit to become even more impermeable. Soon after this, NW-trending vertical natural hydraulic fractures formed. The Rhinestreet appears to have entered the oil window roughly coeval with emplacement of the Blue Ridge-Piedmont Megathrust sheet. However, because the Rhinestreet may not have been in the oil window long enough to achieve little more than modest production, NW joints set did not come close to saturating the source rock. The Rhinestreet shale continued to produce hydrocarbons as it approached its modeled maximum burial depth of ~3.1 km. As a result, ENE joints that formed under the influence of the continued oblique plate convergence in the New England Appalachians came closer to saturating the Rhinestreet source rock. These joints, having more drive behind them, propagated higher in the sequence. ENE joints may have continued to form during post-Alleghanian uplift of the Appalachian Plateau as a consequence of thermal contraction.

Clearly, the geologic history of the Rhinestreet shale differs from other continuous-type hydrocarbon accumulations most notably in the timing of its entry into the oil window and resultant chronology, orientation and density of fracturing. These factors are crucial to exploration and production strategies of such a unit as the Rhinestreet shale. Our ongoing work demonstrates that a fuller understanding of the intricacies of a petroleum system like that of the Rhinestreet shale requires a multi-faceted approach that entails the analysis of the system from the submicroscopic scale to the lithospheric stress level.

REFERENCES

Algeo, T.J., Berner, R.A., Maynard, J.B., and Sheckler, S.E., 1995, Late Devonian oceanic anoxic events and biotic crises: "Rooted" in the evolution of vascular land plants?; GSA Today, v. 5, p. 64-66.

Anderson, T.F., and Arthur, M.A., 1983, Stable isotopes of oxygen and carbon and their application to sedimentologic and environmental problems, in Arthur, M.A., Anderson, T.F., Kaplan, I.R., Veizer, J., and Land, L.S., editors, Stable Isotopes in Sedimentary Geology: Society of Economic Paleontologists and Mineralogists Short Course Notes, 10, p. 1-151.

Aplin, A.C., Matenaar, I.F., and van der Pluijm, B., 2003, Influence of mechanical compaction and chemical diagenesis on the microfabric and fluid flow properties of Gulf of Mexico mudstones: Journal of Geochemical Exploration, v. 78-79, p. 449-451.

Astin, T.R., and Scotchman, I.C., 1988, The diagenetic history of some septarian concretions from the Kimmeridge Clay, England: Sedimentology, v. 35, p. 349-368.

Athy, L.F., 1930, Density, porosity and compaction of sedimentary rocks: American Association of Petroleum Geologists Bulletin, v. 14, p. 1-24.

Audet, D.M., 1996, Compaction and overpressuring in Pleistocene sediments on the Louisiana Shelf, Gulf of Mexico: Marine and Petroleum Geology, v. 13, p. 467-474.

Audet, D.M., and McConnell, J.D.C., 1992, Establishing resolution limits for tectonic subsidence curves by forward basin modeling: Marine and Petroleum Geology, v. 11, p. 283-298.

Baird, G.C., and Brett, C.E., 1991, Submarine erosion on the anoxic sea floor: stratinomic, palaeoenvironmental, and temporal significance of reworked pyrite-bone deposits, *in* Tyson, R.V., and Pearson, T.H., eds., *Modern and Ancient Continental Shelf Anoxia*: Geological Society, London, Special Publication No. 58, p. 233-257.

Baird, G.C., and Brett, C.E., 2003, Shelf and off-shelf deposits of the Tully Formation in New York and Pennsylvania: faunal incursions, eustasy and tectonics: *Cour. Forsch.-Inst. Senckenberg*, v. 242, p. 141-156.

Baird, G.C., and Lash, G.G., 1990, Devonian strata and environments: Chautauqua County region: New York State: New York State Geological Association, 62nd Annual Meeting Guidebook, Sat. A1-A46.

Baldwin, B., and Butler, C.O., 1985, Compaction curves: *American Association of Petroleum Geologists Bulletin*, v. 69, p. 622-626.

Beaumont, C., Quinlan, G.M., and Hamilton, J., 1987, The Alleghanian orogeny and its relationship to the evolution of the eastern interior, North America, *in* Beaumont, C., and Tankard, A.J., eds., *Sedimentary basins and basin-forming mechanisms*: Canadian Society of Petroleum Geologists, Memoir 12, p. 425-446.

Beaumont, C., G. Quinlan, and J. Hamilton, 1988, Orogeny and stratigraphy: numerical models of the Paleozoic in the Eastern Interior of North America: *Tectonics*, v. 7, p. 389-416.

Becker, A., and Gross, M.R., 1996, Mechanism for joint saturation in mechanically layered rocks: an example from southern Israel: *Tectonophysics*, v. 257. p. 223-237.

Bennett, R.H., Bryant, W.R., and Keller, G.H., 1977, Clay fabric and geotechnical properties of selected submarine sediment cores from the Mississippi Delta: NOAA Professional Paper No. 9, U.S. Department of Commerce/NOAA/ERL, 86 p.

Bennett, R.H., Bryant, W.R., and Keller, G.H., 1981, Clay fabric of selected submarine sediments: fundamental properties and models: *Journal of Sedimentary Petrology*, v. 51, p. 217-232.

Bennett, R.H., O'Brien, N.R., and Hulbert, M.H., 1991, Determinants of clay and shale microfabric signatures: processes and mechanisms, *in* Bennett, R.H., Bryant, W.R., and Hulbert, M.H., eds., *Microstructure of Fine-Grained Sediments*: New York, Springer-Verlag, p. 5-31.

Berg, T.M., McInerney, M.K., Way, J.H., and MacLachlan, D.B., 1983, *Stratigraphic correlation chart of Pennsylvania*: Pennsylvania Topographic and Geologic Survey, General Geology Report 75.

Berner, R.A., 1980, *Principles of Chemical Sedimentology*: McGraw-Hill, New York, 240 p.

Blackmer, G.C., Omar, G.I., and Gold, D.P., 1994, Post-Alleghanian unroofing history of the Appalachian Basin, Pennsylvania, from apatite fission track analysis and thermal models: *Tectonics*, v. 13, p. 1259-1276.

Blood, D.R., and Lash, G.G., 2006, Calculation of the fluid retention burial depth for the Upper Devonian Rhinestreet shale, western New York State: Geological Society of America Abstracts with Programs, vol. 38, p. 64.

Bond, G.C., and Kominz, M.A., 1991, Paleozoic sea level and tectonic events in cratonic margins and cratonic interiors of North America: *Journal of Geophysical Research*, v. 96, p. 6619-6639.
Bredehoeft, J.D., Djevanshir, R.D., and Belitz, K.R., 1988, Lateral fluid flow in a compacting sand-shale sequence, south Caspian Sea: *American Association of Petroleum Geologists Bulletin*, v. 72, p. 416-424.
Brett, C.E., and Baird, G.C., 1996, Middle Devonian sedimentary cycles and sequences in the northern Appalachian basin, in Witzke, B.J., Ludvigson, G., and Day, J.E., eds., *Paleozoic sequence stratigraphy*: Geological Society of America, Special Paper 306, p. 213-242.
Broecker, W.S., and Peng, T.-H., 1982, *Tracers in the sea*: Palisades, New York, Lamont-Doherty Geological Observatory, Columbia University, 690 p.
Buggisch, W., 1991, The global Frasnian-Famennian "Kellwasser Event": *Geol. Rundsch.*, v. 80, p. 49-72.
Burland, J.B., 1990, On the compressibility and shear strength of natural clays: *Geotechnique*, v. 40, p. 329-378.
Burrus, J., 1998, Overpressure models for clastic rocks, their relation to hydrocarbon expulsion: a critical reevaluation, *in* Law, B.E., Ulmishek, G.F., and Slavin, V.I., eds., *Abnormal pressures in hydrocarbon environments*: American Association of Petroleum Geologists, Memoir 70, p. 35-63.
Carr, A.D., 2000, Suppression and retardation of vitrinite reflectance, part 1. Formation and significance for hydrocarbon generation: *Journal of Petroleum Geology*, v. 23, p. 313-343.
Chadwick, G.H., 1920, Large fault in western New York: *Geological Society of America Bulletin*, v. 31, p. 117-120.
Charpentier, D., Worden, R.H., Dillon, C.G., and Aplin, A.C., 2003, Fabric development and the smectite to illite transition in Gulf of Mexico mudstones: an image analysis approach: *Journal of Geochemical Exploration*, v. 78-79, p. 459-463.
Clarke, J.M., 1903, *Classification of the New York series of geologic formations*: New York State Museum Handbook, no. 19, 28 p.
Clifton, H.E., 1957, The carbonate concretions of the Ohio Shale: *Ohio Journal of Science*, v. 57, p. 114-124.
Colton, G.W., 1967, Orientation of carbonate concretions in the Upper Devonian of New York: U.S. Geological Survey, Professional Paper 575-B, p. B57-B59.
Coniglio, M., and Cameron, J.S., 1990, Early diagenesis in a potential oil shale: evidence from calcite concretions in the Upper Devonian Kettle Point Formation, southwestern Ontario: *Bulletin of Canadian Petroleum Geology*, v. 38, p. 64-77.
Conybeare, C.E.B., 1967, Influence of compaction on stratigraphic analysis: *Bulletin of Canadian Petroleum Geology*, v. 15, p. 331-345.
Criss, R.E., Cooke, G.A., and Day, S.D., 1988, An organic origin for the carbonate concretions of the Ohio Shale: United States Geological Survey Bulletin 1836, 21 p.
Daly, R.A., 1900, The calcareous concretions of Kettle Point, Lambton County, Ontario: *Journal of Geology*, v. 8, p. 135-150.
Demaison, G., and Huizinga, B.J., 1994, Genetic classification of petroleum systems using three factors: charge, migration, and entrapment, *in* Magoon, L.B., and Dow, W.G., eds., *The Petroleum System--From Source to Trap*: American Association of Petroleum Geologists, Memoir 60, p. 73-89.
de Witt, W., Jr., and Colton, G.W., 1978, Physical stratigraphy of the Genesee Formation (Devonian) in western and central New York: United States Geological Survey Professional Paper 1032-A, p. A1-A22.
de Witt, W., Jr., Roen, J.B., and Wallace, L.G., 1993, Stratigraphy of Devonian black shales and associated rocks in the Appalachian Basin: United States Geological Survey Bulletin 1909, p. B1-B47.
Dickinson, G., 1953, Geological aspects of abnormal reservoir pressures in Gulf Coast Louisiana: *American Association of Petroleum Geologists Bulletin*, v. 37, p. 410-432.
Dix, G.R., and Mullins, H.T., 1987, Shallow, subsurface growth and burial alteration of Middle Devonian calcitic concretions: *Journal of Sedimentary Petrology*, v. 57, p. 140-152.
Dodge, C.H., 1992, Bedrock lithostratigraphy of Warren County, Pennsylvania: Guidebook for the 57th Annual Field Conference of Pennsylvania Geologists, Field Conference of Pennsylvania Geologists, Inc., Harrisburg, Pennsylvania, 1-20.
Duck, R.W., 1990, S.E.M. study of clastic fabrics preserved in calcareous concretions from the late-Devensian Errol Beds, Tayside: *Scottish Journal of Geology*, v. 26, p. 33-39.

Edmunds, W.E., Berg, T.M., Sevon, W.D., Piotrowski, R.C., Heyman, L., and Rickard, L.V., 1979, The Mississippian and Pennsylvanian (Carboniferous) systems in the United States – Pennsylvania and New York: U.S. Geological Survey Professional Paper 1110-B, p. B1-B33.

El Albani, A., Vachard, D., Kuhnt, W., and Thurow, J., 2001, The role of diagenetic carbonate concretions in the preservation of the original sedimentary record: *Sedimentology*, v. 48, p. 875-886.

Engelder, T., 1985, Loading paths to joint propagation during a tectonic cycle: an example from the Appalachian Plateau, USA: *Journal of Structural Geology*, v. 7, p. 459-476.

Engelder, T., 1987, Joints and shear fractures in rock, *in* Atkinson. B. K, ed., *Fracture mechanics of rock*: London, England, Academic Press, p. 27–69.

Engelder, T., and Fischer, M.P., 1996, Loading configurations and driving mechanisms for joints based on the Griffith energy-balance concept: *Tectonophysics*, v. 256, p. 253-277.

Engelder, T., and Geiser, P.A., 1980, On the use of regional joint sets as trajectories of paleostress fields during the development of the Appalachian Plateau, New York: *Journal of Geophysical Research*, v. 94, p. 6319-6341.

Engelder, T., and Gross, M., 1993, Curving cross joints and the neotectonic stress field in eastern North America: *Geology*, v. 21, p. 863-866.

Engelder, T., and Lacazette, A., 1990, Natural hydraulic fracturing, *in* Barton, N. and Stephansson, O., eds., *Rock Joints*: A.A. Balkema, Rotterdam, p. 35-43.

Engelder, T., and Oertel, G., 1985, The correlation between undercompaction and tectonic jointing within the Devonian Catskill Delta: *Geology*, v. 13, p. 863-866.

Engelder, T., and Whitaker, A., 2006, Post-Desomoinesian epeirogenic deformation as a prelude to the Alleghanian orogeny: *Geology*, v. 34, p. 581-584.

Espitalie, J., 1986, Use of T_{max} as a maturation index for different types of organic matter. Comparison with vitrinite reflectance, *in*, Burrus, J., ed., *Thermal Modeling in Sedimentary Basins*: Editions Technip, Paris, p. 475-496.

Ettensohn, F.R., 1985, The Catskill Delta Complex and the Acadian Orogeny: A model, *in* Woodrow, D.L., and Sevon, W.D., eds., *The Catskill Delta*: Geological Society of America, Special Paper 201, p. 39-49.

Ettensohn, F.R., 1987, Rates of relative plate motion during the Acadian orogeny based on the spatial distribution of black shales: *Journal of Geology*, v. 95, p. 572-582.

Ettensohn, F.R., 1992, Controls on the origin of the Devonian-Mississippian oil and gas shales, east-central United States: *Fuel*, v. 71, p. 1487-1492.

Ettensohn, F.R., and Chesnut, D.R., Jr., 1989, Nature and probably origin of the Mississippian-Pennsylvania unconformity in the eastern United States: Internationale Congres de Stratigraphic et Geologie du Carbonifere, Beijing, 11th, Compte Rendu 4, p. 145-159.

Evans, M.A., 1994, Joints and decollement zones in the Middle Devonian shale: evidence for multiple deformation event in the central Appalachian Plateau: *Geological Society of America Bulletin*, v. 106, p. 447-460.

Faas, R.W., and Crocket, D.S., 1983, Clay fabric development in a deep sea core: Site 515, Deep Sea Drilling Project Leg 72: Initial Reports of the Deep Sea Drilling Project, v. 72, p. 519-535.

Faill, R.T., 1997, A geologic history of the north-central Appalachians, part 2: the Appalachian basin from the Silurian through the Carboniferous: *American Journal of Science*, v. 297, p. 729-761.

Falvey, D.A., and Deighton, I., 1982, Recent advances in burial and thermal geohistory analysis: *Journal of the Australian Petroleum Exploration Association*, v. 22, p. 65-81.

Filer, J.K., 2002, Late Frasnian sedimentation cycles in the Appalachian basin – possible evidence for high frequency eustatic sea-level changes: *Sedimentary Geology*, v. 154, p. 31-52.

Filer, J.K., 2003, Stratigraphic evidence for a Late Devonian possible back-bulge basin in the Appalachian basin, United States: *Basin Research*, v. 15, p. 1-13.

Finley, W.R., 1990, Differential compaction influences on structure in West Cameron Block 225 Field: *American Association of Petroleum Geologists Bulletin*, v. 74, p. 1495.

Fischer, M., Gross, M.R., Engelder, T., and Greenfield, R.J., 1995, Finite element analysis of the stress distribution around a pressurized crack in a layered elastic medium: implications for the spacing of fluid-driven joints in bedded sedimentary rock: *Tectonophysics*, v. 247, p. 49-64.

Folk, R.L., 1965, Some aspects of recrystallization in ancient limestones, *in* Pray, L.C., and Murray, R.C., editors, *Dolomitzation and Limestone Diagenesis: A symposium*: Society of Economic Paleontologists and Mineralogists, Special Publication 13, p. 14-48.

Gallagher, K., 1989, An examination of some uncertainties associated with estimates of sedimentation rates and tectonic subsidence: *Basin Research*, v. 2, p. 97-114.
Gallagher, K., and Lambeck, K., 1989, Subsidence, sedimentation and sea-level changes in the Eromanga Basin, Australia: *Basin Research*, v. 2, p. 115-131.
Gates, A. E. and Glover, L., III, 1989, Alleghanian tectonothermal evolution of the dextral transcurrent Hylas Zone, Virginia; *Journal of Structural Geology*, v. 11, p. 407-419.
Gautier, D.L., 1982, Siderite concretions: indicators of early diagenesis in the Gammon shale (Cretaceous): *Journal of Sedimentary Research*, v. 52, p. 859-871.
Gerlach, J.B., 1987, Post-Devonian burial history of the New York state Appalachian Basin based on Lopatin modeling of regional variations in vitrinite reflectance trends: M.S. Thesis, State University of New York at Stony Brook, Stony Brook, New York, 135 p.
Gerlach, J.B., and Cercone, K.R., 1993, Former Carboniferous overburden in the northern Appalachian Basin: a reconstruction based on vitrinite reflectance: *Organic Geochemistry*, v. 20, p. 223-232.
Giles, M.R., Indrelid, S.L., and James, D.M.D., 1998, Compaction - the great unknown in basin modeling, *in* Duppenbecker, S.J., and Iliffe, J.E., eds., *Basin modeling: practice and progress*: Geological Society, London, Special Publication 141, p. 15-43.
Goulty, N.R., 2004, Mechanical compaction behaviour of natural clays and implications for pore pressure calculation: *Petroleum Geoscience*, v. 10, p. 73-79.
Gradstein, F.M., OGG, J.G. and Smith, A.G., 2004, *A geologic time scale 2004*: Cambridge University Press, New York, 610 p.
Grauls, D., 1998, Overpressure assessment using a minimum principal stress approach, *in* Mitchell, A., and Grauls, D., eds., *Overpressures in Petroleum Exploration*: Elf EP-Editions, Pau, France, 22, p. 137-147.
Hallam, A., 1962, A band of extraordinary calcareous concretions in the Upper Lias of Yorkshire, England: *Journal of Sedimentary Petrology*, v. 32, p. 840-847.
Ham, H.H., 1966, New charts help estimate formation pressures: *Oil and Gas Journal*, v. 64, p. 58-63.
Hamilton, E.L., 1976, Variations of density and porosity with depth in deep-sea sediments: *Journal of Sedimentary Petrology*, v. 46, p. 280-300.
Hamilton-Smith, T., 1993, Stratigraphic effects of the of the Acadian orogeny in the authochthonous Appalachian basin, *in* Roy, D.C., and Skehan, J.W., eds., *The Acadian orogeny: recent studies in New England, Maritime Canada, and the autochthonous foreland*: Geological Society of America, Special Paper 275, p. 153-164.
Hansen, S., 1996, A compaction trend for Cretaceous and Tertiary shales on Norwegian Shelf based on sonic transit times: *Petroleum Geoscience*, v. 2, p. 159-166.
Harrison, W. J., and Summa, L. L., 1991, Paleohydrology of the Gulf of Mexico basin: *American Journal of Science*, v. 291, p. 109–176.
Harrold, T.W.D., Swarbrick, R.E., and Goulty, N.R., 1999, Pore pressure estimation from Mudrock porosities in Tertiary Basins, Southeast Asia: *American Association of Petroleum Geologists Bulletin*, v. 83, p. 1057-1067.
Harrold, T.W.D., Swarbrick, R.E., and Goulty, N.R., 2000, Pore pressure estimation from mudrock porosities in Tertiary basins, southeast Asia, *in* Swarbrick, R.E., ed., *Overpressure 2000 – workshop proceedings*: CD volume, paper OP2000_9, 6 p.
Hart, B.S., Flemings, P.B., and Deshpande, A., 1995, Porosity and pressure: Role of compaction disequilibrium in the development of geopressures in a Gulf Coast Pleistocene basin: *Geology*, v. 23, p. 45-48.
Hatcher, R.D., Jr., 2002, Alleghanian (Appalachian) orogeny, a product of zipper tectonics: rotational transpressive continent-continent collision and closing of ancient oceans along irregular margins, *in* Martínez Catalán, J.R., Hatcher, R.D., Jr., Arenas, R., and Díaz García, F., eds., *Variscan-Appalachian dynamics: the building of the late Paleozoic basement*: Geological Society of America, Special Paper 364, p. 199-208.
Hatcher, R.D., Jr., Thomas, W.A., Geiser, P.A., Snoke, A.W., Mosher, S., and Wiltschko, D.V., 1989, Alleghanian orogen, *in* Hatcher, R.D., Jr., Thomas, W.A., and Viele, G.W., eds., *The Appalachian-Ouachita Orogen in the United States*: Boulder, Colorado, Geological Society of America, The Geology of North America, v. F-2, p. 233-318.
Heckel, P.H., 1973, *Nature, origin, and significance of the Tully limestone: An anomalous unit in the Catskill Delta, Devonian of New York*: Geological Society of America, Special Paper 138, 243 p.

Hedberg, H.D., 1926, The effect of gravitational compaction on the structure of sedimentary rocks: *American Association of Petroleum Geologist, Bulletin*, v. 10, p. 1035-1072.
Hedberg, H.D., 1936, Gravitational compaction of clays and shales: *American Journal of Science*, v. 31, p. 241-287.
Hegarty, K.A., Weissel, J.K., and Mutter, J.C., 1988, Subsidence history of Australia's southern margin: constraints on basin models: *American Association of Petroleum Geologists Bulletin*, v. 72, p. 615-633.
Heling, D., 1970, Micro-fabrics of shales and their rearrangement by compaction: *Sedimentology*, v. 15, p. 247-260.
Heppard, P.D., Cander, H.S., and Eggerston, E.B., 1998, Abnormal pressure and the occurrence of hydrocarbons in offshore eastern Trinidad, West Indies, *in* Law, B.E., Ulmishek, G.F., and Slavin, V.I., eds., *Abnormal pressures in hydrocarbon environments*: American Association of Petroleum Geologists, Memoir 70, p. 215-246.
Hermanrud, C., 1993, Basin modeling techniques – an overview, *in* Dore, A.G., et al., eds., *Basin modeling: advances and applications*: Norwegian Petroleum Society, Memoir 3, p. 1-34.
Hermanrud, C., Wensaas, L., Teige, G.M.G., Vik, E., Nordgard Bolas, H.M., and Hansen, S., 1998, Shale porosities from well logs on Haltenbanken (offshore mid-Norway) show no influence of overpressuring, *in* Law, B.E., Ulmishek, G.F., and Slavin, V.I., eds., *Abnormal pressures in hydrocarbon environments*: American Association of Petroleum Geologists, Memoir 70, p. 65-85.
Ho, N.C., Peacor, D.R., and Van der Pluijm, B.A., 1999, Preferred orientation of phyllosilicates in Gulf Coast mudstones and relation to smectite-illite transition: *Clays and Clay Mineralogy*, v. 47, p. 495-504.
Hosterman, J.W., 1993, Illite crystallinity as an indicator of the thermal maturity of Devonian black shales in the Appalachian Basin: United States Geological Survey, Professional Paper 1909, G1-G9.
Huang, Z., and Gradstein, F., 1990, Depth-porosity relationship from deep sea sediments: *Scientific Drilling*, v. 1, p. 157-162.
Hudak, P.F., 1992, Terminal decollement tectonics in the Appalachian Plateau of northwestern Pennsylvania: *Northeastern Geology*, v. 14, p. 108-112.
Hudson, J.D., 1977, Stable isotopes and limestone lithification: *Quarterly Journal of the Geological, London*, v. 133, p. 637-660.
Hudson, J.D., 1978, Concretions, isotopes and the diagenetic history of the Oxford Clay (Jurassic) of central England: *Sedimentology*, v. 25, p. 339-370.
Hudson, J.D., and Anderson, T.F., 1989, Ocean temperatures and isotopic compositions through time: *Transactions of the Royal Society of Edinburgh*, v. 80, p. 183-192.
Irwin, H., Curtis, C.D., and Coleman, M.L., 1977, Isotopic evidence for source of diagenetic carbonates formed during burial of organic rich sediments: *Nature*, v. 29, p. 209-213.
Jacob, C.E., 1949, Flow of Ground Water, *in* Rouse, H., ed., *Engineering hydraulics*: John Wiley and Sons, Inc., New York, p. 321-386.
Jacobi, R. D., 2002, Basement faults and seismicity in the Appalachian Basin of New York State: *Tectonophysics*, v. 353, p.75-113.
Jacobi, R. D. and Fountain, J. C., 1993, The Southern Extension & Reactivations of the Clarendon-Linden Fault System: *Geographie Physique et Quaternaire*, v.47, n.3, p.285-302.
Joachimski, M.M., and Buggisch, W., 1993, Anoxic events in the late Frasnian – causes of the Frasnian-Famennian faunal crisis?: *Geology*, v. 21, p. 675-678.
Johnson, J. G., 1970, Taghanic onlap and the end of North American provinciality: *Geological Society of America Bulletin*, v. 81, p. 2077-2106.
Johnson, J. G., G. Klapper, and C. A. Sandberg, 1985, Devonian eustatic fluctuations in Euramerica: *Geological Society of America Bulletin*, v. 96, p. 567-587.
Jones, M.E., and Addis, M.A., 1986, The application of stress path and critical state analysis to sediment deformation: *Journal of Structural Geology*, v. 8, p. 575-580.
Kaufmann, B., 2006, Calibrating the Devonian time scale: a synthesis of U-Pb ID-TIMS ages and conodont stratigraphy: *Earth-Science Reviews*, v. 75, p. 175-190.
Kawamura, K., and Ogawa, Y., 2004, Progressive change of pelagic clay microstructure during burial process: examples from piston cores and ODP cores: *Marine Geology*, v. 207, p. 131-144.
Kay, S.M., Snedden, W.T., Foster, B.P., and Kay, R.W., 1983, Upper mantle and crustal fragments in the Ithaca kimberlites: *Journal of Geology*, v. 91, p. 277-290.

Keller, G.H., 1982, Organic matter and the geotechnical properties of submarine sediments: *Geo-Marine Letters*, v. 2, p. 191-198.
Kooi, H., 1997, Insufficiency of compaction disequilibrium as the sole cause of high pore fluid pressures in pre-Cenozoic sediments: *Basin Research*, v. 9, p. 227-241.
Lacazette, A., and Engelder, T., 1992, Fluid-driven cyclic propagation of a joint in the Ithaca siltstone, Appalachian Basin, *in* Evans, B., and Wong, T.-F., eds., *Fault Mechanics and Transport Properties of Rocks*: Academic Press, London, p. 297-324.
Ladeira, F.L., and Price, N.J., 1981, Relationship between fracture spacing and bed thickness: *Journal of Structural Geology*, v. 3, p. 179-183.
Lash, G.G., 2006a, The Upper Devonian Rhinestreet shale: an unconventional fractured reservoir in western New York State: AAPG 2006 Annual Convention, Abstracts Volume, p. 61.
Lash, G.G., 2006b, Top seal development in the shale-dominated Upper Devonian Catskill Delta Complex, western New York State: *Marine and Petroleum Geology*, v. 23, p. 317-335.
Lash, G.G., 2006c, The Upper Devonian Rhinestreet shale, western New York state: from seal to fractured reservoir: AAPG 2006 Annual Convention, Abstracts Volume, p. 61.
Lash, G.G., and Blood, D.R., 2004a, Depositional clay fabric preserved in early diagenetic carbonate concretion pressure shadows, Upper Devonian (Frasnian) Rhinestreet shale, western New York: *Journal of Sedimentary Research*, v. 74, p. 110-116.
Lash, G.G., and Blood, D.R., 2004b, Geochemical and textural evidence for early diagenetic growth of stratigraphically confined carbonate concretions, Upper Devonian Rhinestreet black shale, western New York: *Chemical Geology*, v. 206, p. 407-424.
Lash, G.G., and Engelder, T., 2005, An analysis of horizontal microcracking during catagenesis: an example from the Catskill delta complex: *American Association of Petroleum Geologists*, v. 89, p. 1433-1449.
Lash, G.G., Loewy, S., and Engelder, T., 2004, Preferential jointing of Upper Devonian black shale, Appalachian Plateau, USA: evidence supporting hydrocarbon generation as a joint-driving mechanism, *in* Cosgrove, J., and Engelder, T., eds., *The initiation, propagation, and arrest of joints and other fractures*: Geological Society, London, Special Publication 231, p. 129-151.
Lindberg, F.A., 1985, *Northern Appalachian Region: COSUNA Project*: AAPG Bookstore, Tulsa Oklahoma.
Lippmann, F., 1955, Ton, Geoden und Minerale des Barreme von Hoheneggelsen: *Geologische Rundschau*, v. 43, p. 475-503.
Liu, G., and Roaldset, E., 1994, A new decompaction model and its application to the northern North Sea: *First Break*, v. 12, p. 81-89.
Lo, H.-B., 1993, Correction criteria for the suppression of vitrinite reflectance in hydrogen-rich kerogens: preliminary guidelines: *Organic Geochemistry*, v. 20, p. 653-657.
Loewy, S., 1995, The post-Alleghanian tectonic history of the Appalachian Basin based on joint patterns in Devonian black shales: M.S. Thesis, The Pennsylvania State University, University Park, Pennsylvania, 179 p.
Lüning, S., and Kolonic, S., 2003, Uranium spectral gamma-ray response as a proxy for organic richness in black shales: applicability and limitations: *Journal of Petroleum Geology*, v. 26, p. 153-174.
Luo, X., and Vasseur, G., 1992, Contributions of compaction and aquathermal pressuring to geopressure and the influence of environmental conditions: *American Association of Petroleum Geologists Bulletin*, v. 76, p. 1550-1559.
Luo, X., Brigaud, F., and Vasseur, G., 1993, Compaction coefficients of argillaceous sediments: their implications, significance and determination, *in* Dore, A.G., et al., eds., *Basin modeling: advances and applications*: Norwegian Petroleum Society, 3, p. 321-332.
Luther, D.D., 1903, Stratigraphy of Portage Formation between the Genesee Valley and Lake Erie: New York State Museum Bulletin, v. 69, p. 1000-1029.
Magara, K., 1978, *Compaction and fluid migration, practical petroleum geology*: Elsevier, Amsterdam, 296 p.
Magara, K., 1980, Comparison of porosity-depth relationships of shale and sandstone: *Journal of Petroleum Geology*, v. 3, p. 175-185.
Mann, D.M., and Mackenzie, A.S., 1990, Prediction of pore fluid pressures in sedimentary basins: *Marine and Petroleum Geology*, v. 7, p. 55-65.

McConaughy, D.T., and Engelder, T., 1999, Joint interaction with embedded concretions: joint loading configurations inferred from propagation paths: *Journal of Structural Geology*, v. 21, p. 1637-1652.
McGhee, G.R., Jr., 1990, The Frasnian-Famennian mass extinction record in the eastern United States, *in* Kauffman, E.G., and Walliser, O.H., eds., *Extinction events in Earth history*: Lecture Notes in earth Sciences, 30, Springer-Verlag, New York, p. 161-168.
McTavish, R.A., 1978, Pressure retardation of vitrinite diagenesis, offshore north-west Europe: *Nature*, v. 271, p. 648-650.
McTavish, R.A., 1998, The role of overpressure in the retardation of organic matter maturation: *Journal of Petroleum Geology*, v. 21, p. 153-186.
Meade, R.H., 1966, Factors influencing the early stages of compaction of clays and sands – review: *Journal of Sedimentary Petrology*, v. 36, p. 1085-1101.
Meckel, L.D., 1967, Origin of Pottsville conglomerates (Pennsylvanian) in the central Appalachians: *Geological Society of America Bulletin*, v. 78, p. 223–258.
Miller, D.S., and Duddy, I.R., 1989, Early Cretaceous uplift and erosion of the northern Appalachian Basin, New York, based on apatite track analysis: *Earth and Planetary Science Letters*, v. 93, p. 35-49.
Mozley, P.S., 1996, The internal structure of carbonate concretions in mudrocks: a critical evaluation of the conventional concentric model of concretion growth: *Sedimentary Geology*, v. 103, p. 85-91.
Müller, G., 1967, Diagenesis in argillaceous sediments, *in* Larson, G., and Chilinger, G.V., eds., *Diagenesis in Sediments*: Developments in Sedimentology, 8, p. 127-177.
Narr, W., 1991, Fracture density in the deep subsurface: techniques with application to Point Arguello Oil Field: *American Association of Petroleum Geologists Bulletin*, v. 75, p. 1300-1323.
Nuccio, V.F., and Hatch, J.R., 1996, Vitrinite reflectance suppression in the New Albany Shale, Illinois Basin - Vitrinite reflectance and Rock-Eval data: U.S. Geological Survey Open-File Report 96-665, p. 37.
O'Brien, N.R., 1995, Origin of shale fabric – clues form framboids: *Northeastern Geology and Environmental Sciences*, v. 17, p. 146-150.
O'Brien, N.R., and Slatt, R.M., 1990, *Argillaceous rock atlas*: SpringerVerlag, New York, 141 p.
Oertel, G., and Curtis, C.D., 1972, Clay ironstone concretion preserving fabrics due to progressive compaction: *Geological Society of America Bulletin*, v. 83, p. 2597-2606.
Oliver, W.A., Jr., de Witt, Wallace, Jr., Dennison, J.M., Hoskins, D.M., and Huddle, J.W., 1969, Correlation of Devonian rock units in the Appalachian basin: U.S. Geological Survey Oil and Gas Investigations Oil Chart OC-64.
Over, D.J., 1997, Conodont biostratigraphy of the Java Formation, Upper Devonian, and the Frasnian-Famennian in western New York, *in* Klapper, G., Murphy, M.A., and Talent, J.A., eds., *Paleozoic sequence stratigraphy, biostratigraphy, and biogeography: studies in honor of J. Granville ("Jess") Johnson*: Geological Society of America, Special Publication 321, p. 161-178.
Peacock, D.C.P., and Mann, A., 2005, Evaluation of the controls of fracturing in reservoir rocks: *Journal of Petroleum Geology*, v. 28, p. 385-396.
Pearson, M.J., and Small, J.S., 1988, Illite-smectite diagenesis and palaeotemperatures in northern North Sea Quaternary to Mesozoic shale sequences: *Clay Minerals*, v. 23, p. 111-132.
Pepper, J.F., de Witt, Jr., W., and Colton, G.W., 1956, Stratigraphy of the West Falls Formation of Late Devonian age in western and west-central New York : U.S. Geological Survey Oil and Gas Investigations, Chart OC 55.
Pettijohn, F.J., 1975, *Sedimentary rocks*, 3rd ed.: New York, Harper & Row, 628 p.
Price, L.C., and C.E. Barker, 1985, Suppression of vitrinite reflectance in amorphous rich kerogen - a major unrecognized problem: *Journal of Petroleum Geology*, v. 8, p. 59-84.
Raiswell, R., 1971, The growth of Cambrian and Liassic concretions: *Sedimentology*, v. 17, p. 147-171.
Raiswell, R., 1987, Non-steady state microbial diagenesis and the origin of carbonate concretions and nodular limestones, *in* Marshall, J.D., ed., *Diagenesis of Sedimentary Sequences*: Geological Society of London, Special Publication 36, p. 41-54.
Raiswell, R., 1988, A chemical model for the origin of minor limestone-shale cycles by anaerobic methane oxidation: *Geology*, v. 16, p. 641-644.
Raiswell, R., and Fisher, Q.J., 2000, Mudrock-hosted carbonate concretions: a review of growth mechanisms and their influence on chemical and isotopic composition: *Geological Society of London Journal*, v. 157, p. 239-251.

Raiswell, R., and White, N.J.M., 1978, Spatial aspects of concretionary growth in the Upper Lias of N.E. England: *Sedimentary Geology*, v. 20, p. 291-300.
Reed, J.S., Spotila, J.A., Eriksson, K.A., and Bodnar, R.J., 2005, Burial and exhumation history of Pennsylvanian strata, central Appalachian basin: an integrated study: *Basin Research*, v. 17, p. 259-268.
Repetski, J.E., Ryder, R.T., Harper, J.A., and Trippi, M.H., 2002, Thermal maturity patterns (CAI and $\%R_o$) in the Ordovician and Devonian rocks of the Appalachian basin in Pennsylvania: U.S. Geological Survey Open-File Report 02-302, 57 p.
Rickard, L.V., 1989, *Stratification of the subsurface low and mid-Devonian of New York, Pennsylvania, Ohio, and Ontario*: New York State Museum and Science Map and Chart Series 39, 59 p.
Rieke, H.H., III, and Chilingarian, C.V., 1974, *Compaction of Argillaceous Sediments*: Elsevier, New York, 424 p.
Rimmer, S.M., and Cantrell, D.J., 1988, Organic maturation of the Cleveland Member of the Ohio Shale, eastern Kentucky: *Proc. Eastern Oil Shale Symposium*, Lexington, Kentucky, Inst. Min. Miner. Res., p. 401-410.
Rimmer, S.M., Cantrell, D.J., and Gooding, P.J., 1993, Rock-Eval pyrolysis and vitrinite reflectance trends in the Ohio Shale, eastern Kentucky: *Organic Geochemistry*, v. 20, p. 735-746.
Rives, T., Razack, M., Petit, J.P., and Rawnsley K.D., 1992, Joint spacing; analogue and numerical simulations: *Journal of Structural Geology*, v. 14, p. 925-937.
Rowan, E.L., Ryder, R.T., Repetski, J.E., Trippi, M.H., and Ruppert, L.F., 2004, Initial results of a 2D burial/thermal history model, central Appalachian Basin, Ohio and West Virginia: U.S. Geological Survey Open-File Report 2004-1445, 12 p.
Ryder, R.T., 1996, Fracture patterns and their origin in the Upper Devonian Antrim Shale gas reservoir of the Michigan basin: A review: U.S. Geological Survey Open-File Report 96-23.
Sandberg, Z.A., Ziegler, W., Dressen, R., and Butler, J.L., 1988, Late Devonian mass extinction: conodont event stratigraphy, global changes, and possible causes: *Courier Forsch. Senckenb.*, v. 102, p. 263-307.
Schmoker, J. W., 1979, Determination of organic content of Appalachian Devonian shales from formation-density logs: *American Association of Petroleum Geologists Bulletin*, vol. 63, p. 1504-1509.
Schmoker, J.W., 1981, Determination of organic-matter content of Appalachian Devonian shales from gamma-ray logs: *American Association of Petroleum Geologists Bulletin*, v. 65, p. 1285-1298.
Schmoker, J.W., and Oscarson, S.A., 1995, Descriptions of cntinuous-type (unconventional) plays of the U.S. Geological Survey 1995 National Assessment of United State oil and gas resources: U.S. Geological Survey Open-File Report 95-75B, p. 21.
Sclater, J.G., and Christie, P.A.F., 1980, Continental stretching: an explanation of the post-mid-Cretaceous subsidence of the central North Sea basin: *Journal of Geophysical Research*, v. 85, p. 3711-3739.
Smith, J.W., and Young, N.B., 1964, Specific-gravity to oil-yield-relationships for black shales of Kentucky's New Albany Formation: U.S. Bureau of Mines Report Investigation 6531, 13 p.
Sorby, H.C., 1908, On the application of quantitative methods to the study of the structure and history of rocks: *Geological Society of London Quarterly Journal*, v. 64, p. 171-233.
Stewart, J., and Watts, A.B., 1997, Gravity anomalies and spatial variations of flexural rigidity at mountain ranges: *Journal of Geophysical Research*, v. 102, p. 5327-5352.
Strickler, M.E., and Ferrell, R.E., 1989, Provenance and diagenesis of Upper Wilcox Formation clay minerals: 9th International Clay Conference, Strasbourg, p. 379.
Swarbrick, R.E., and Osborne, M.J., 1998, Mechanisms that generate abnormal pressures: an overview, *in* Law, B.E., Ulmishek, G.F., and Slavin, V.I., eds., *Abnormal pressures in hydrocarbon environments*: American Association of Petroleum Geologists, Memoir 70, p. 13-34.
Swarbrick, R.E., Osborne, M.J., and Yardley, G.S., 2002, Comparison of overpressure magnitude resulting from the main generating mechanisms, *in* Huffman, A.R., and Bowers, G.L., eds., *Pressure regimes in sedimentary basins and their prediction*: American Association of Petroleum Geologists, Memoir 76, p. 1-12.
Sweeney, J. J., and Burnham, A.K., 1990, Evaluation of a simple model of vitrinite reflectance based on chemical kinetics: *American Association of Petroleum Geologists Bulletin*, v. 74, p. 1559-1570.
Tankard, A.J., 1986, On the depositional response to thrusting and lithospheric flexure: examples from the Appalachian and Rocky Mountain basins, *in* Allen, P.A., and Homewood, P., eds., *Foreland Basins*: Special Publications of the International Society of Sedimentologists, 8, p. 369-392.

Terzaghi, K., and Peck, R.B., 1948, *Soil mechanics in engineering practice*: John Wiley and Sons, Inc., New York.

Tingay, M.R.P., Hillis, R.R., Swarbrick, R.E., Mildren, S.D., Morley, C.K., and Okpere, E.C., 2000, The sonic and density log expression of overpressure in Brunei Darussalam, *in* Swarbrick, R.E., ed., *Overpressure 2000 – workshop proceedings*: CD volume, paper OP2000_21, 8 p.

Tissot, B.P., and Welte, D.H., 1984, *Petroleum formation and occurrence*, 2nd ed.: SpringerVerlag, New York., 720 p.

Towarak, M.J., 2006, Differential compaction and porosity loss in Devonian shale of the Catskill Delta Complex: M.S. Thesis, The Pennsylvania State University, University Park, Pennsylvania, 85 p.

Ujiié, Y., Sherwood, N., Faiz, M., and Wilkins, R.W.T., 2004, Thermal maturity and suppressed vitrinite reflectance for Neogene petroleum source rocks of Japan: *American Association of Petroleum Geologists Bulletin*, v. 88, p. 1335-1356.

van Geldern, R., Joachimski, M.M., Day, J., Alvarez, F., Jansen, U., and Yolkin, E.A., 2001, Secular changes in the stable isotopic composition of Devonian brachiopods: Eleventh Annual V.M. Goldschmidt Conference, Hot Springs, Virginia, Abstract 3532, LPI Contribution No. 1088, Lunar and Planetary Institute, Houston, Texas (CD-ROM).

van Ruth, P.J., Hillis, R.R., and Tingate, P.R., 2004, The Origin of Overpressure in the Carnarvon Basin, Western Australia: Implications for Pore Pressure Prediction: *Petroleum Geoscience*, v. 10, p. 247-257.

Veevers, J.J., and Powell, C. McA., 1987, Late Paleozoic glacial episodes in Gondwanaland reflected in transgressive-regressive depositional sequences in Euramerica: *Geological Society of America Bulletin*, v. 98, p. 475-487.

Velde, B., 1996, Compaction trends of clay-rich deep sea sediments: *Marine Geology*, v. 133, p. 193-201.

Ver Straeten, C.A., and Brett, C.E., 2000, Bulge Migration and Pinnacle Reef Development, Devonian Appalachian Foreland Basin: *Journal of Geology*, vol. 108, p. 339-352.

von Engelhardt, W., 1977, The origin of sediments and sedimentary rocks, III., *in* von Engelhardt, W., Füchtbauer, H., and Müller, G., eds., *Sedimentary petrology*: Wiley, New York, 359 p.

Weary, D.J., Ryder, R.T., and Nyahay, R., 2000, Thermal maturity patterns (CAI and $\%R_o$) in the Ordovician and Devonian rocks of the Appalachian basin in New York State: U.S. Geological Survey Open-File Report 00-496, 39 p.

Weeks, L.G., 1957, Origin of carbonate concretions in shales, Magdalena Valley, Columbia: *Geological Society of America Bulletin*, v. 68, p. 95-102.

Weller, J.M., 1959, Compaction of sediments: *American Association of Petroleum Geologists*, v. 43, p. 273-310.

Werne, J.P., Sageman, B.B., Lyons, T.W., and Hollander, D.J., 2002, An integrated assessment of a "type euxinic" deposit: evidence for multiple controls on black shale deposition in the Middle Devonian Oatka Creek Formation: *American Journal of Science*, v. 302, p. 110-143.

Wetzel, A., 1992, An apparent concretionary paradox: *Zentralblatt für Geologie und Paläontologie, Teil I*, v. H12, p. 2823-2830.

Woodland, B.G., 1984, Fabric of the clastic component of Carboniferous concretions and their enclosing matrix, *in* Belt, E.S., and Macqueen, R.W., eds., Neuvième Congrès International de Stratigraphie et de Géologie du Carbonifère, vol. 3: Washington and Champaign-Urbana, p. 694-701.

Woodrow, D.L., Dennison, J.M., Ettensohn, F.R., Sevon, W.T., and Kirchgasser, W.T., 1988, Middle and Upper Devonian stratigraphy and paleogeography of the central and southern Appalachians and eastern Midcontinent, U.S.A., *in* McMillan, N.J., Embry, A.F., and Glass, D.J., eds., *Devonian of the world*: : *proceedings of the Second International Symposium on the Devonian System*, v. 1: Canadian Society of Petroleum Geologists, Calgary, Canada, p. 277-301.

Wright, N.A., 1973, Subsurface Tully limestone New York and northern Pennsylvania: New York State Museum and Science Service, Map and Chart Series Number 14, 15 p.

Zangerl, R., Woodland, B.G., Richardson, E.S., Jr., and Zachry, D.L., Jr., 1969, Early diagenetic phenomena in the Fayetteville black shale (Mississippian) of Arkansas: *Sedimentary Geology*, v. 3, p. 87-119.

Zhao, M., and Jacobi, R.D., 1997, Formation of regional cross-fold joints in the northern Appalachian Plateau: *Journal of Structural Geology*, v. 19, p. 817-834.

ROAD LOG AND STOP DESCRIPTIONS

Total Miles	Miles from Last Point	Route Description
0.0	0.0	Depart Adams Mark heading east on Church St. to its intersection with Route. 5.
0.2	0.2	Bear right onto Route 5 West.
15.3	15.1	Intersection of Route 5 with South Creek Road. Turn right onto South Creek Road.
15.6	0.3	Turn left onto Lake Shore Road.
17.5	1.9	Park in the small lot at the Erie County Water Authority building or at the intersection of Sweetland Road a short distance ahead. Walk down to Pike Creek.

STOP 1: PIKE CREEK/LAKE ERIE SHORELINE

Significance: I) the preferential generation of early NS-trending joints at the contacts of gray shale and black shale;
II) geographic variations in the magnitude of the pre-Upper Devonian or Taghanic unconformity and the significance of the so-called "Driller's Tully";
III) preferential propagation of NW and ENE joints in the Rhinestreet black shale.

I. Working down creek toward Lake Erie, the first exposure encountered reveals the contact of the West River gray shale and overlying Middlesex black shale (Fig. 40). A prominent NS-trending joint set as well as ENE-trending joints can be observed here (Fig. 41). The NS joints terminate at the contact or a short distance above it, a theme common to other Upper Devonian black shale units of western New York state as described earlier. We interpret the generation of the NS joints to be a response to the passage of a peripheral bulge produced by loading of the Laurentian plate edge at the onset of the Alleghanian orogeny across the western New York state region of the Appalachian Basin. Reduced compressive stress as a consequence of uplift-related thermoelastic loading initiated joints in higher modulus diagenetic carbonate. Propagation of these joints through the host gray shale was aided by moderately overpressured pore fluids at the top of the gray shale, perhaps sealed in by the overlying low permeability black shale.

II. The mouth of Pike Creek exposes the Middle-Upper Devonian interval from the Tichenor limestone (perhaps the top of the Ludlowville shale, depending upon the lake level) to roughly two-thirds the way up the Middlesex black shale (Fig. 40). This exposure provides the opportunity to (1) consider the magnitude of the Taghanic unconformity in the subsurface of western New York state and (2) offer some preliminary thoughts on the subsurface stratigraphy of the Moscow-Tully interval in this region of the basin. De Witt and Colton (1978) placed the unconformity at the contact of the Penn Yan shale of the Geneseo Formation and the North Evans limestone of the underlying Moscow shale, Hamilton Group (Fig. 40). Rocks absent this exposure include, in descending order, an unknown thickness of the Penn Yan shale and the underlying Geneseo black shale, the Tully limestone, and some thickness of the Moscow shale (Windom Member). The hiatal extent or magnitude of the Taghanic unconformity diminishes to the south and east as the Moscow shale increases in thickness and the Geneseo black shale and Tully limestone appear and thicken (Fig. 42). De Witt et al. (1993) maintained that the disconformity confined the Middle Devonian Geneseo black shale to the eastern region of the basin in New York state; however, Upper Devonian black shales, including the Dunkirk, Pipe Creek, and Rhinestreet shales were largely restricted to the western part of the basin by the unconformity. However, the distribution of the Middle Devonian Oatka Creek black shale of the Marcellus Formation (Hamilton Group) appears to have been unaffected by the Taghanic unconformity.

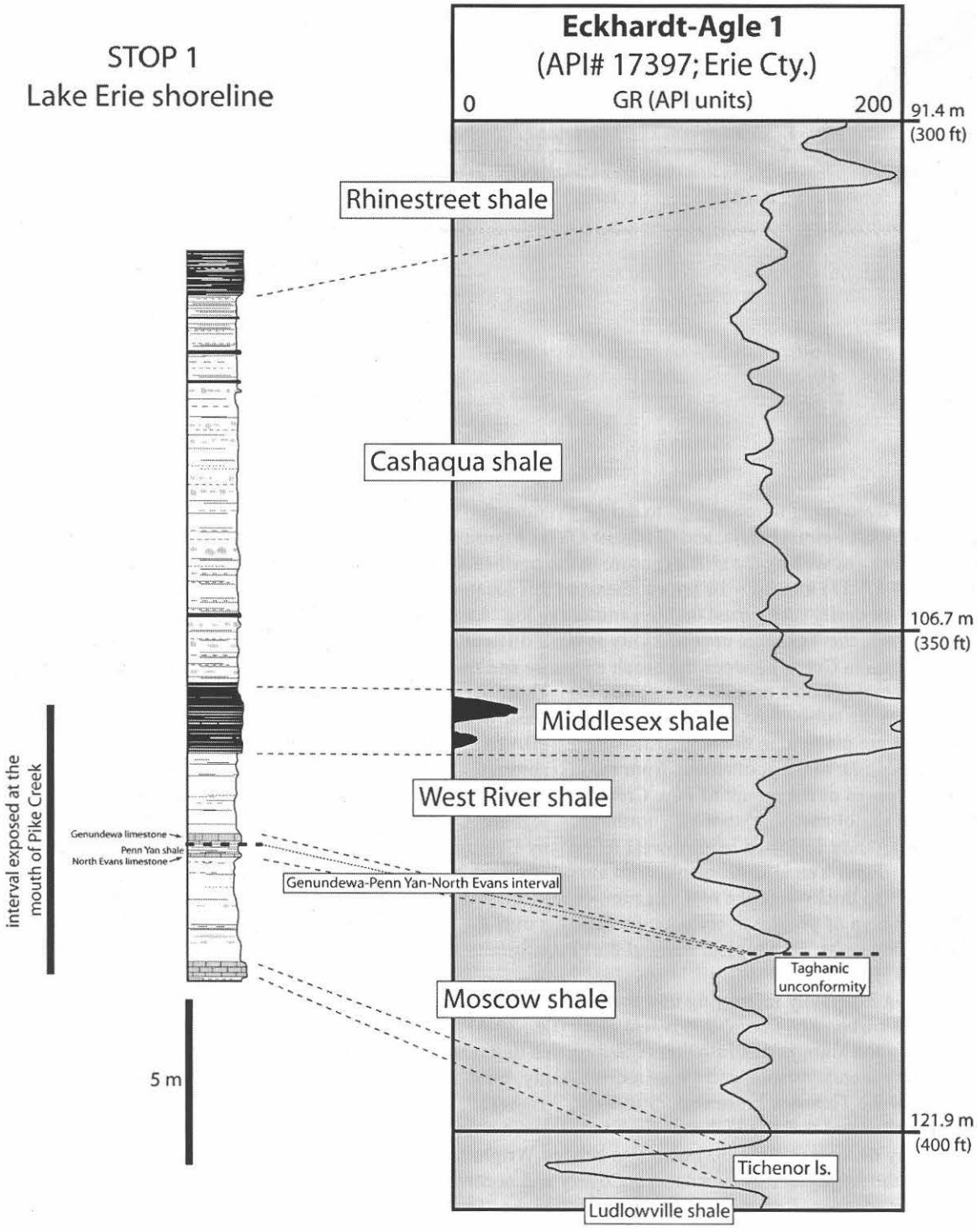

Fig. 40: Stratigraphic section of the beach cliff northeast of the mouth of Pike Creek (showing the interval exposed at the mouth of Pike Creek). The lithologic log is based on measurements made along the lakeshore and Eighteenmile Creek. This section is traced into the subsurface to the Eckhardt-Agle 1 gas well (see Fig. 42 for location of this well).

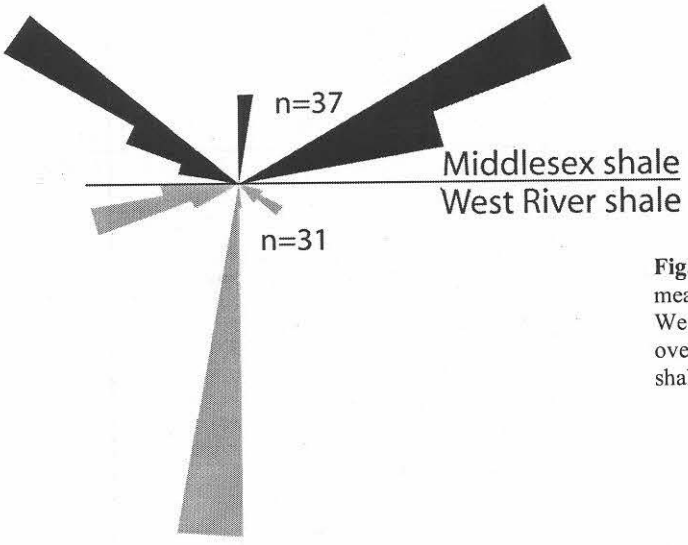

Fig. 41: Rose plot of joints measured at the contact of the West River gray shale and overlying Middlesex black shale along Pike Creek.

We are using wireline logs to define stratigraphic trends in the subsurface of western New York state, northwest Pennsylvania, and northeast Ohio. Figure 40 links the stratigraphy observed at the mouth of Pike Creek (as well as the cliff exposure to the northeast along the beach) to the Eckhardt-Agle 1 gas well (API# 17937) located ~ 10 km southeast of this location (Fig. 42). The Middlesex shale and Tichenor limestone are easily recognized on the gamma-ray log. Locating the North Evans-Genundewa interval, and, therefore, the Taghanic unconformity is more difficult. The Genundewa limestone, ~21 – 30 cm thick on Eighteenmile Creek between the beach exposure and the Eckhardt-Agle 1 well (Fig. 42), is difficult at best to be resolved on a normal gamma-ray log. Thus, our placement of the unconformity is based on extension of the subsurface stratigraphy from the east, where the Tully limestone and overlying Geneseo black shale are present, to the Eckhardt-Agle 1 well. There is a marked increase in the thickness of the West River shale to the south away from the lakeshore (Fig. 40). Cross-section 1 (Fig. 42) carries the interval exposed at the mouth of Pike Creek (i.e., the base of the Tichenor limestone to the base of the Middlesex shale) east-southeast into northeast Alleghany County. The Geneseo black shale first appears in Wyoming County followed in northwest Alleghany County by the Tully limestone. Notice also that the West River/Penn Yan interval displays an almost six-fold increase in thickness to the east. The Tichenor limestone also thickens to the east. In sum, cross-section 1 displays, over a relatively short distance, the westward onlap of progressively younger deposits over the Taghanic unconformity as well as the truncation of underlying units, both typical traits of the unconformity elsewhere in the Appalachian Basin (Hamilton-Smith, 1993).

An especially interesting unit that we are mapping in the subsurface, the so-called "Driller's Tully," is a carbonate interval that is less clean (i.e., 20 API units or more) than the true Tully limestone. There is a good amount of confusion regarding this unit; Oliver et al. (1969) placed the "Driller's Tully" of Erie County, Pennsylvania, and Chautauqua County, New York, well down the Hamilton Group, perhaps at the level of the Tichenor limestone. Similarly, Wright (1973) referred to the "Driller's Tully" as limestone "B" and suggested that the Tichenor limestone is a tongue of limestone "B." This interpretation was accepted by de Witt et al. (1993) who also echoed Wright's proposition that the Tully limestone is not present in the subsurface of Chautauqua County and northwest Pennsylvania. De Witt et al. (1993) pointed out that conodonts collected from the upper part of the "Driller's Tully" in a core from the Eastern Gas Shales Project well PA3 in Erie County, Pennsylvania, included elements of *Polygnathus linguiformis*,

Fig. 42 (next page): Stratigraphic cross-section (gamma-ray logs) of the interval observed at the mouth of Pike Creek east into northern Allegany County (datum = base of the Middlesex shale).

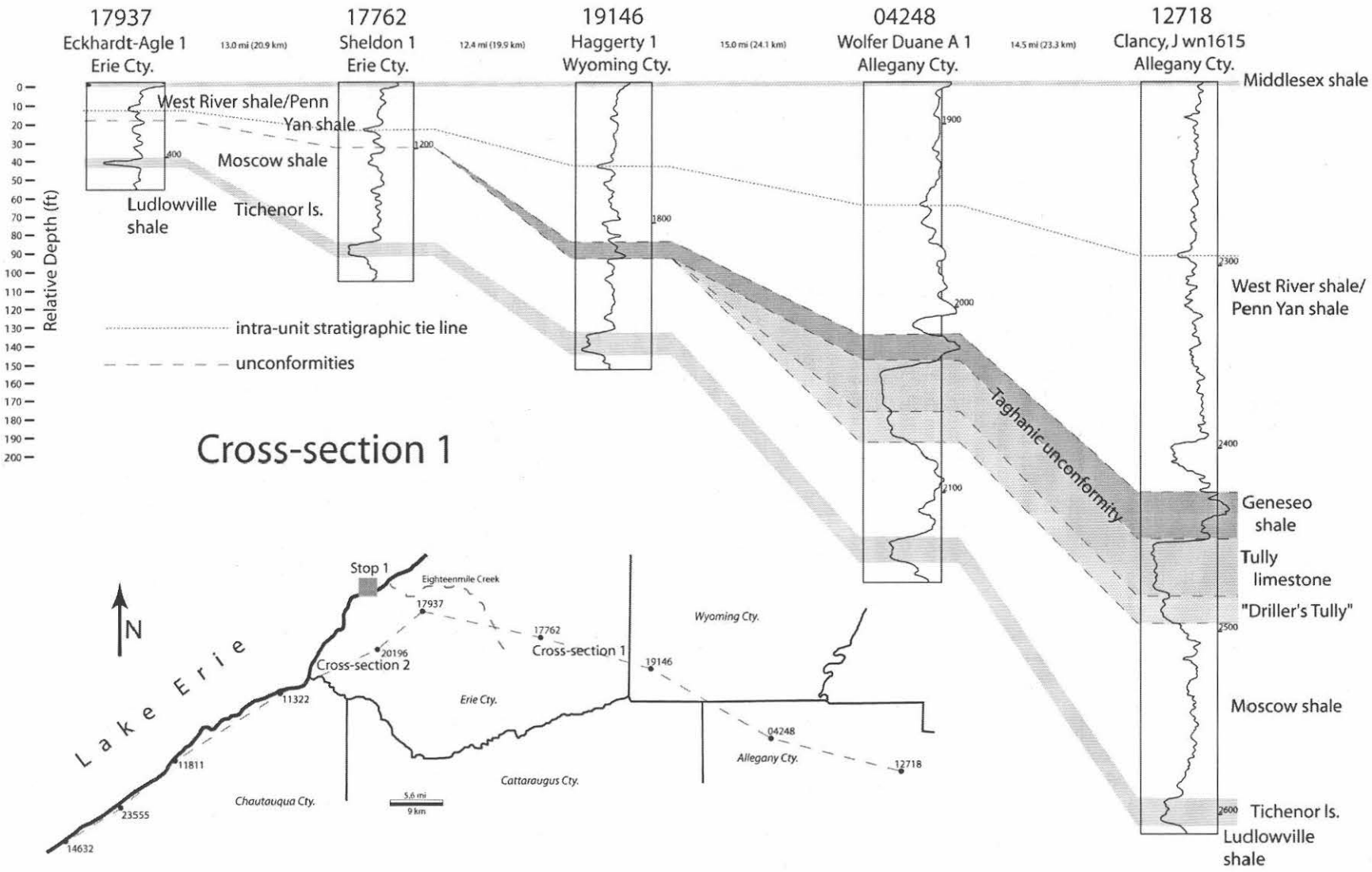
17937
Eckhardt-Agle 1
Erie Cty.
13.0 mi (20.9 km)
17762
Sheldon 1
Erie Cty.
12.4 mi (19.9 km)
19146
Haggerty 1
Wyoming Cty.
15.0 mi (24.1 km)
04248
Wolfer Duane A 1
Allegany Cty.
14.5 mi (23.3 km)
12718
Clancy, J wn1615
Allegany Cty.
Relative Depth (ft)
West River shale/Penn Yan shale
Moscow shale
Ludlowville shale
Tichenor ls.
intra-unit stratigraphic tie line
unconformities
Cross-section 1
Middlesex shale
West River shale/ Penn Yan shale
Taghanic unconformity
Geneseo shale
Tully limestone
"Driller's Tully"
Moscow shale
Tichenor ls.
Ludlowville shale
Stop 1
Eighteenmile Creek
Lake Erie
N
Cross-section 2
Wyoming Cty.
Erie Cty.
Allegany Cty.
Chautauqua Cty.
Cattaraugus Cty.
5.6 mi
9 km
14632
23555
11811
11322
20196
17937
17762
19146
04248
12718

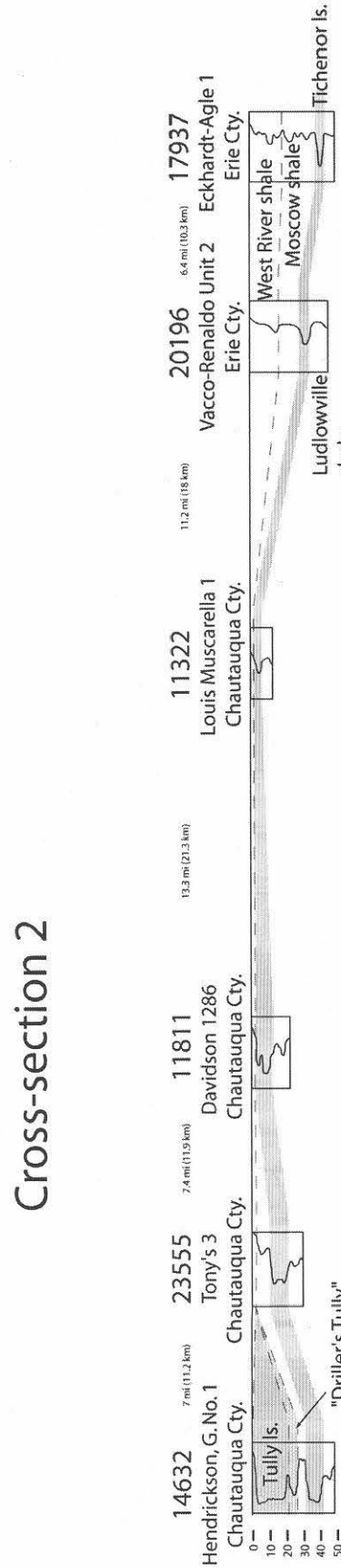

Fig. 43: Stratigraphic cross-section (gamma-ray logs) of the interval observed at the mouth of Pike Creek west into northern Chautauqua County (datum = base of the Middlesex shale).

We agree with Rickard (1989) that the Tully limestone is present in the subsurface of Chautauqua County and northwest Pennsylvania. Indeed, our analysis of close-spaced wells in far western Chautauqua County indicates that Wright's (1973) Tichenor limestone and limestone "B" is actually the Tully limestone and underlying "Driller's Tully," the latter resting unconformably on the Tichenor limestone. However, we interpret the "Driller's Tully" to be a discrete unit in erosional contact with the Moscow shale, and locally the Tichenor limestone, rather than a stratigraphic equivalent of the Moscow shale and Tichenor limestone as suggested by Rickard (1989). Truncated calcareous intervals of the Moscow shale and locally abrupt changes in thickness of the "Driller's Tully" confirm the erosional contact of this unit with underlying deposits. The "Driller's Tully" is recognized in the subsurface of northern Allegany County, that area of Chautauqua County where the Tully is present (Fig. 43) and parts of Warren and Erie counties, Pennsylvania. The contact of the "Driller's Tully" and overlying Tully limestone is a thin shaley interval (Figs. 42 and 43). However, the local absence of this interval and as well as the occasional absence of the "Driller's Tully" beneath the Tully suggests that the contact of these units is an unconformity.

Cross-section 2 extends southwest along the Lake Erie shoreline from the Eckhardt-Agle 1 well to Westfield, New York, northern Chautauqua County (Fig. 43). Noteworthy features in this section include: (1) the thickening of the Tichenor limestone to the west of Erie County; (2) the appearance of the Tully and underlying "Driller's Tully" in the Westfield area; and (3) the thinning of the interval between the base of the Tichenor limestone and the base of the Middlesex shale to the southwest (the Middlesex and Tichenor are separated by less than one meter of gray shale in the Muscarella 1 well; Fig. 43) followed by its rapid thickening as the Tully reappears near Westfield. This latter point is consistent with localized uplift. That the Middlesex shale and younger deposits show no evidence of this event provides clues to the timing of uplift, perhaps a reflection of localized tectonic activity of the post-Tully basin in advance of the Acadian thrust load and related forebulge (e.g., Tankard, 1986; Beaumont et al., 1988; Hamilton-Smith, 1993; Ver Straeten and Brett, 2000; Filer, 2003). Indeed, Filer (2003) defined a Famennian forebulge in West Virginia based on isopach and sedimentary facies maps that, when traced north, extends through the eastern Chautauqua County-Erie County region. We are just beginning to consider this event in a regional

sense based on subsurface information from western New York state, northwest Pennsylvania, and northeast Ohio.

The Taghanic unconformity appears to be erosional throughout western New York state (Johnson, 1970; Wright, 1973; Baird and Brett, 2003). Heckel (1973) maintained that the contact is a slight diastem in central New York state, increasing in stratigraphic magnitude to the west where the disconformity represents an increasing period of nondeposition. However, our ongoing investigation of the subsurface stratigraphy of western New York state reveals a more complex situation made more so by the presence of the "Driller's Tully." Indeed, the initial event may have been that phase of erosion that occurred before deposition of the "Driller's Tully," which locally rests unconformably on the Tichenor limestone.

Heckel (1973) pointed out that the Geneseo black shale conformably overlies the Tully limestone east of Cayuga Lake. West of this meridian, however, the contact becomes one of disconformity as progressively younger deposits onlap westward above the unconformity (de Witt et al., 1993) until the Geneseo shale feathers out in easternmost Chautauqua County into eastern Wyoming County (Fig. 42). Rickard (1989) suggested that the post-Tully unconformity was entirely subaqueous. Similarly, Baird and Brett (1991) postulated that the erosional contact of the Geneseo black shale and underlying Tully limestone is a submarine erosional feature (maximum flooding surface) related to the abrupt increase in water depth, likely the result of the sudden sinking of a forebulge in response to tectonic loading to the east (e.g., Hamilton-Smith, 1993).

III. Moving northeast along the beach for perhaps a kilometer enables us to observe in cliff exposure the entire Moscow shale – basal Rhinestreet shale interval (Fig. 40). Note the diagenetic carbonate intervals within the Cashaqua shale. The heavily fractured Rhinestreet black shale at the top of the exposure is easily recognized from the beach. The upper several meters of the Cashaqua and lower few meters of the Rhinestreet shale carry the older NS-trending joints, similar to what we saw on Pike Creek and likely for the same reasons. NW- and younger ENE-trending joints, most densely formed in the basal organic-rich interval of the Rhinestreet shale, formed as a consequence of catagenesis as these source rocks approached and finally reached their modeled maximum burial depth of ~3.1 km (see Fig. 9). This exposure demonstrates the strong stratigraphic control on jointing in these rocks. The NW joints probably formed soon after the rocks had entered the oil window and at that time that the basin was feeling the same remote stress field responsible for emplacement of the Blue Ridge-Piedmont Megathrust. The younger ENE-trending joints propagated after the Rhinestreet shale had been in the oil window for a protracted period of time, thus their greater density. The stress field under which these joints formed reflected the oblique convergence of Laurentia and Africa and had been responsible for the generation of the early (perhaps Chesterian) ENE-trending coal cleat throughout the Appalachian Basin and similarly oriented joints in the deeply buried Frasnian black shales of the Finger Lakes District (Engelder and Whitaker, 2006).

Total Miles	Miles from Last Point	Route Description
17.5	0.0	Head east on Lake Shore Road.
19.4	1.9	Turn right (south) onto South Creek Road.
19.7	0.3	Intersection of South Creek Road and Route 5. Remain on South Creek Road.
21.2	1.5	Cross Versailles Plank Road.
21.5	0.3	Intersection of South Creek Road and Route 20 (Southwestern Boulevard). Remain on South Creek Road.
21.6	0.1	Park along the shoulder of South Creek Road at the North Evans Cemetery. Cross South Creek Road and walk down the gravel path to Eighteenmile Creek heading toward the white Route 20 bridge.

STOP 2: EIGHTEENMILE CREEK/ROUTE 20 BRIDGE

Significance: I) approximately the lower half of the Rhinestreet shale can be observed in the east wall of the creek exposure immediately south of the Route 20 bridge over Eighteenmile Creek;
II) the presence of NS joints at the contact of the Cashaqua gray shale and overlying Rhinestreet shale, and the high density of NW- and younger ENE-trending joints at the organic-rich base of the Rhinestreet shale;
III) basin modeling of measured vitrinite reflectance and the possibility of vitrinite suppression;
IV) recognition of the Cashaqua-Rhinestreet contact in the subsurface – gamma-ray vs. bulk density logs.

I. A bit less than the lower half of the Rhinestreet shale is visible in the cliff exposure immediately north of the Route 20 bridge. We will have an opportunity to look at the concretion horizon – the middle concretion horizon – visible at the top of the cliff – ~34 m above the bottom contact (see Fig. 1) - at Stop 4. The Rhinestreet section displayed in the cliff contains two intervals of gray shale and thin-bedded black shale at ~10.0-12.5 m and 27.5-29.3 m above the contact (Fig. 1). These horizons, which probably represent eustatic oscillations, can be observed in gamma-ray and bulk density logs (Fig. 44). Moreover, the lower gray shale interval contains a lenticular limestone bed as thick as 20 cm, one of Luther's (1903) scraggy layers and our lower scraggy layer (see Fig. 1). The geochemistry of the scraggy layers, discussed above, confirms their early diagenetic origin and suggests that they formed in a manner similar to the concretions. The scraggy layers, which are consistently found associated with organic-lean gray shale intervals (see Fig. 1), are recognized in gamma-ray logs as a sharp deflection to the left (Fig. 44) and may serve as markers for basinwide correlation. The fact that the limestone deflection on the gamma-ray logs cannot always be correlated among neighboring offset wells demonstrates the discontinuous nature of these deposits, which is evident in field exposures.

II. The Cashaqua shale-Rhinestreet shale contact is exposed beneath the bridge. The Cashaqua shale along Eighteenmile Creek comprises ~11.5 m of silty, organic lean (TOC < 0.7%) gray shale and nodular limestone horizons. The overlying Rhinestreet shale is composed of ~54 m of organic-rich black shale, much lesser gray shale, sparse thin siltstone beds, and several carbonate concretion horizons and nodular limestone intervals, the latter termed "scraggy layers" by Luther (1903; see Fig. 1 for the measured Rhinestreet section along Eighteenmile Creek). TOC content of the Rhinestreet shale at its base is 8.09%, diminishing upward (Fig. 1; Lash and Blood, 2004b; Lash et al., 2004). Vitrinite reflectance of the Rhinestreet shale at its base along Eighteenmile Creek is 0.74%, indicating that these rocks entered the oil window during their burial history (Lash, 2006c).

Joints of the three dominant sets carried by the Rhinestreet shale are represented at this exposure. Several long NS-trending joints, can be seen at the contact. We contend that uplift of the Upper Devonian sedimentary succession in response to passage of a peripheral bulge at the onset of the Alleghanian orogeny, and resultant thermoelastic loading, induced the NS joints in the high modulus carbonate. These joints propagated upward under the influence of moderately overpressured pore fluid at the top of the Cashaqua shale. Elevated pore pressure may have resulted from a combination of disequilibrium compaction and the tight, impermeable nature of the organic-rich Rhinestreet shale. The lack of bioturbation in the finely laminated organic-rich sediment preserved a strong strength anisotropy that precluded easy vertical movement of fluid. The squeezing of ductile organic matter into voids and pore throats further reduced the permeability of the black shale (Lash, 2006b).

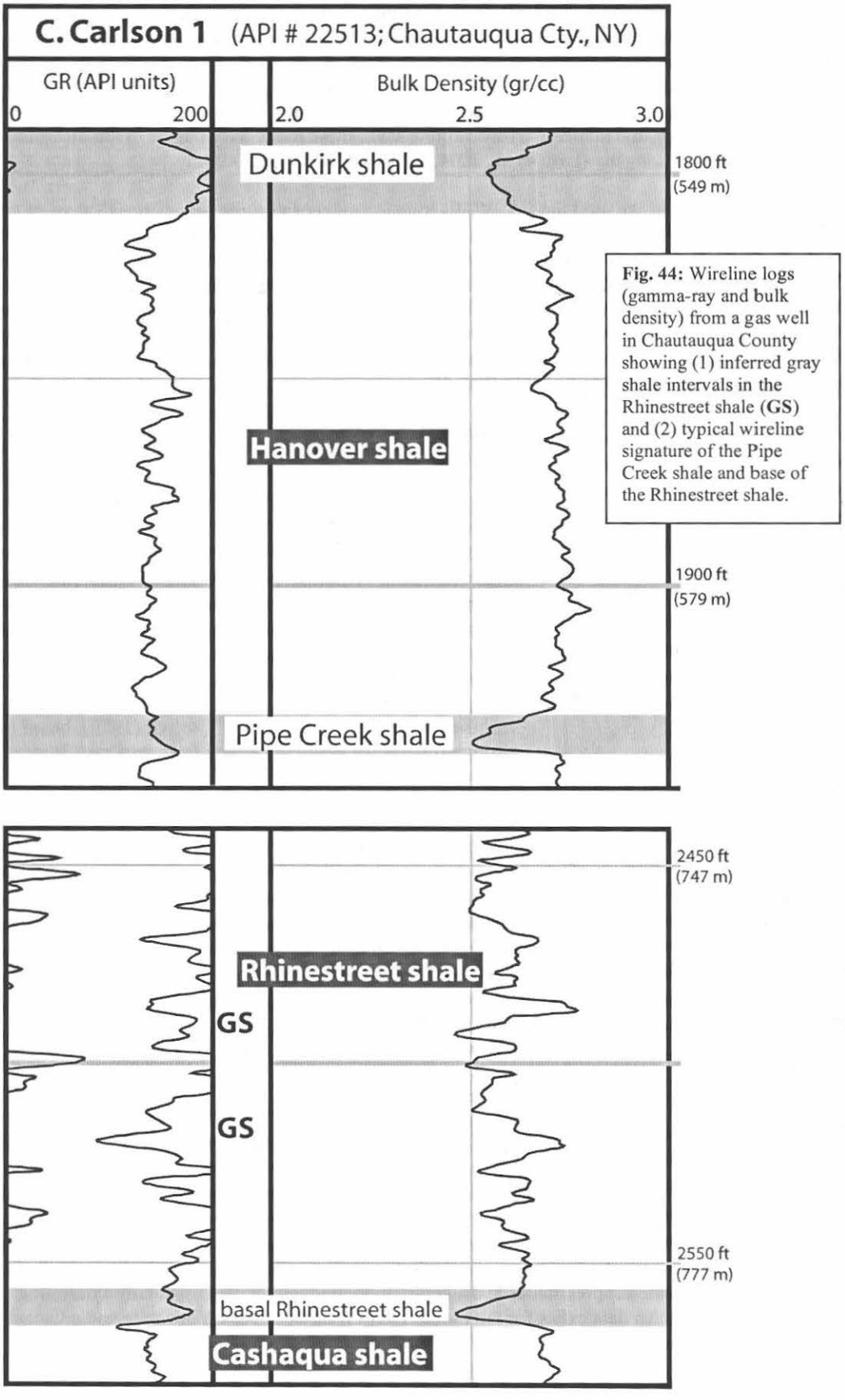

Fig. 44: Wireline logs (gamma-ray and bulk density) from a gas well in Chautauqua County showing (1) inferred gray shale intervals in the Rhinestreet shale (**GS**) and (2) typical wireline signature of the Pipe Creek shale and base of the Rhinestreet shale.

NW- and ENE-trending joints are densely formed in the black shale immediately above the contact with the Cashaqua shale (station EMC 13 and 16, Fig. 38). A similar relationship of joint density and TOC has been observed in the Dunkirk shale along the Lake Erie shoreline as well as in the Geneseo shale of the Finger Lakes District (Loewy, 1995; Lash et al., 2004). The correlation of joint density with TOC provides compelling evidence that the joints formed as natural hydraulic fractures as a consequence of the transformation of organic matter to hydrocarbons when these rocks were buried to the oil window during the Alleghanian orogeny (Lash et al., 2004; Lash and Engelder, 2005).

III. As noted earlier, we used the EASY%R_o kinetic model of vitrinite reflectance (Sweeney and Burnham, 1990) to model the burial/thermal history of the Rhinestreet black shale. Thermal modeling by use of the EASY%Ro algorithm requires knowledge of (1) the age(s) of the unit(s) of interest (the base of the Rhinestreet shale), (2) at least a partial thickness of the local stratigraphic sequence, and (3) the measured vitrinite reflectance of the unit(s) of interest (vitrinite reflectance of the base of the Rhinestreet shale = 0.74%). Our model for the Rhinestreet shale, which includes passage of the early Alleghanian peripheral bulge (see Fig. 9), requires ~1.5 km of Permian strata in this area of the basin, an amount close to that modeled by Beaumont et al. (1988) (Fig. 45).

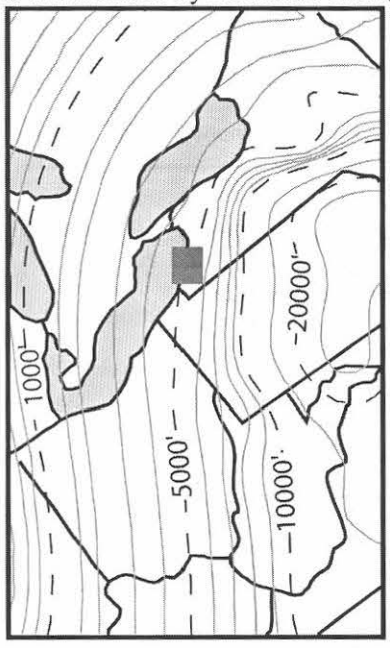

Fig. 45: Modeled thickness of Permian strata in the Appalachian Basin (modified after Beaumont et al., 1987).

Our method of modeling the burial/thermal history of the Rhinestreet shale depends on accurate %R_o values. However, several workers (e.g., Nuccio and Hatch, 1996; Rimmer and Cantrell, 1988; Rimmer et al., 1993; Rowan et al., 2004) have recognized the likely occurrence of vitrinite suppression in Devonian-Mississippian black shales, including those of the Appalachian Bain. Suppression of vitrinite leads to an underestimation of thermal maturity and, therefore, an underestimated burial depth. Suppression is most readily recognized by anomalously low %R_o on maturity profiles of wells or stratigraphic columns (e.g., Price and Barker, 1985). There are several lines of evidence suggesting that Devonian black shales of the Appalachian Basin have been affected to some extent by vitrinite suppression. Rimmer and Cantrell (1988), based on a vitrinite reflectance gradient derived from coal rank trends, claim that measured %R_o values of the Cleveland Member of the Ohio shale in eastern Kentucky are suppressed by as much as 0.3 – 0.5%R_o. More recently, Rowan et al. (2004), in the course of their burial/thermal modeling of a cross-section from central West Virginia to northeast Ohio, demonstrated that the predicted %R_o of Devonian shale is locally twice the measured %R_o. Rowan et al. (2004) constrained their burial/thermal model with measured %R_o of Pennsylvanian coals and color alteration index values of conodonts recovered from Ordovician and Devonian limestones.

We suggest that Middle and Upper Devonian black shale of the western New York state and northwest Pennsylvania region of the Appalachian Basin was also been affected by suppression. Our data base includes published thermal/maturity values (Weary et al., 2000; Repetski et al., 2002) and %R_o and Rock-Eval data from our work on the Upper Devonian shale succession of the Lake Erie District. We limited our data to the western New York state and northwest Pennsylvania region of the basin in order to assume a common thermal history for these deposits. A plot of Rock-Eval HI versus %R_o of Appalachian Basin black shale samples, principally from the Marcellus shale, reveals a trend similar to that observed by Nuccio and Hatch (1996) for the Upper Devonian-Mississippian New Albany shale, which has been affected by vitrinite suppression (Fig. 46). The higher HI samples, including samples collected from the Dunkirk and Rhinestreet shales, fall along a relatively narrow %Ro trend; however, at an HI of ~125 mg/g, measured %R_o increases rapidly from ~ 0.75 to > 2.5 as HI drops to near zero (Fig. 46). This plot appears to show suppressed values in the lower to mid oil window (%R_o = ~0.7 to 1.0), consistent with Lo's (1993) findings regarding vitrinite suppression of hydrogen-rich organic matter. An especially interesting subpopulation of Marcellus data exists for the Finger Lakes District of New York state and adjacent Potter and Tioga counties, Pennsylvania (Fig. 46). These data are defined by %R_o ranging from 0.5 to 1.0 and HI

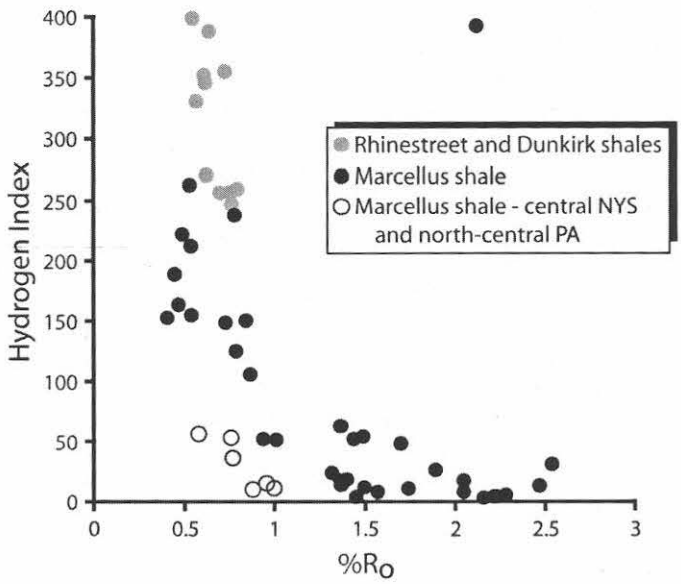

Fig. 46: Rock-Eval HI versus $\%R_o$ for Middle and Upper Devonian shale samples collected from the western New York state and northwest Pennsylvania region of the Appalachian Basin.

< 55 (Fig. 46). These samples, which appear severely suppressed, were collected from that part of the basin affected by emplacement of Cretaceous ultramafic intrusions (Kay et al., 1983).

Upper Devonian black shales exposed along the Lake Erie shoreline show a good amount of variation in measured $\%R_o$ over a relatively small distance (see Fig. 7). Measured %Ro in a well cutting sample collected from the base of the Rhinestreet shale in northern Chautauqua County is 0.51%. The $\%R_o$ of the same stratigraphic interval ~40-45 km to the northeast is 0.73 – 0.77 based on the analysis of four outcrop samples. Finally, a sample collected from the base of the Rhinestreet 7.25 km to the east on Cazenovia Creek has a $\%R_o$ of 0.59. We recognize similar erratic variations in the measured $\%R_o$ for Dunkirk shale samples. Rowan et al. (2004) suggest that variations in the type of organic matter in marine sediments may account for erratic variations in $\%R_o$ (e.g., Ujiié et al., 2004).

Vitrinite suppression has also been attributed to the overpressuring of rocks (McTavish, 1978 1998; Carr, 2000). Pervasive natural hydraulic fractures in the Rhinestreet shale provides evidence that these rocks were overpressured during their burial history, which could have contributed to suppression of virinite reflectance. Regardless of its mode of origin, suppression of vitrinite reflectance is a phenomenon that should be taken into account in any exploration and production considerations of Devonian black shales.

IV. The contact of the Cashaqua gray shale and overlying Rhinestreet black shale is readily defined in the field; both color contrast and relative weathering profile provide easy means for making this recognition. The contact is rather obvious in gamma-ray logs, which provide a measure of the intensity of natural gamma-rays (uranium concentration) emitted by a formation (Fig. 44). Still, the initial deflection marking the contact is not what one might expect based on the abrupt contact between the low-TOC (<0.7%) Cashaqua shale and the carbonaceous (TOC>8%) Rhinestreet shale. However, the Cashaqua-Rhinestreet contact is very obvious in bulk density logs (Fig. 44), no doubt a reflection of the low density of organic matter relative to shale minerals (Smith and Young, 1964; Schmoker, 1979). Schmoker (1981) claimed that the bulk density log is a more accurate proxy for organic matter content than the gamma-ray API value. Indeed, the strong inverse relationship of bulk density and TOC in Upper Devonian black shale of western New York state has been confirmed by a proprietary data set we have had the opportunity to study (Lash, 2006c). It is interesting to note that the organic-rich Pipe Creek black shale (TOC = 3.2 - 7.9%) is not easily recognized on the gamma-ray log, but is readily picked on the bulk density log (Fig. 44).

On the other hand, the base of the overlying Dunkirk shale is readily recognized on both types of logs (Fig. 44).

Lüning and Kolonic (2003) have pointed out that many black shale deposits show a strong correlation of uranium, manifested by gamma-radiation in API units, and TOC. However, they also note those examples where the correlation is weak at best. The basal Rhinestreet shale and the Pipe Creek shale provide examples of the latter phenomenon. Indeed, a spectral gamma-ray log from a well in northeast Chautauqua County reveals the base of the Rhinestreet shale to be marked by an increase in uranium from 6 to 10 ppm; the Pipe Creek shale is defined by an increase of only 2 ppm. Lüning and Kolonic (2003) suggest that the precipitation of uranium from seawater onto the surface of organic particles under anoxic conditions is governed by several factors, including carbonate content, sedimentation rate, and primary uranium content of the seawater. Upper Devonian shales of western New York state are defined by very low $CaCO_3$ abundances ruling out the first factor. Lüning and Kolonic (2003) point out that the longer organic matter is in contact with seawater, the greater the amount of uranium that can precipitate onto organic grains. Low sedimentation rates favor high uranimum/TOC ratios. The anomalously low API values of the most organic-rich interval of the Rhinestreet shales (as deduced by TOC analysis of field samples and bulk density values determined from wireline logs) may indicate a high sedimentation rate of this interval such that lesser amounts of uranium were fixed onto organic particles. The same can be said of the Pipe Creek shale. The organic-rich base of the Dunkirk shale (Lash et al, 2004; Lash and Engelder, 2005), however, defined by the highest API value and lowest bulk density of the unit, would have accumulated relatively slowly.

Finally, it is possible that the introduction of low uranium freshwater into the Devonian Sea, such as might be expected as a consequence of the reduction of polar ice volume, was responsible for some of the variations in gamma-ray response observed in wireline logs of the base of the Rhinestreet shale and especially the Pipe Creek shale, which has been correlated with the Lower Kellwasser Bed recognized in Europe (Over, 1997). The concentration of uranium in seawater is an order of magnitude greater than freshwater (Broecker and Peng, 1982). The presence of the diagnostic uranium signature of the Pipe Creek shale in well logs recovered from northwest Pennsylvania, western New York state, northeast Ohio, and northernmost West Virginia suggests a basinwide cause. The Pipe Creek interval is a particularly interesting horizon. McGhee (1990) argued that this interval is a significant crisis interval similar to the younger Frasnian-Famennian boundary. In fact, he suggested that the Pipe Creek interval was more critical in terms of the maximum number of species extinctions and the extinction rate. It has been suggested that the Kellwasser Beds, including the Pipe Creek shale, resulted from eustatic transgressions perhaps caused by a reduction in polar ice volume (Sandberg et al., 1988; Buggisch, 1991; Joachimski and Buggisch, 1993). It may be that the same global mechanism that created the Pipe Creek crisis – rapid climatic warming – also accounts for the unique wireline log signature of the Pipe Creek shale.

Total Miles	**Miles from Last Point**	**Route Description**
21.6	0.0	Head north on South Creek Road.
21.7	0.1	Intersection of South Creek Road and Route 20. Remain on South Creek Road.
23.8	2.1	Turn left onto Lake Shore Road.
25.8	2.0	Intersection of Sweetland Road and Lake Shore Road.
27.0	1.2	Turn right onto Sturgeon Point Road.
27.9	0.9	Follow Sturgeon Point Road into the Sturgeon Point Marina. Continue through the marina (slowly) to the lower (east) parking area.

STOP 3: STURGEON POINT

Significance: I) comparison of the degree of jointing in black shale versus gray shale and the preferential generation of NS systematic joints in gray shale at contacts with overlying black shale;
II) carbonate concretions in black shale and analysis of compaction strain;
III) variation in the thickness of the bottom gray shale interval of the Rhinestreet shale.

I. Depart the parking area walking northeast toward the bedrock cliff a few hundred meters distant. We will follow this exposure of gray and black shale of the Rhinestreet shale for perhaps 0.75 km. The 2.75-m-thick gray shale interval exposed at the west end of the exposure is the equivalent of the lower gray shale interval of the Rhinestreet shale on Eighteenmile Creek (see Fig. 1; 9.9-12.5 m). The gray shale includes several horizons of high aspect ratio (lenticular) carbonate concretions and thin grayish-black shale layers. One can readily observe differences in the degree (density) of jointing between black and gray shale in this exposure. Black shale above and below the gray shale carries NW joints and younger ENE-trending systematic joints (Fig. 47). NW and ENE joints can be observed in the gray shale, but these deposits also contain the older NS-trending systematic joints (Fig. 47). The black shale clearly is more densely jointed than the gray shale, a recurring theme throughout the Appalachian Plateau (Fig. 48; Loewy, 1995; Lash et al., 2004). Moreover, ENE joints are more densely formed (i.e., closer to saturation) than are the older NW joints. This latter observation can also be made of ENE and NW joints in the gray shale (Fig. 48). NS-trending systematic joints in the gray shale are more densely formed than are the younger NW joints. As described earlier, the NS joints are interpreted to have originated in the higher modulus carbonate concretions as a consequence of thermoelastic loading caused by passage of a peripheral bulge across the Appalachian Basin at the onset of the Alleghanian orogeny. Indeed, it is more common for a NS joint to penetrate or cut a higher modulus carbonate concretion than it is for ENE and NW joints to cleave concretions. Note also that very few NS joints penetrate more than a few tens of cm into the overlying black shale; more often than not, they are arrested at the base of the organic-rich deposits. This exposure presents a nice example of the stratigraphic control on jointing in these rocks.

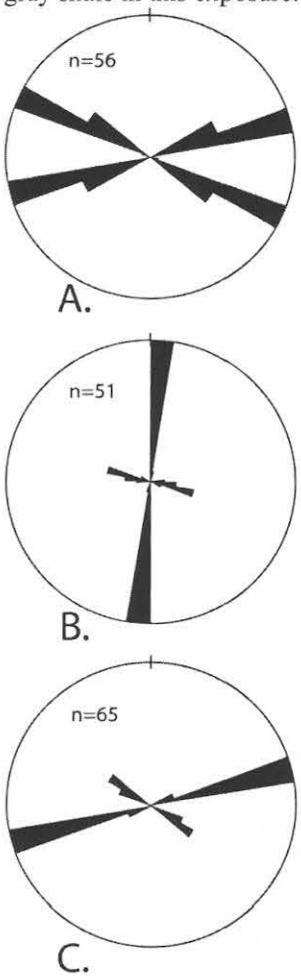

Fig. 47: Rose plots of joints in the (A) upper black shale, (B) gray shale interval, and (C) lower black shale at Stop 3.

Continue NE along the beach toward a large drainage pipe in the cliff. Careful observations of the gray shale horizon while working along the beach to this location would have revealed a gradual decrease in thickness of this interval. The thickness of the gray shale immediately east of the drainage pipe (determined by digging through beach sand to black shale) is ~ 80 cm, markedly reduced from what is was at the start of this trek along the beach. Note also that the gray shale is not as complexly jointed here; indeed, the median spacing of NS joints is 50% greater than at the western end of the exposure (Fig. 48). Finally, the thickness of the gray shale interval at the NE end of the exposure is at least 1.5 m. NW- and NS-trending joints are carried by the gray shale in this area. Further, NS joints are more densely formed at this location of the exposure than elsewhere along the beach (Fig. 48).

There is a school of thought that holds that all jointing in the exposed Devonian succession of the Appalachian Plateau of western New York state is a consequence of post-Alleghanian (perhaps even post-glacial) uplift of the Appalachian Basin. This view fails to take into account the

Fig. 48: Box-and-whisker diagrams representing joint spacing distribution for NS, NW, and ENE joints along the length of the Stop 3 exposure from the southwest (closest to parking area at the Sturgeon Point Marina) to the east. Spacing data for the lower black shale exposed at the southwest end of the exposure is included for comparison.

well-defined chronology of the joints (Engelder and Geiser, 1980; Lash et al., 2004) and the fact that the joints provide information regarding the orientation of the remote or lithospheric (Engelder and Whitaker, 2006) stress field that was responsible for their formation. There are likely subtle differences in rock properties between the black and gray shale that perhaps played some ancillary role in the jointing of these rocks. We suggest that the black shale, principally by virtue of its greater amount of ductile organic matter, was not as stiff (i.e., lower modulus) as the gray shale, a view at odds with the more common thinking regarding heavily fractured black shale. Accordingly, gray shale, as a consequence of its higher porosity and locally greater abundance of calcite cement (e.g., Lash, 2006b) would have had the higher modulus. Joints driven by fluid decompression, natural hydraulic fractures, form at great burial depth and, therefore, under high confining pressure. All else being equal, it would have been more difficult to initiate open mode cracks in higher modulus organic-lean gray shale under these conditions. Moreover, movement of the black shale into the oil window and resultant transformation of kerogen to hydrocarbons would more readily create a negative effective stress necessary for the propagation of natural hydraulic fractures, their growth direction being controlled by the remote stress field. NW-trending joints were produced by an Alleghanian remote stress field that was responsible for emplacement of the Blue Ridge-Piedmont Megathrust sheet; ENE joints, however, reflect a longer-standing lithospheric scale stress field related to continued oblique approach of the African portion of Gondwana against the Laurentian plate boundary (Engelder and Whitaker, 2006).

The remaining question, then, relates to the preferential formation of NS joints in the gray shale as observed at this exposure. Passage of the peripheral bulge across the Appalachian Basin at the onset of the Alleghanian orogeny and related uplift of the Upper Devonian shale-dominated succession of the Lake Erie District subjected these rocks to thermoelastic contraction. The higher modulus rock - the gray shale – would have carried a higher tensile stress and, therefore, would have been closer to the negative effective stress necessary to initiate joints. The inferred contrast in modulus between black and gray shale may explain why the NS joints terminate at gray shale-black shale contacts; i.e., the lower modulus black shale carried a lower tensile stress than the gray shale. However, the highest modulus rocks in the Rhinestreet shale were the carbonate concretions. As described earlier, concretions remained in compression during catagenesis so that fluid-driven NW and ENE joints were unable to penetrate them any more than a cm or so. However, during thermoelastic contraction, the concretions carried a high level of tensile stress (higher than that of the gray shale and certainly much higher than that of the black shale) making them more likely to fail under true tension. Initiation of the NS joints in the diagenetic carbonate was followed by their propagation through the host gray shale aided by a modest pore pressure.

In sum, this exposure, like others in this region of the Lake Erie District, provide evidence that systematic joints carried by the Upper Devonian shale succession resulted from two different loading mechanisms before post-Alleghanian uplift of the Appalachian foreland. However, we are investigating the intriguing possibility that an ENE-trending set of joints, some of which cut diagenetic carbonate, formed as a consequence of the uplift of the Appalachian Plateau. These joints appear to have been driven by thermoelastic contraction under a remote stress field perhaps induced by spreading at the Mid-Atlantic Ridge; thus their ENE strike.

II. This exposure also allows for the differentiation of concretionary carbonate found in gray shale from concretions common to black shale (spectacular examples of this latter type will be seen at Stop 4). The former are defined by high aspect ratios (they may better be described as lenticular diagenetic limestone) and lack obvious internal structures, principally layering. The scraggy layers are an example of this type of diagenetic carbonate. Carbonate concretions in the black shale have lower aspect ratios and display nicely preserved layers of the host organic-rich sediment. The above distinctions is readily made at this exposure.

Numerous small, internally laminated concretions can be observed in black shale within a meter or so of the upper contact of the gray shale interval, especially along the eastern stretch of the exposure. These concretions lend themselves to compaction strain analysis as described earlier (Fig. 49). Compaction strain is determined by measuring a stratigraphic interval within the concretion, T_i, and that same interval traced into the host shale but far enough beyond the strain shadow to provide a full measure of compaction strain, T_o (Fig. 49). The following equation is used to calculate compaction strain, ε_3:

$$\varepsilon_3 = \frac{T_i - T_o}{T_i}.$$

Estimated compaction strain of six concretions at this exposure is 60.8%, ~ 9% higher than the average for the Rhinestreet shale as discussed earlier. We believe that this reflects concretionary growth in a stratigraphic horizon that had not compacted to the extent that most of the unit did before the onset of normal compaction (see earlier discussion).

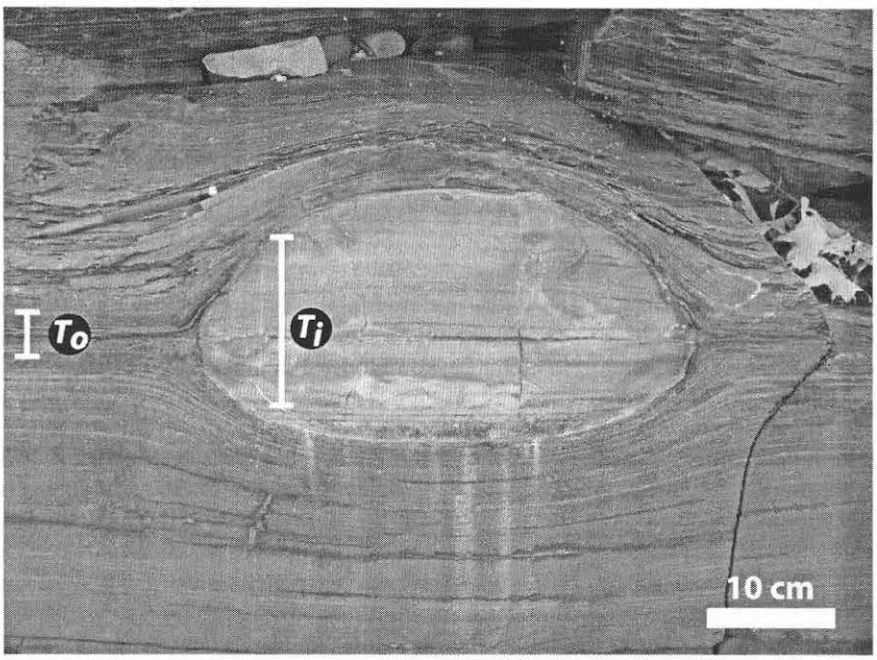

Fig. 49: Ellipsoidal carbonate concretion in Rhinestreet black shale at Stop 3. Refer to text for discussion.

III. Moving SW to NE along the beach, we observed the thickness of the gray shale interval diminish from ~2.75 m to ~ 0.8 m; farther along, though the thickness increases to at least 1.5 m. We observed no evidence of faulting that might account for the described change in thickness. Perhaps we are looking at the effects of differential compaction (e.g., Conybeare, 1967; Finely, 1990; Ryder, 1996). Indeed, the local presence of flame-like structures at the top of the gray shale interval suggests that these deposits were rather mobile and perhaps characterized by moderately high pore pressures, as suggested by the NS joints. Indeed, the relatively low density of NS systematic joints in the middle interval of this exposure where the gray shale is thinnest may reflect the effects of differential dewatering and resultant differential compaction. Preferential dewatering of the gray shale could account for (1) the reduced thickness of the gray shale at this location of the exposure and (2) a reduction in pore pressure, which would not have favored the generation of NS-trending joints in these rocks. Clearly, much more work is needed to elucidate this hypothesis.

Total Miles	Miles from Last Point	Route Description
27.9	0.0	Depart the marina onto Sturgeon Point Road.
28.8	0.9	Turn left (east) onto Lake Shore Road.
30.9	2.1	Intersection of Sweetland Road and Lake Shore Road.

31.0	0.1	Cross Pike Creek.
32.9	1.9	Turn right onto South Creek Road.
33.2	0.3	Intersection of South Creek Road and Route 5. Remain on South Creek Road.
34.1	0.9	Pass under railroad bridge.
35.0	0.9	Intersection of South Creek Road and Route 20. Turn left (east) onto Route 20.
36	1.0	Turn right (south) onto Lakeview Road.
36.4	0.4	Crossing over the New York State Thruway.
37.1	0.7	Turn right onto an unnamed road.
37.2	0.1	Turn right (west) at the stop sign onto North Creek Road.
37.8	0.6	Pull off onto the wide shoulder on the right. Cross North Creek Road and take the path down to Eighteenmile Creek.

STOP 4: **EIGHTEENMILE CREEK (main branch)**

Significance: I) the contact of the Rhinestreet shale and overlying Angola gray shale;
II) general characteristics of the carbonate concretions.

I. Follow the creek upstream (to the left) to where the east branch of Eighteenmile Creek enters the main creek. Cross the east branch just upstream from this point and follow a trail through the woods for roughly several hundred meters or until the path approaches the main branch. Cross the creek and walk to where you can view the cliff exposure across the creek. The middle concretion horizon will be visible a meter or so above the waterline. The upper ~21 m of the Rhinestreet shale and lower few meters of the Angola shale are exposed in the cliff (see Fig. 1). The Rhinestreet-Angola contact is transitional and marked by an increase in the frequency of less resistant (to the effects of weathering) gray shale layers, which can be observed both in the field at this stop and in well logs (Figs. 1 and 50). Luther (1903) suggested that the contact be placed at an easily recognizable discontinuous nodular limestone bed locally as thick as ~ 30 cm, the upper scraggy layer (see Fig. 1), which can be seen near the top of the exposure. The upper scraggy layer can also be recognized in some gamma-ray logs by a sharp deflection to the left (e.g., Fig. 20).

II) Carbonate concretionary horizons like the one exposed here are conspicuous in Middle and Upper Devonian black shale units of central and western New York state (Dix and Mullins, 1987; Lash and Blood, 2004a,b), southwestern Ontario (Daly, 1900; Coniglio and Cameron, 1990) and Ohio (Clifton, 1957; Criss et al., 1988) suggesting that diagenetic conditions favorable to the formation of these features existed regionally. Concretions are especially useful in the analysis of the early post-depositional history of encapsulating shale, for not only can they preserve the depositional texture of the host sediment (e.g., Woodland, 1984; Duck, 1990), but they carry a record of the evolution of pore fluids carried by the sediment (e.g., Hudson, 1978; Coniglio and Cameron, 1990). Details of our work on the carbonate concretions of the Rhinestreet shale can be found in Lash and Blood (2004a,b) and are presented in an abbreviated format above.

The concretions visible here are among the most spectacular in the world. They are similar to those described from such well known units as the Kimmeridge Clay (Astin and Scotchman, 1988) and the Jet Rock (Hallam, 1962). Close inspection of the exposed Rhinestreet concretions reveals their laminated

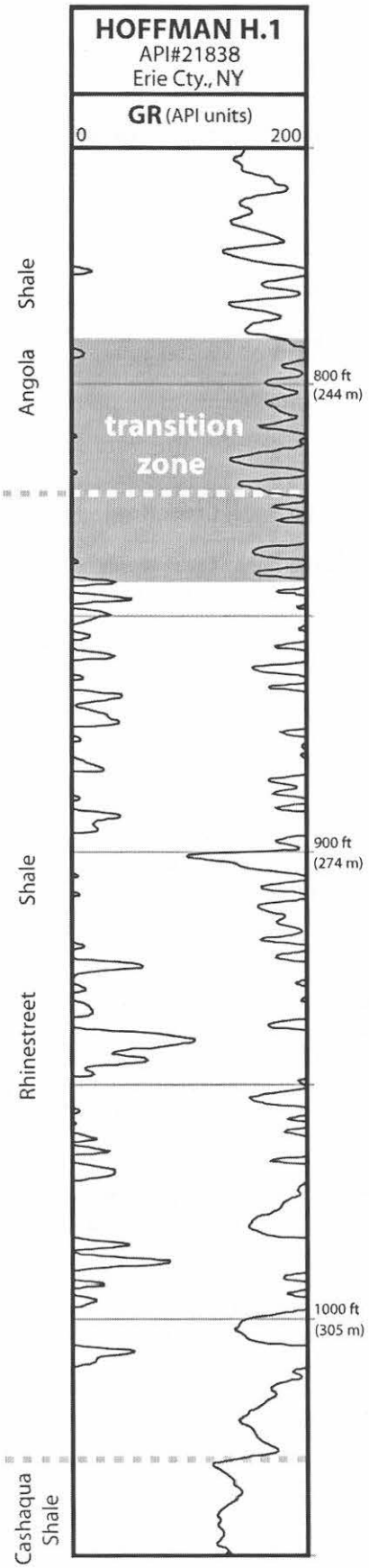

Fig. 50: Gamma-ray log from a gas well in Erie County showing the transitional contact of the Rhinestreet shale and overlying Angola shale. Note the frequency of gray (organic lean) shale-black shale alternations in the transition zone. The contact (dashed line) is based on bulk density (the upper contact of the Rhinestreet is arbitrarily set at that level where bulk density > 2.55 gr/cm^3; Lash, 2006a).

nature and presence of septaria. Our principal interest in the concretions has been their use as compaction strain indicators. However, before they could be used in this way, we had to understand their mode of origin and depth of growth, which was considered earlier. Most carbonate concretions of the Rhinestreet shale are found in three stratigraphically confined but laterally persistent horizons (see Fig. 1) – a lower horizon ~ 6 m above the base of the unit, a middle interval slightly more than halfway up the Rhinestreet (Stop 4), and an upper, less well defined, horizon ~ 43 m above the base of the unit. Most concretions are oblate ellipsoids with maximum diameters and thicknesses ranging up to 2.7 m and 1.1 m, respectively (Lash and Blood, 2004b); coalesced concretions have also been observed and are locally abundant. We carried out a detailed analysis of the dimensions and general shapes of concretions of the lower and middle horizons (Fig. 51). The dimensional data for both horizons reveals an especially intriguing feature; the maximum vertical dimension of the bulk of the concretions is ~ 80 cm (Fig. 51). However, the scatter of data from the middle horizon suggests that some concretions stopped growing in the vertical dimension at ~ 80 cm but continued to form laterally (Fig. 51). This suggests that the middle concretion horizon remained in the zone of anaerobic methane oxidation (AMO) longer than the lower concretion horizon.

Crucial to precipitation of diagenetic carbonate by the AMO mechanism discussed earlier is a marked reduction in sedimentation/burial, which would stabilize the sediment in the AMO zone thereby enabling protracted carbonate precipitation in that horizon (Raiswell, 1987, 1988). Two observations considered earlier provide evidence of a marked reduction in burial rate during concretion growth: (1) little or no change in carbonate volume percentage outward from the centers of studied concretions and (2) negligible variations in laminae thickness across concretions (Lash and Blood, 2004b).

The middle and lower concretion horizons differ in a fundamental way that yields indirect information regarding such parameters as the *magnitude* and *duration* of the change in sedimentation/burial rate. The middle horizon, 1 to 2.5 m-thick, contains concretions distinctly larger in the horizontal dimension than are concretions of the roughly 2.5-m-thick lower horizon (Fig. 51). The thickness of a concretion horizon is interpreted to be proportional to the change in sedimentation/burial rate; i.e., a marked reduction in burial rate yields the minimum vertical range of carbonate precipitation because the zone of AMO in the sediment stabilized (Raiswell, 1987, 1988). The more oblate, occasionally flat-topped, concretions in the middle horizon, then, likely reflect the restriction of carbonate precipitation to a relatively

narrow, fixed zone defined by the upper limit of methane and CO_3^{2-} diffusion and the maximum depth to which seawater sulfate can diffuse (Raiswell, 1988). Thus, the generally larger horizontal dimensions of concretions of the middle horizon indicate that the break in sedimentation persisted longer at this time than during formation of the lower concretionary horizon.

The middle Rhinestreet concretion horizon, by virtue of its limited thickness and the geometry of its concretions, records a reduction in sedimentation/burial rate of greater magnitude than that which led to formation of the thicker lower concretionary interval (Lash and Blood, 2004b). However, the thickness and geometry of the scraggy layers likely reflects an even greater duration of the break in sedimentation/burial and, therefore, a protracted period of time that isotopically light methane and ^{13}C-enriched dissolved carbonate were delivered to the stationary AMO zone (Raiswell, 1987, 1988). That is, the near cessation of sedimentation and, more importantly, subsidence, resulted in confinement of carbonate precipitation to a narrow, fixed zone defined by the upper limit of methane diffusion and the maximum depth to which seawater sulfate could diffuse (Raiswell, 1988). Because the events that contributed to the reduction in sedimentation/burial rate may have been basinwide, concretionary horizons may serve as time lines in establishing regional time-stratigraphic relationships.

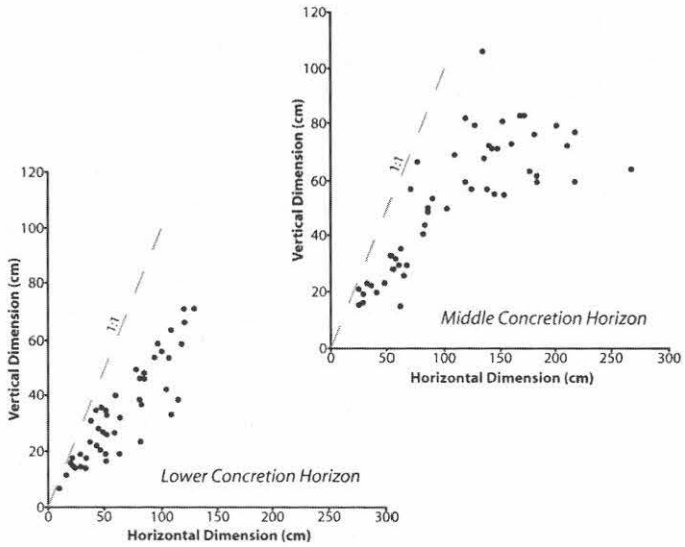

Fig. 51: Horizontal versus vertical dimensions of carbonate concretions of the lower (n = 50) and middle (n = 52) concretion horizons of the Rhinestreet shale.

END OF FIELDTRIP – return to vehicles

Total Miles	Miles from Last Point	Route Description
37.8	0.0	Continue along North Creek Road to Route 20.
39.0	1.2	Turn left (west) onto Route 20.
39.4	0.4	Turn right onto South Creek Road.
41.2	1.8	Turn right onto Route 5 and return to Adams Mark in Buffalo.